

Distribution Agreement

In presenting this thesis or dissertation as a partial fulfillment of the requirements for an advanced degree from Emory University, I hereby grant to Emory University and its agents the non-exclusive license to archive, make accessible, and display my thesis or dissertation in whole or in part in all forms of media, now or hereafter known, including display on the world wide web. I understand that I may select some access restrictions as part of the online submission of this thesis or dissertation. I retain all ownership rights to the copyright of the thesis or dissertation. I also retain the right to use in future works (such as articles or books) all or part of this thesis or dissertation.

Signature:

Yun Wei

Date

Identifying a novel therapeutic target in Sonic Hedgehog medulloblastoma

By

Yun Wei
Doctor of Philosophy

Graduate Division of Biological and Biomedical Sciences
Cancer Biology

Anna Marie Kenney, Ph.D.
Advisor

Lawrence Boise, Ph.D.
Committee Member

Dolores Hambarzumyan, Ph.D.
Committee Member

David C. Pallas, Ph.D.
Committee Member

Maureen Powers, Ph.D.
Committee Member

Wei Zhou, Ph.D.
Committee Member

Accepted:

Lisa A. Tedesco, Ph.D.
Dean of the James T. Laney School of Graduate Studies

Date

Identifying a novel therapeutic target in Sonic Hedgehog medulloblastoma

By

Yun Wei
Bachelor's of Science, 2012

Advisor: Anna Marie Kenney, Ph.D.

An abstract of
A dissertation submitted to the Faculty of the
James T. Laney School of Graduate Studies of Emory University
in partial fulfillment of the requirements for the degree of
Doctor of Philosophy
in Cancer Biology
2018

Abstract

Identifying a novel therapeutic target in Sonic Hedgehog medulloblastoma

By

Yun Wei

Medulloblastomas are the most common malignant pediatric brain tumors. The World Health Organization classified medulloblastomas into four molecular subgroups, including WNT-activated, SHH-activated *TP53*-mutant, SHH-activated *TP53*-wildtype, and non-WNT/SHH (also known as Group 3 and Group 4) in 2016. SHH-activated medulloblastomas have been well established, most of which harbor the aberrant driver Sonic Hedgehog signaling. However, the cure rate has reached a plateau over the past decade, due to the underrepresented integration of molecular discoveries into the stratification system or treatment protocols. Moreover, the lack of targeted therapy leads to the over-treatment of some patients, and the inadequacy to cure some other patients. This underscores the necessity to identify novel therapeutic targets for these patients. Even within SHH medulloblastomas, the intra-subgroup heterogeneity hinders the development of a “one-for-all” drug. Therefore, my research project focuses on 1) untangling the intra-subgroup heterogeneity of SHH medulloblastomas in respect of age demographics, signaling crosstalk, the tumor microenvironment compositions, and the possible epigenetics attributions, and 2) identifying I2PP2A as a novel therapeutic target for SHH medulloblastoma patients harboring wildtype *TP53*. We summarized the recent findings in SHH medulloblastoma research utilizing mouse models, patient samples, and the implications of these discoveries in guiding future stratification or treatment for SHH medulloblastoma patients. We postulated that the more refined stratification system and more tailored treatment protocols would benefit SHH medulloblastoma patients in the future, considering the intra-subgroup heterogeneity of this disease. Furthermore, we showed that I2PP2A, inhibitor 2 of protein phosphatase 2A, could be a potential target, which can be inhibited to restore TP53 function. In a SHH medulloblastoma mouse model, we tested the hypothesis that I2PP2A upregulates p-MDM2^{S166} by suppressing PP2A dephosphorylation activity, and that the subsequent accumulation of p-MDM2^{S166} degrades wildtype p53. We also demonstrated that targeting I2PP2A caused tumor cell death through inhibiting p-MDM2^{S166} and restoring p53 activity in both SHH medulloblastoma mouse model and patient-derived cell lines. We hope to facilitate improvements in refining current stratification and treatment protocols by illustrating the tumor heterogeneity and by identifying a novel therapeutic target for a subset of SHH medulloblastoma patients.

Identifying a novel therapeutic target in Sonic Hedgehog medulloblastoma

By

Yun Wei
Bachelor's of Science,

Advisor: Anna Marie Kenney, Ph.D.

A dissertation submitted to the Faculty of the
James T. Laney School of Graduate Studies of Emory University
in partial fulfillment of the requirements for the degree of
Doctor of Philosophy
in
Graduate Division of Biological and Biomedical Sciences
Cancer Biology
2018

Acknowledgements

Many people deserve my appreciation and acknowledgment in helping me to complete my Ph.D. and to get the training I need for my career.

To my husband and best friend, for many supports, he has provided in past years. I met him at the point when I felt unsure about the future, being alone in a foreign country struggling with the academic performances. Though being quiet in most times, he supports me through his love for me and his devotion to family. We don't share the same interests or career path, but we always find the balancing point and coordinate well in times when I need to work hours over the weekend, when I need my own space to focus on writing, and when I need a getaway from research. He is supportive of my science career and understands the difficult choices that I made along the way. I can't be luckier in getting married to a man who always sees good things in people, and who is passionate about life.

To my mentor Dr. Anna Kenney, for her accepting me to the Kenney lab and the following mentoring. She is open-minded and runs an inclusive lab with diversity which encourages the cooperation among lab members. I would never forget the time when she encountered me in the hallway and asked if I want to join her lab after my rotations. It's the time when my research journey begins, and the time when I feel needed by people in the United States. I don't know how to define a good mentor, but she is among a few that I have in my career. She gives me space and time to make research progress and provides alternatives when I feel frustrated with failures in testing some scientific ideas. Anna cares about me, and instead of pushing me forward, she provides me with what she can, with different resources, opportunities, and connections with other great scientists in the field whenever needed. I feel self-motivated and become more confident and independent in performing science along the way, primarily due to her way of mentoring.

My next acknowledgement goes to other lab members, including the postdoc Victor Maximov, who helped me in developing the experimental designs and data analysis, postdocs Anshu and Abhi, who are always there to help me with lab techniques, another PhD student Hope Robinson, who came to the lab later but helped me a lot in writing and idea developing, and last but not the least, Chad Potts, the best lab technician ever. I also got help from other lab members, who came and left during my Ph.D. Day to day lab work is not easy, but is made pleasant by these lovely people.

To my parents and other family members, who support my choice of going abroad for advanced training. I especially need to thank my mom, who did not even complete the middle school. She is open-minded and always believes in me since I was a kid. She couldn't go too far in providing academic support, but could always find ways to hold me up when I feel crumbled occasionally. To my father, who has taught me to enjoy life while pursuing career success. It's my parents who made me strong enough mentally to face any challenges in life and academia.

To all my committee members, Drs. Lawrence Boise, Dolores Hambardzumyan, David Pallas, Maureen Powers, and Wei Zhou, for providing the insightful feedback in committee meetings. I would never forget the time when I saw Larry's video congratulating on me getting the offer to Emory, while I was still in China. Being the first international students of Cancer Biology Program, I felt lucky and honored to be recruited by Larry. I would also like to thank Dolores in giving me the praise for every bit progress I've made. She is the person who helps me lay out the timeline for graduation and the plan for my Ph.D. completion. To Dr. Zhou and Powers for insightful and practical suggestions in committee meetings, and to David Pallas for the collaboration and the detailed feedback for the research article manuscript. All my committee members are available any time for help, which makes me feel confident in conducting the good science.

To lab members from the same floor of our research building, including people from Craig Castellino, Tobey MacDonald, Dolores Hambarzumyan, Kelly Goldsmith and Chris Potter labs, who helped me by generously lending their equipment, the experimental materials, and technical support.

Last but not the least, my acknowledgment goes to the Cancer Biology students and faculty, staff, who welcome me and help me in every aspect of my coursework, oral presentations, and academic planning. I feel there are many people behind me whom I can count on even we have a different cultural background, skin colors or ways of comprehending. I get plenty of respect and encouragement for me to work through my Ph.D., due to the help from these diligent and devoted people.

Table of Contents

Chapter 1. Introduction	1
1.1 Medulloblastoma	1
1.1.1 Medulloblastoma overview	1
1.1.2 Sonic-hedgehog activated medulloblastoma	8
1.1.3 Challenges in treating SHH medulloblastoma patients	10
1.2 p53 and SHH medulloblastoma	12
1.2.1 <i>TP53</i> mutations in SHH medulloblastoma	12
1.2.2 p53 deficiency as a “second-hit” in promoting SHH medulloblastoma	15
1.2.3 The aberrant regulators of p53 in SHH medulloblastoma	19
1.3 I2PP2A in SHH medulloblastoma	22
1.3.1 PP2A as a possible MDM2 suppressor	22
1.3.2 The role of oncoprotein I2PP2A/SET in cancers	25
1.3.3 Hypothesis: I2PP2A compromises wildtype p53 in SHH medulloblastoma	28
1.4 Dissertation goals	31
1.4.1 Untangling the tumor heterogeneity of SHH medulloblastoma	31
1.4.2 Investigating the interaction of I2PP2A-p53 in SHH medulloblastoma	32
Chapter 2. Untangling tumor heterogeneity in Sonic Hedgehog medulloblastomas	33
2.1 Introduction	35
2.2 Intra-subgroup heterogeneity of SHH medulloblastoma	37

2.3	Aberrant signaling crosstalk	41
2.4	Epigenetics	49
2.5	Tumor microenvironment	52
2.6	Conclusions	58
Chapter 3. p53 Function is Compromised by Inhibitor 2 of Phosphatase 2A in Sonic Hedgehog Medulloblastoma		60
3.1	Introduction	62
3.2	Materials and Methods	66
3.3	Results	73
3.4	Discussion	94
Chapter 4. Preliminary data of I2PP2A characterization		107
4.1	The oncogenic role of I2PP2A <i>in vivo</i>	107
4.2	I2PP2A and MDM2 during cerebellar development	110
4.3	The possible upstream regulator of I2PP2A protein stabilization	112
4.4	The role of p53 and p-AKT post-irradiation	115
Chapter 5. Summary and Future Directions		117
5.1	Summary	117
5.1.1	Treatment options to target heterozygous SHH medulloblastomas	117
5.1.2	I2PP2A as a possible target in TP53 wildtype SHH medulloblastoma patients	123
5.2	Future directions	125
5.2.1	I2PP2A in SHH medulloblastoma patients	125
5.2.3	Implications of TP53 in radiation therapy for SHH medulloblastoma patients	127

References

List of Figures

Figure 1.1. Pathological histology of medulloblastomas.....	2
Figure 1.2. Consensus on four molecular subgroups of medulloblastoma.	3
Figure 1.3. Postnatal cerebellar development of mice.	9
Figure 1.4. Overall survival curve of SHH and WNT medulloblastomas with wild type or mutant <i>TP53</i>	14
Figure 1.5. Chromothripsis model of SHH medulloblastoma with <i>TP53</i> mutations.....	18
Figure 1.6. Identification and characterization of I2PP2A in SHH medulloblastoma.	27
Figure 1.7. Heterozygous <i>NeuroD2: SmoA1</i> SHH medulloblastoma mouse model.	30
Figure 2.1. Signaling crosstalk in SHH medulloblastoma cells.....	42
Figure 2.2. Various cell populations in the tumor microenvironment (TME) of SHH medulloblastoma.	53
Figure 3.1. p-MDM2S166 is upregulated in Trp53-wildtype SHH-activated medulloblastoma.....	75
Figure 3.2. Inhibitor 2 of Phosphatase 2A is elevated in SHH medulloblastoma.....	79
Figure 3.4. I2PP2A knock-down decreases p-MDM2S166, cell viability and proliferation of SmoA1 tumor cells.....	86
Figure 3.5. I2PP2A knock-down effects on SHH MBCs are dependent on p53.....	89
Figure 3.6. I2PP2A knockdown-mediated loss of viability requires wild-type p53 function in patient-derived medulloblastoma cells.....	92
Figure S3.1. Nutlin-3a treatment caused apoptosis and cell cycle arrest.....	97
Figure S3.2. Whole blots of MDM2 and p-MDM2S166 in SmoA1 tumors.....	99

Figure S3.3. Normalized expression levels of I2PP2A mRNA in medulloblastoma patients showed a small difference between SHH medulloblastoma samples and cerebellar controls.....	100
Figure S3.4. Brief characterization of I2PP2A in SHH medulloblastoma.	101
Figure S3.5. p-MDM2 is regulated by both PP2A and p-Akt.....	103
Figure S3.6. Lentivirus and retrovirus infection on SmoA1 MBCs are successful.	104
Figure S3.7. I2PP2A knockdown affected p53 targets and SHH signaling only in ONS76 cells...	105
Figure 4.1. I2PP2A knockdown delayed tumor progression in an allograft model.	109
Figure 4.2. Expression of I2PP2A protein during postnatal cerebellar development of wildtype pups.....	111
Figure 4.3. Preliminary data of I2PP2A protein stability.	114
Figure 4.4. Reaction of tumor cells to radiation within 24 hours.	116
Figure 5.1. PFS curves for patients divided into (a) three or (b) four risk groups.....	122

List of Tables

Table 1.1. PP2A subunit isoforms and corresponding encoding genes.	24
Table 2.1. Subtypes of SHH medulloblastoma.	40

List of Abbreviations

In alphabetical order

AIF1 -Allograft Inflammatory Factor 1

ANOVA -Analysis of Variance

APC -Adenomatous Polyposis Coli

ATOH1 -Atonal BHLH Transcription Factor 1

ATP -Adenosine triphosphate

BAX -Bcl-2-associated X protein

BBB -Blood Brain Barrier

BCOR -BCL6 co-repressor

BID -BH3 interacting-domain death agonist

BOC -Brother of CDO

BrdU -Bromodeoxyuridine

BTSC -Brain Tumor Stem cells

CB -Cerebellum

CBP -CREB-binding protein

CC3 -Cleaved caspase 3

CDC25 -Cell division cycle 25

CDK6 -Cyclin-dependent kinase 6

CDO -Cysteine Dioxygenase

CGNP -Cerebellar granule neuron precursor

CLL -Chronic Lymphocytic Leukemia

CNS -Central Nervous System

CSF1R -Colony Stimulating Factor 1 Receptor

CTD -C-terminal domain

DDX3X -DEAD-Box Helicase 3 X-Linked

DNA -Deoxyribonucleic acid

EGL -External Granule Layer

EMT -Epithelial-mesenchymal transition

ERK -Extracellular-signal-regulated kinase

FACS -Fluorescence-activated cell sorting

GFAP -Glial fibrillary acidic protein

GFP -Green fluorescent protein

GLI -Glioma-associated oncogene

GPS2 -G Protein Pathway Suppressor 2

GSK3 β -Glycogen synthase kinase 3 beta

GUSB -Glucuronidase Beta

HAT -Histone Acetyltransferase

HDAC -Histone Deacetylase

HE staining -Hematoxylin and eosin stain

HIF1 α -Hypoxia-Inducible factor 1 alpha

HNSCC -Head and neck squamous cell carcinoma

HP1 -Heterochromatin protein 1

HRP -Horseradish peroxidase

ID2 -DNA-binding protein inhibitor 2

IGF1R -Insulin-like growth factor receptor 1

IGF2 -Insulin-like growth factor 2

IgG -Immunoglobulin G

IGL -Internal Granule Layer

IHC -Immunohistochemistry

INHAT -Inhibitor of acetyltransferase

INK4A -Cyclin-dependent kinase inhibitor 2A

IR -Irradiation

KAP1 -KRAB-associated protein-1

KAT2B -Lysine Acetyltransferase 2B

KDM1A -Lysine Demethylase 1A

KIF7 -Kinesin family member 7

LCA -Large Cell/Anaplastic

LDB1 -LIM Domain Binding 1

LFS -Li-Fraumeni Syndrome

LOH -Loss of heterozygosity

LSD1 -Lysine-specific histone demethylase 1A

MAPK -Mitogen-activated protein kinase

MB -Medulloblastoma

MBC -Medulloblastoma cell

MBEN -Medulloblastoma with extensive nodularity

MDM2 -Mouse double minute 2

MLL2 -Myeloid/Lymphoid Or Mixed-Lineage Leukemia 2

MOI -Multiplicity of infection

MRI -Magnetic resonance imaging

mRNA -message ribonucleic acid

MS -Multiple Sclerosis

mTOR -mechanistic target of rapamycin

MTT -3-(4,5-dimethylthiazol-2-yl)-2,5-diphenyltetrazolium bromide

NAP -Nucleosome assembly protein

NCBI -National Center for Biotechnology Information

NHEJ -Non-Homologous End Joining

NME1 -Nonmetastatic marker 1

PCAF -P300/CBP-associated factor

PCNA -Proliferating cell nuclear antigen

PCR -Polymerase chain reaction

PD-1 -Programmed cell death protein 1

PFA -Paraformaldehyde

PFS -Progression-free survival

PI3K -Phosphatidylinositol-4,5-bisphosphate 3-kinase

PIP3 -Phosphatidylinositol (3,4,5)-trisphosphate

PKA -Protein kinase A

PLK2 -Serine/threonine-protein kinase

PNET -Primitive neuroectodermal tumor

PP1 -Protein Phosphatase 1

PP2A -Protein Phosphatase 2A

PP2B -Protein Phosphatase 2B

PPM1D -Protein Phosphatase, Mg²⁺/Mn²⁺ Dependent 1D

PRC1 -Polycomb repressive complex 2

PTCH -Patched

PTEN -Phosphatase and tensin homolog

PVN -Perivascular niche

RAC1 -Ras-related C3 botulinum toxin substrate 1

RB -Retinoblastoma protein

S6RP -S6 ribosomal protein

SCID -Severe combined immune deficiency

SHH -Sonic Hedgehog

shRNA -Short hairpin RNA

SMO -Smoothened

SOX2 -SRY (sex determining region Y)-box 2

SUFU -Suppressor of Fused

TERT -Telomerase reverse transcriptase

TET -Ten-eleven Translocation

TME -Tumor Microenvironment

UV -Ultraviolet

VEGF -Vascular endothelial growth factor

WGS -Whole Genome Sequencing

WHO -World Health Organization

WNT -Wingless

YAP1 -Yes-associated protein 1

ZIC5 -C2H2-type zinc finger protein 5

Chapter 1. Introduction

1.1 Medulloblastoma

1.1.1 Medulloblastoma overview

Medulloblastoma is the most common malignant pediatric brain tumor, accounting for 1.5 cases per million each year in the United States (1, 2). The 5-year overall survival rate has been brought up to ~70% after combination therapy composed of surgery, craniospinal radiation, and chemotherapy (3). However, survivors are beset with lifelong side effects including developmental, neurological, neuroendocrine, and psychosocial deficits. Medulloblastoma was first considered to be among primitive neuroectodermal tumors (PNET) but was later distinguished and histologically characterized as a separate entity by Bailey and Cushing in 1930s (4). The histological subtypes of medulloblastomas include classic, desmoplastic/medulloblastoma with extensive nodularity (MBEN), anaplastic, and large cell, as illustrated in **Figure 1.1** (5). Though medulloblastomas have long been considered as heterozygous diseases with distinct molecular profiles, it was not until the burst of sequencing at the beginning of the 21st century generated the subgrouping of medulloblastomas based on patients' gene expression, and DNA methylation data. Patients classified into the same molecular subgroup share similar clinical features/histology, cytogenetic alterations, demographics within each group, but are quite distinct from patients in the other subgroups. At the 2010 Boston Society for Neuro-oncology meeting, a consensus was reached that medulloblastoma can be molecularly classified into at least four subgroups, namely, WNT, SHH, Group 3 and Group 4 (6-9). As shown in **Figure 1.2**, each molecular subgroup presents with specific cytogenetic aberrations, demographic distribution, local or broad genetic alteration patterns, and clinical features.

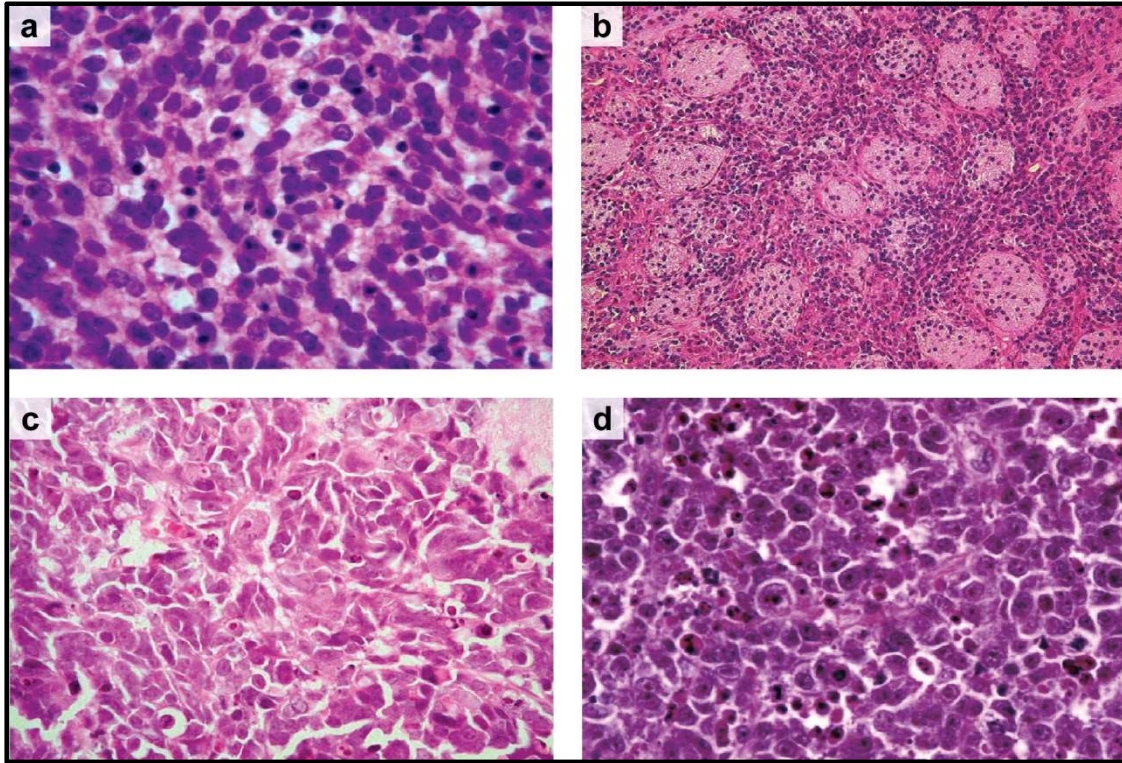

















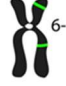
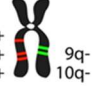
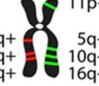
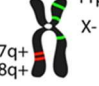
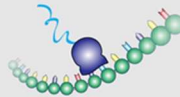


Figure 1.1. Pathological histology of medulloblastomas. Taken from (5) with permission. There are four different histological classes observed by clinicians or pathologists post HE staining, including (a) classic, densely-packed cells with small blue nuclei, (b) desmoplastic/MBEN, with extensive nodules, (c) anaplastic with necrotic areas and disoriented cells, and (d) large cells featured with cells of various sizes.

Molecular Subgroups of Medulloblastoma				
CONSENSUS	WNT	SHH	Group 3	Group 4
Cho (2010)	C6	C3	C1/C5	C2/C4
Northcott (2010)	WNT	SHH	Group C	Group D
Kool (2008)	A	B	E	C/D
Thompson (2006)	B	C, D	E, A	A, C
DEMOGRAPHICS				
Age Group:   	  	   	  	  
Gender: ♀ ♂	♂ : ♀ ♀ ♀	♂ ♂ ♂ : ♀ ♀	♂ ♂ ♂ : ♀	♂ ♂ ♂ : ♀
CLINICAL FEATURES				
Histology	classic, LCA	desmoplastic/nodular, classic, LCA	classic, LCA	classic, LCA
Metastasis	rarely M+	uncommonly M+	very frequently M+	frequently M+
Prognosis	very good	infants good, others intermediate	poor	intermediate
GENETICS				
	 CTNNB1 mutation	 PTCH1/SMO/SUFU mutation GLI2 amplification	 i17q MYC amplification	 i17q CDK6 amplification
GENE EXPRESSION				
	WNT signaling MYC +	SHH signaling MYCN +	Photoreceptor/GABAergic MYC +++	Neuronal/Glutamergic minimal MYC / MYCN

© Taylor MD. *et al.* 2011

Figure 1.2. Consensus on four molecular subgroups of medulloblastoma. Taken from (6) with permission. Four molecular subgroups of medulloblastomas are named WNT, SHH, Group 3 and Group 4 after 2010 Boston Society for Neuro-oncology meeting. These four subgroups show differences in demographics (age groups and sex), clinical features (histology, metastases, prognosis), broad and focal genetic alterations (chromosome loss/gain, gene amplification or deletion, gene mutation).

WNT-activated medulloblastoma

The WNT-activated subgroup accounts for approximately 10% of all medulloblastoma cases and is primarily distributed in children (3-16 years old), with an optimal five-year overall survival >90% (6-8). This subgroup is the most homogeneous with a handful of gene mutations identified, including factors involved in the WNT signaling pathway, such as *CTNNB1*, *APC* and *AXIN* (10-14). *CTNNB1* encodes β -catenin, the major downstream activator of WNT signaling, which enters the nucleus and binds directly to transcriptional factors when induced. Both APC and AXIN are components of the destruction complex which degrades β -catenin when WNT ligand is absent. Germline mutations of *APC* are implicated in Turcot Syndrome, and a subset of these patients are predisposed to colorectal cancers or WNT medulloblastomas (15). Over 90% of WNT-activated medulloblastomas harbor an activating mutation of *CTNNB1*, generating constitutively active β -catenin which accumulates in the nucleus and can be histologically diagnosed by nuclear staining (11). The second most frequently mutated gene in WNT medulloblastomas is *DDX3X*, DEAD-Box Helicase 3 X-Linked, found to be mutated in ~50% of all WNT cases. *DDX3X* encodes for a protein shown to have ATPase activity and which regulates transcription and translation (16). The function of *DDX3X* in WNT medulloblastoma development has not been fully elucidated though it has been suggested that *DDX3X* is required to maintain the differentiation potential of lower rhombic lip progenitors, the proposed cell-of-origin for WNT tumors in mouse models (17). Currently, two mouse models of WNT medulloblastoma have been developed, namely, *Blbp-cre; Ctnnb1^{+/-lox(ex3)}; Trp53^{flx/flx}* and the other with further *Pi3kca^{E545K}* mutation (18). BLBP, brain lipid binding protein, is a molecular marker for radial glia in the developing central nervous system. The activating mutation in *Pi3kca* increases the tumor incidence and shortens the latency period in the *Blbp-cre; Ctnnb1^{+/-lox(ex3)}; Trp53^{flx/flx}* mouse model. According to mouse studies and sequencing data, WNT tumors are proposed to derive from lower rhombic lip/brainstem neuron progenitor cells, unlike the other three medulloblastoma subgroups

(19). As patients in this subgroup present the best prognosis among the four subgroups, currently de-escalation trials (lower dosage of radiation or chemotherapy) with the aim to lessen the treatment burden on patients with WNT medulloblastoma have been proposed.

SHH-activated medulloblastoma

SHH-activated medulloblastoma comprises ~30% of all medulloblastoma cases and shows an average 5-year overall survival of ~70% (6-8). This subgroup has a bimodal curve in age distribution, predominantly infant (<3 years old) and adult cases (>16 years old). Patient samples of this subgroup are histologically heterogeneous, containing classic, desmoplastic, large cell/anaplastic (LCA) morphology. As its name indicates, SHH medulloblastoma has alterations of genes implicated in the Sonic Hedgehog pathway, including amplifications in *MYCN*, *GLI*, *YAP1*, and mutations in *PTCH*, *SMO*, *SUFU* (20-26). Some patients with Gorlin syndrome, harboring germline mutations of *PTCH*, are predisposed to SHH medulloblastomas (27, 28). SHH medulloblastoma are proposed to originate from cerebellar granule neuron precursor cells of the external granule layer (EGL) in developing cerebellum (29-31). Multiple mouse models exist for SHH medulloblastoma studies, among them are *PTCH*^{+/-} and *SmoA1* mouse models, which have altered SHH signaling components that confer constitutively activated mitogenic signals in a tissue-specific manner (18). Targeted therapy, Smoothed inhibitors, has been tested in clinical trials to treat SHH medulloblastoma patients, but resistance occurs in most of these patients (32, 33). Further introduction of SHH medulloblastoma can be found in 1.1.2, and heterogeneity of this subgroup is further discussed in Chapter 2.

Group 3 and Group 4 medulloblastoma

The World Health Organization (WHO) published classification of CNS tumors in 2016, integrating the molecular findings into their stratification system for the first time (34). Group 3 and Group 4 tumors are named as non-WNT/SHH tumors due to the lack of well-established driver mutations in

these two subgroups (16). These two subgroups have distinct gene expression and DNA methylation profiles as compared to WNT or SHH activated medulloblastomas. Epigenetic changes in Group 3 and Group 4 tumors are predominant, including aberrantly modified histones, which alter chromatin compaction for transcriptional regulation. Frequently mutated genes identified in these two subgroups belong to chromatin modifiers or transcription regulators such as *MYC*, *KDM6A*, *MLL2* and *MLL3* (16). These genetic mutations alter the histone or DNA modification landscape, thus regulating gene expression by controlling the availability of the genome to transcription factors. Recent research has indicated that alterations in intergenic regions of the genome could also participate in regulating critical unidentified oncogenes or tumor suppressors in these two groups. For example, structural variants at chromosome 9q34.13 pose proto-oncogenes *GFI1* and *GFI1B* in proximity (hundreds of kilobases) with the gene *DDX31*, rendering the expression of these two oncogenes under the control of an active enhancer that facilitates *DDX31* overexpression in Group 3 and Group 4 medulloblastomas (35).

Patient samples from these two subgroups differ regarding the DNA methylation patterns, gene expression profiles, and clinical features. Group 3 patients have only ~50% 5-year overall survival and have the most abundant anaplastic histology, which has long been considered a poor prognostic marker for “high-risk” medulloblastoma patients (3). Even worse, group 3 tumors show frequent metastases including leptomeningeal spread and systemic metastasis at diagnosis or post-treatment (6). The combination of a *Myc* mutation and *Trp53* deficiency generated a mouse model that represents group 3 medulloblastomas, but the fidelity remains questionable as *TP53* mutations are rarely observed in group 3 tumors (18, 36, 37). Group 4 patients account for the largest class of medulloblastoma patients, corresponding to two in five medulloblastoma cases (16). The prognosis of group 4 tumors is intermediate, likely due to the neuronal differentiation signatures possessed by this subgroup tumors(16). Currently, no mouse model has been developed for this subgroup. The lack of known

oncogenic drivers poses challenges in devising effective targeted therapies for patients classified into these two molecular groups.

1.1.2 Sonic-hedgehog activated medulloblastoma

Since the *Patched* heterozygous mouse model was developed in the 1990s, Sonic Hedgehog signaling in cerebellar development and medulloblastoma has been extensively studied and well-established (38). SHH medulloblastomas are proposed to derive from cerebellar granule neuron precursors (CGNPs) of the external granule layer (EGL) during early cerebellar development (39, 40). As depicted in **Figure 1.3**, the EGL consists of rapidly dividing CGNPs in the early postnatal days of mice. Sonic Hedgehog, a cholesterol-modified protein primarily secreted by Purkinje cells from the Molecule Layer (MOL) promotes the proliferation of these CGNPs through a diffused SHH gradient (41). These cells exit the cell cycle and migrate inward to form the internal granule layer (IGL), the location with the most abundant neurons. Though Sonic Hedgehog is still present after postnatal day 15 of mice, the EGL has been depleted, and granule neurons stop proliferating in the matured mouse cerebellum.

The Sonic Hedgehog signaling pathway was first illustrated in *Drosophila melanogaster* and later proved to be conserved in vertebrates (42, 43). Upon binding of SHH, Patched, a twelve-transmembrane protein is released from inhibiting Smoothed, the activation of which induces the transcriptional activity of GLI proteins. GLI proteins transactivate downstream gene expression including CDKs (Cyclin-dependent kinases), and Cyclins, which are involved in regulating the cell cycle. The mitogenic and morphogenic SHH signaling is finely regulated and coordinated during embryonic development in a timely manner, which decides the intricate foliation, structure, and patterning of the adult cerebellum. The aberration of SHH signaling in early cerebellum development is proposed to cause SHH medulloblastomas. SHH medulloblastoma will be the focus of the work presented in the dissertation, and a more detailed SHH signaling pathway can be found in Chapter 2 and **Figure 2.1**.

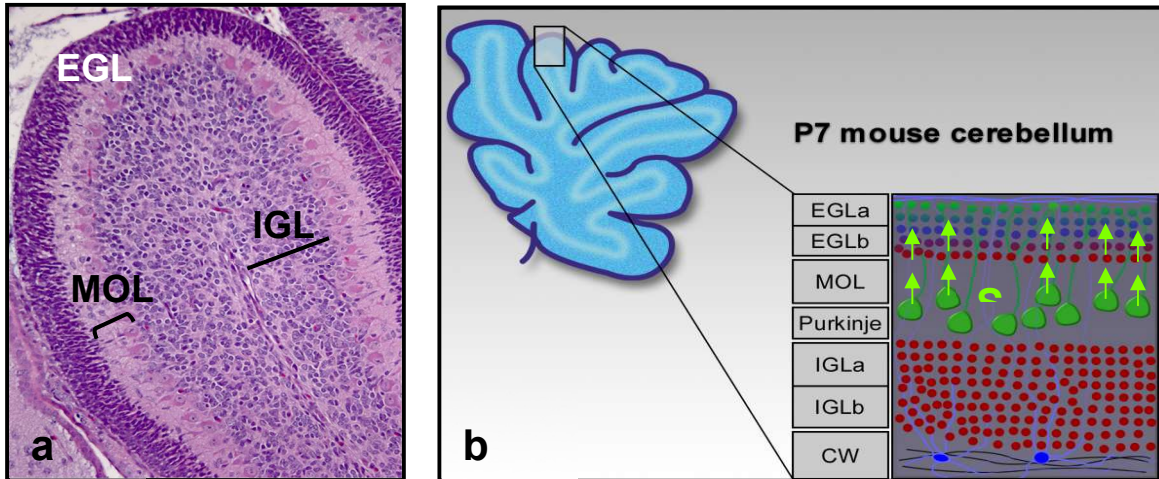


Figure 1.3. Postnatal cerebellar development of mice. Adapted from (39) with permission. **a**, HE staining of postnatal day 7 of wildtype cerebellum folium. EGL, the external granular layer where cerebellar granule neuron precursor cells reside. MOL, molecular layer where Purkinje cells, Bergmann glial cells reside. IGL, internal granule layer composed of non-dividing cells derived from EGL. **b**, schematic view of how SHH signaling impacts the EGL during early cerebellar development. Arrowheads indicate the diffusion of Sonic Hedgehog molecules.

1.1.3 Challenges in treating SHH medulloblastoma patients

The cure rate of medulloblastoma has come to a plateau over the past decade, not yet integrating the molecular subgrouping of medulloblastoma into the stratification system or treatment protocols (8). Even within SHH medulloblastomas, intra-subgroup heterogeneity might contribute to treatment failures in subsets of SHH patients, which will be further discussed in Chapter 2. Challenges in treating these patients include the inadequacy of treating molecularly “high-risk” patients, over-treatment of patients with optimal prognosis, and the same treatment protocol for adult medulloblastoma patients which are considerably different from infant and pediatric age groups (3).

Targeted therapy such as the Smoothed inhibitor vismodegib has been tested to treat SHH medulloblastoma patients (44, 45). However, patients in clinical trials developed resistance to vismodegib by gaining novel mutations in Smoothed which reduces the binding affinity of the mutated protein to the drug (33). Moreover, other problems occur including bone toxicity in younger patients, and primary resistance because a high percentage of SHH medulloblastoma patients harbor alterations such as *MYCN/GLI2* amplification or *SUFU* mutations, which are downstream of *Smoothed*, as indicated by **Figure 2.1** (32, 46). As PI3K/AKT signaling pathway activation was observed in a subset of SHH medulloblastoma patients, the combination therapy of targeting PI3K and Smoothed inhibitor has been proposed and showed promising synergy in SHH medulloblastoma mouse models (47). The WHO classification in 2016 also takes the *TP53* mutational status into account, considering the critical prognosis value of *TP53* mutation for SHH subgroup (34). However, except for the relatively higher *PTCH* mutation rate (~20% of all SHH MBs), the mutation rate of any single gene is low, making it challenging to find a “one-for-all” target for SHH medulloblastoma patients. Though *MYC* family proteins are highly expressed in medulloblastoma cases across all four subgroups, no effective *MYC*/*MYCN* inhibitor or antagonists have been utilized in current targeted therapy.

The intra-subgroup heterogeneity of SHH medulloblastoma urges better understanding of molecular profiles and cellular components of this subgroup tumors to deal with challenges mentioned above. Though not as frequent as in Group 3 and Group 4 tumors, SHH medulloblastoma tumors also present epigenetic changes which may provide clues for future novel therapeutic strategies. For example, HDAC (histone deacetylase) inhibitors have been proposed to treat medulloblastomas and showed efficacy in reducing tumor growth in mouse xenografts with patient-derived SHH medulloblastoma cells (48). As a CNS tumor, the SHH medulloblastoma was firstly considered immune-privileged, but now with accumulating evidence that immune cells like macrophages and microglia can be found in the tumor microenvironment. As the precision medicine era develops, molecular profiles of patients will be readily collected and assessed, which may benefit individual patients with a more tailored therapeutic strategy. Additionally, understanding the tumor microenvironment could arm us with better knowledge in drug delivery and efficacy prediction.

1.2 p53 and SHH medulloblastoma

1.2.1 *TP53* mutations in SHH medulloblastoma

Medulloblastomas are occasionally seen in patients of Li-Fraumeni Syndrome (LFS), who harbor germline *TP53* mutations (28). However, early detection of *TP53* mutations in medulloblastoma patients was not frequent due to the limited number of patients available (49, 50). One report of eight patient samples identified one *TP53* mutation and no amplification of *MDM2*, which encodes the central negative regulator of *p53* and is found to be overexpressed in other solid tumors (49). The discovery of *TP53* as a tumor suppressor gene is also very interesting; p53 was found to accumulate in the progressive tumors associated with poorer prognosis and thus was considered as oncogenic until researchers detected mutations of this gene in these tumors (51). Under normal conditions, p53 has a very short half-life in mammalian cells, as it is degraded by proteasomes within an hour after production. However, mutant p53 could not be recognized by its antagonist MDM2 for subsequent proteolysis, and thus these non-degradable p53 proteins accumulate in cancer cells. The positive staining of p53 in clinical samples was utilized in pathology as a marker of mutant p53.

As studies in medulloblastoma accumulated, conclusions about the prognosis of *TP53* mutations were controversial. Some researchers found that patients with mutant *TP53* and metastases had a poorer prognosis; others indicated p53 mutations were associated with better survival in WNT subgroup tumors (52-56). Hill *et al.* showed that *MYCN* amplification and *TP53* mutations together were frequently found in recurrent tumors and predicted a poor prognosis (57). It was not until 2013, Zhukov *et al.* combined two different large cohort studies of patient samples and showed that *TP53* mutations exclusively occurred in WNT (~15%) and SHH (~21%) subgroups. Moreover, the prognostic value of *TP53* mutation was subgroup-dependent (**Figure 1.4**). No difference in 5-year overall survival or progression-free survival was observed in WNT medulloblastoma patients with either wildtype or mutant *TP53*. In contrast, SHH patients with wildtype *TP53* showed a much better

5-year overall survival (~80%) than SHH patients with mutant *TP53* (~40%) (58). The authors of this paper also proposed different treatment strategies should be used to treat SHH medulloblastoma with either wildtype or mutant *TP53*. The WHO classified SHH medulloblastomas into SHH *TP53-wildtype* and SHH *TP53-mutant* subgroups based on these studies (34).

In contrast to the controversial results from patient medulloblastoma studies, p53 has long been considered as a critical tumor suppressor in SHH medulloblastoma mouse models. For example, in the first-ever SHH medulloblastoma mouse model, *Ptc1* heterozygous mice, the homozygous loss of p53 brought the tumor incidence from ~15% to over 90% and shortened the latency period by facilitating tumor growth (18, 59). Additionally, the deficiency in the DNA repair machinery was mimicked in *Lig4^{+/-}p53^{-/-}* mice, which also developed medulloblastomas that resembled SHH medulloblastomas (60, 61). DNA ligase 4 (*Lig4*) is a protein heavily involved in non-homologous end joining, employed primarily by mammalian somatic cells to repair DNA damages. The deficiency in DNA ligase 4 and p53 leads to error-prone DNA replications during cell divisions, causing genome instability. The cerebellum was proposed to be the organ that is susceptible to these changes, and thus medulloblastomas were seen in these *Lig4^{+/-}p53^{-/-}* mice. SHH downstream targets such as *Atob1*, *Gli1* were found to be overexpressed in these tumors, suggesting SHH-subgroup affiliation of these tumors.

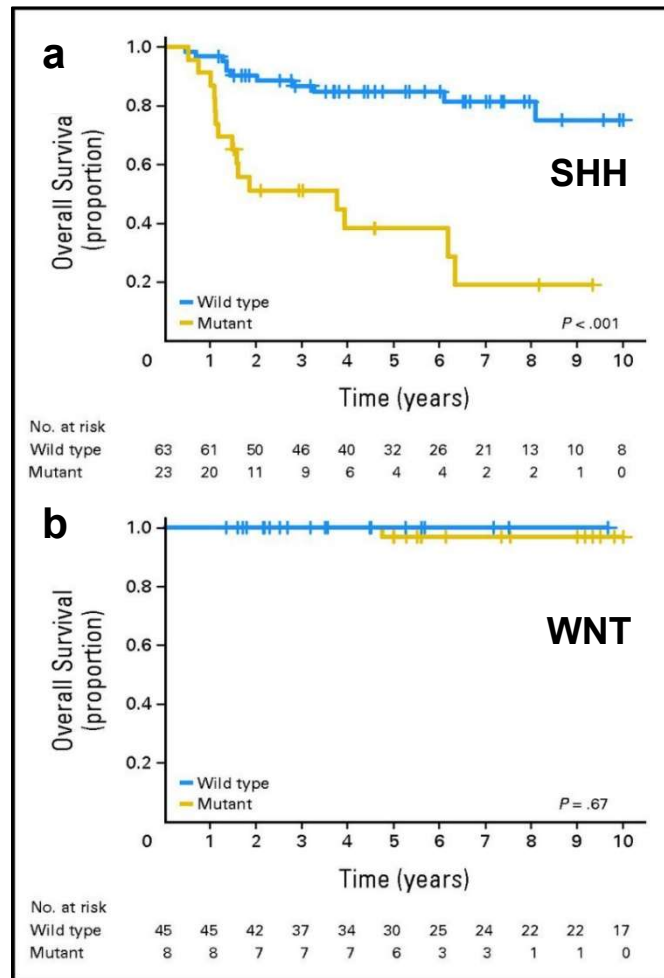


Figure 1.4. Overall survival curve of SHH and WNT medulloblastomas with wild type or mutant *TP53*. Taken from (58) with permission. **a**, 5-year overall survival of SHH medulloblastoma patients with wildtype or mutant *TP53* is ~80% and ~40% respectively, and the survival rates in these two groups are statistically different, $p < 0.001$. **b**, 5-year overall survival of WNT medulloblastoma patients with wildtype or mutant *TP53* is ~100% and ~90% respectively, $p = 0.67$. Patient numbers are indicated below the graphs.

1.2.2 p53 deficiency as a “second-hit” in promoting SHH medulloblastoma

Though it is now acknowledged that *TP53* loss-of-function mutations are associated with lower rates of survival in SHH medulloblastoma patients, an understanding of how p53 deficiency contributes to medulloblastoma development remains elusive. Some proposed mechanisms based on the investigation of mouse models and patient genomics and chromosome aberrations suggest that p53 deficiency might serve as a “second-hit” for medulloblastoma progression in addition to the first-step event of SHH signaling activation. These studies provide insights into possible mechanisms mediated by p53 as a tumor suppressor during SHH medulloblastoma development which will be further discussed below.

A senescence evasion model was proposed by Tamayo-Orrego *et al.* in 2016 showing that in *Ptch*^{+/-} heterozygous mouse model, *Trp53* mutations or *p16*^{ink4a} low-expression is mutually exclusive and facilitates malignancy by empowering “preneoplastic” cells to evade senescence check (62, 63). Their studies were built on analyzing preneoplastic lesions of *Ptch*^{+/-} mice at 3-4 weeks after birth. In *Ptch*^{+/-} mice, only ~16% of mice develop medulloblastomas at 3-6 months after birth, whereas the majority of these mice show ectopic cells (densely-packed cells with a relatively higher nuclei: cytosol ratio) on the surface of their cerebellum 3-4 weeks after birth, not seen in normal cerebellar development at this stage (38, 64, 65). Oliver *et al.* and Kessler *et al.* from the Wechsler-Reya group characterized these ectopic cells and named them as “preneoplastic cells” (29, 66). They discovered that over 90% of *Ptch*^{+/-} mice showed loss of heterozygosity (LOH) in the *Ptch* allele 3-4 weeks after birth, indicating most of these mice completely lose Patched expression and therefore have Shh signaling activation at an early stage. However, only a small portion of these mice developed tumors, indicating there must be a “second-hit” required in addition to SHH signaling activation. Kessler *et al.* proposed that *MYCN* could serve as a “second-hit” as preneoplastic cells isolated from *Ptch*^{+/-} with additional *Nmyc* overexpression could lead to a 100% tumor incidence in SCID mice, as compared to ~30% tumor

incidence in mice transplanted with preneoplastic cells infected with empty vector. Tamayo-Orrego *et al.* also analyzed the preneoplastic lesions at an earlier stage, postnatal day 14 mice, and observed aberrantly upregulated senescence markers such as p21 and p16^{ink4a} proteins in these cells as compared to both postnatal day-7 EGL and advanced tumors of *Ptch*^{+/-} mice (62, 63). As senescence could be overcome by the loss of the tumor suppressor gene *Trp53*, the authors further checked *Trp53* status in these advanced *Ptch*^{+/-} tumors as compared to preneoplastic cells. They observed *Trp53* somatic mutations in 36% (7/19) of advanced tumors, and a further 60% (6/10) of tumors with low p16^{ink4a} expression in medulloblastomas without *Trp53* mutations, the alterations of which were not found in preneoplastic lesions. As *TP53* mutations have been found in ~20% of SHH medulloblastoma patients, they analyzed p16^{ink4a} status in patient samples and observed point mutations, as well as hypermethylation of regulatory regions of the *CDKN2A* gene in a subset of SHH patients. In cancer studies, mice seem to require fewer mutation events to develop advanced tumors, sometimes mutations in two genes cause progressive tumors, which were frequently seen in mouse models for SHH medulloblastomas (36, 59, 61). In contrast, there exists a higher mutational load in patients than mouse tumor models, with an average of 5.7 non-synonymous SNVs in SHH medulloblastoma patients (67). Still, these investigations of SHH mouse models provide clues that additional events other than *Shh* signaling activation are critical for eventual malignancy of SHH medulloblastomas.

The whole-genome-sequencing (WGS) of SHH medulloblastoma patients with the *TP53* loss (Li-Fraumeni Syndrome) also suggested a “chromothripsis” mechanism mediated by *TP53* loss in these patients (68). Chromothripsis means a catastrophic event of drastic chromosome rearrangements at one point during tumor development. Rausch *et al.* first performed and analyzed the WGS data of one LFS SHH medulloblastoma patient, and observed a relatively higher SNV(single nucleotide variant) number, 24 as compared to the average 5.7 nonsynonymous SNVs found in sporadic pediatric medulloblastoma exome sequencing data (67). They observed complex chromosome rearrangements

in this specific LFS SHH medulloblastoma patient, including amplification of specific chromosome segments, interchromosomal rearrangements, and double-minute chromosomes (extrachromosomal DNA). When they checked the DNA copy number profiling of 98 patient samples irrespective of their subgroup affiliations, 13 out of 98 patients showed chromosome rearrangements consistent with chromothripsis, and 11 out of 13 belonged to SHH medulloblastomas. Of these 11 patients, 10 harbored mutant *TP53*, 5 of which were germline mutations, the other 5 were somatic mutations. Among these 10 patients, they further performed WGS on three additional LFS SHH medulloblastoma patients and obtained similar results that chromosome rearrangements were more frequent in these tumors as compared to SHH tumors without *TP53* mutations. Furthermore, oncogenes such as *GLI2*, *MYCN*, and *BOC* amplifications involved in SHH signaling pathway were found to be enriched due to chromosome rearrangements. The authors also did computational simulations which indicated that a progressive rearrangement model was unlikely by analyzing all four LFS SHH medulloblastoma patients, and thus proposed the chromothripsis model during SHH medulloblastoma with mutant *TP53* development (**Figure 1.5**). They also observed this chromothripsis phenomenon in *Ptc1*^{+/-} mice, which develop SHH medulloblastomas with *Trp53* mutations as described earlier. All these studies suggest that *TP53* mutations might serve as a “second-hit” for SHH medulloblastoma patients, where the genomic instability such as chromosome rearrangements caused by *TP53* deficiency enable tumor cells to evade senescence or apoptosis as a critical step for final malignancy.

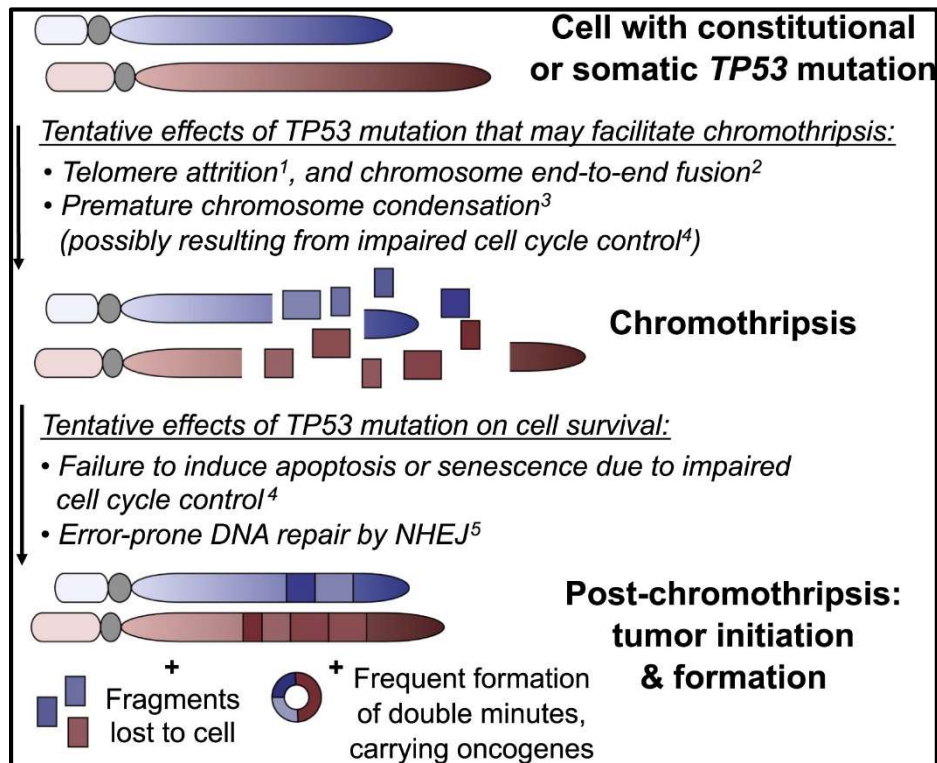


Figure 1.5. Chromothripsis model of SHH medulloblastoma with *TP53* mutations. Taken from (68) with permission. A three-step model of tumorigenesis mediated by *TP53* mutation induced chromothripsis. Step one, cells with constitutional or somatic *TP53* mutation may cause defects in cell cycle control. Chromothripsis happen and further promote error-prone DNA repair by NHEJ. The chromothripsis caused amplification of oncogenes or deletion of tumor suppressor genes could further contribute to tumor initiation and formation.

1.2.3 The aberrant regulators of p53 in SHH medulloblastoma

Utilizing mouse models, researchers have demonstrated the critical role of functional p53 in keeping SHH medulloblastoma cells in check against malignancy. However, the mutation rate of *TP53* in medulloblastoma overall is very low, with the highest percentage of ~20% in the SHH medulloblastoma subgroup. Scientists have questioned whether abnormalities in negative regulators of p53 exist in SHH medulloblastoma or other subgroups. Investigations of WIP1 (wildtype p53 induced phosphatase 1) and MDM2 (mouse double minute 2) shed light on the possible mechanisms of wildtype TP53 dysregulation in SHH medulloblastomas. As its name indicates, WIP1 is a phosphatase which can be induced only by wildtype p53. WIP1 dephosphorylates p53 at Ser15 and promotes its further degradation by MDM2 (69, 70). MDM2 is an E3 ubiquitin ligase which adds ubiquitin and facilitates wildtype p53 degradation by the proteasome (71).

WIP1 amplifications were first observed by Castellino *et al.* by analyzing the expression of *WIP1* in 33 medulloblastomas (72). Of these 33 medulloblastomas, 16 of them showed chromosome 17q gain, which was shown to be associated with overexpression of *WIP1* in other tumors, considering that the *WIP1* gene is at chromosome locus 17q22-q23. Importantly, these *WIP1* amplifications were not only found in patient samples with 17q gain but also in medulloblastomas without 17q chromosome aberration, indicating the possible inhibition of wildtype p53 mediated by upregulated WIP1 protein. Furthermore, they observed a negative correlation between *WIP1* expression and phosphorylated/total p53 level in these patient medulloblastoma samples. When they overexpressed *WIP1* in patient-derived medulloblastoma cell lines and exposed these cells to UV light, they observed that cells with *WIP1* overexpression showed a much lower p53 induction. Doucette *et al.* further extended this research and showed that *WIP1* overexpression could accelerate tumor formation when combined with SHH signaling using *RCAS-tna* system, where they induced overexpression of both *WIP1* and *Sonic Hedgehog* by adding RCAS avian virus which targets the TVA receptor specifically

expressed in early cerebellar development (73). The overexpressed *WIP1*, together with SHH signaling activation, in granule neuron progenitors, significantly increased tumor incidence as compared to that in *Sbb*-overexpression only group. Of note, *WIP1* overexpression was more frequently seen in Group 3 and Group 4 medulloblastomas as compared to WNT or SHH subgroup. Importantly, Group 3 and Group 4 tumors display a lower frequency of *TP53* mutation, indicating *WIP1* overexpression is dominant in these subgroups and may serve to compromise wildtype p53 function.

Like the results from *Lig4^{+/-}p53^{-/-}* mouse studies where researchers proposed that cerebellum is the organ most susceptible to genome instability caused by DNA damage repair deficiency (60, 61), Malek *et al.* observed that lower expression of the *Mdm2* gene in mice caused a significant shrinkage in cerebellum size but not in total body weight or other organs, indicating the more dominant role of the MDM2-p53 interaction in cerebellar development as opposed to their roles in growth of other organs (74). In 1994, Adesina *et al.* observed one *TP53* mutation and no *MDM2* amplifications in eight medulloblastoma samples they analyzed, thus concluding that *TP53* mutation or *MDM2* amplification was not frequent in medulloblastomas. Since then, quite limited research has been focused on MDM2 in medulloblastomas. However, investigations in other systems might provide insights into the interaction between MDM2 and SHH signaling. For example, utilizing MEFs, researchers have shown that SHH signaling suppresses p53 function by activating MDM2 (75). The authors demonstrated that actively-mutated *Smoothened* suppressed the stability of p53 proteins. Furthermore, they observed higher p-MDM2 at Ser166 and Ser186 with mutant *Smoothened* overexpression, correlated with more ubiquitinated p53 and lower p53 levels. Phosphorylation of MDM2 at Serine residues 166 and 186 was previously shown to be an activating modification of MDM2 in facilitating p53's degradation (76). Though amplification of *MDM2* has not been reported in medulloblastomas, researchers have shown that Nutlin-3a, a potent pharmacological suppressor of MDM2 which functions by disrupting the binding between MDM2 and p53 could induce cell death in patient-derived medulloblastoma cell lines,

including SHH medulloblastoma cell lines Daoy and ONS76 (77, 78). More importantly, it has been demonstrated that Nutlin-3a displayed significantly better toxic effects on patient-derived medulloblastoma cell lines with wildtype *TP53*, including ONS76, as compared to that in cell lines with mutant *TP53*. Though *MDM2* amplifications are not frequently seen in SHH medulloblastomas, aberrantly activated MDM2 such as upregulated p-MDM2^{S166/S186} might contribute to the compromising of TP53 function in these tumors, notably when we observed quantitative cellular death caused by the MDM2 inhibitor Nutlin-3a.

1.3 I2PP2A in SHH medulloblastoma

1.3.1 PP2A as a possible MDM2 suppressor

Protein phosphatase 2A (PP2A) is among the major serine/threonine phosphatases in mammalian cells. PP2A is a heterotrimer enzyme composed of structural A (support both B and C), regulatory B (define substrate specificity), and catalytic C (perform dephosphorylation activity) subunits. As reviewed by Wlodarchak and Xing, PP2A holoenzyme is suggested or confirmed to dephosphorylate ~300 protein substrates and play essential roles in negatively controlling cell cycles, thus proposed to be a tumor suppressor in various cancers (79). Both A and C have two separate isoforms, named as α or β . The C subunit needs first to be “primed” and activated to bind to A, which allows for further docking of B subunit to play its full dephosphorylation function. The versatile function of PP2A is primarily mediated through the four families of the regulatory B subunits, including B, B', B'', and B'''. In each family, different isoforms with sequence homology exist to contribute further to the diversity of B subunits, enabling PP2A to recognize various substrates specifically. After the assembly of all three PP2A subunits, it can dephosphorylate protein substrates by removing the phosphorylation on either serine or threonine residues. Although there are large numbers of PP2A holoenzymes that can form with different subunit isoforms, the genes encoding them are quite limited, as summarized in **Table 1.1**.

Although PP2A has been proven to positively regulate proliferation through some signaling pathways, most of the dephosphorylation events mediated by PP2A are suppressing cell proliferation or growth (79). For example, PP2A negatively regulates PI3K/AKT/mTOR signals, which have been demonstrated to promote cancer cell survival and facilitate protein synthesis needed for rapid cell growth. PP2A also dephosphorylates critical factors involved in cell cycle, such as the checkpoint protein Rb, DNA replication initiation complex component CDC6, as well as WEE1 and CDC25, the dephosphorylation of which will prevent cells from entering mitosis. In addition to negatively

regulating cell proliferation, PP2A has been shown to be involved in cell migration or other cellular activities. PP2A can dephosphorylate ERK, the effector of MAPK pathway, and PAK, which are downstream of Rho-GTPase to regulate cytoskeleton dynamics during cell migration (79, 80). Importantly, MDM2 Ser166 phosphorylation mentioned previously could be removed by PP2A in a study performed by Okamoto *et al.*, suggesting that PP2A might be a negative regulator of MDM2 function in suppressing p53 in SHH medulloblastomas (81).

According to the R2: Genomics Analysis and Visualization Platform (r2.amc.nl), which facilitates aggregation of medulloblastoma patient samples genomic and transcriptomic data, no mutations of any listed PP2A subunit gene (**Table 1.1**) have been reported, although expression levels of some subunit genes were different between subgroups. Mainwaring and Kenney showed that PP2A B' γ subunit could be upregulated by SHH signaling in primary cerebellar granule neuron precursors (CGNPs), the putative cell-of-origin for SHH medulloblastoma (82). However, as it has proven challenging to target a tumor suppressor like PP2A, it would be interesting to study its endogenous inhibitors in the context of SHH medulloblastomas, which might serve as a potential therapeutic target for SHH medulloblastomas. As further discussed in Chapter 3, we analyzed three endogenous inhibitors of PP2A, namely I1PP2A (Inhibitor 1 of PP2A), I2PP2A (Inhibitor 2 of PP2A), and CIP2A (Cancerous Inhibitor of PP2A), and observed statistically significant upregulated I2PP2A protein in SHH medulloblastomas based on transgenic mouse studies.

Table 1.1. PP2A subunit isoforms and corresponding encoding genes.

Function	Gene	Protein	Note
Structural subunit A	<i>PPP2R1A</i>	PP2A 65kDa regulatory subunit A α isoform	subunit A, PR65- α isoform
	<i>PPP2R1B</i>	PP2A 65kDa regulatory subunit A β isoform	subunit A, PR65- β isoform
Regulatory subunit B	<i>PPP2R2A</i>	PP2A 55kDa regulatory subunit B α isoform	subunit B, B- α isoform
	<i>PPP2R2B</i>	PP2A 55kDa regulatory subunit B β isoform	subunit B, B- β isoform
	<i>PPP2R2C</i>	PP2A 55kDa regulatory subunit B γ isoform	subunit B, B- γ isoform
	<i>PPP2R2D</i>	PP2A 55kDa regulatory subunit B δ isoform	subunit B, B- δ isoform
	<i>PPP2R3A</i>	PP2A 72/130 kDa regulatory subunit B	subunit B, B''-PR72/PR130
	<i>PPP2R3B</i>	PP2A 48kDa regulatory subunit B	subunit B, B''-PR48 isoform
	<i>PPP2R3C</i>	PP2A regulatory subunit B'' subunit γ	Subunit B, B''-G5PR
	<i>PPP2R4</i>	PP2A regulatory subunit B'	subunit B', PR53 isoform
	<i>PPP2R5A</i>	PP2A 56kDa regulatory subunit α isoform	subunit B, B' α isoform
	<i>PPP2R5B</i>	PP2A 56kDa regulatory subunit β isoform	subunit B, B' β isoform
	<i>PPP2R5C</i>	PP2A 56kDa regulatory subunit γ isoform	subunit B, B' γ isoform
	<i>PPP2R5D</i>	PP2A 56kDa regulatory subunit δ isoform	subunit B, B' δ isoform
	<i>PPP2R5E</i>	PP2A 56kDa regulatory subunit ϵ isoform	subunit B, B' ϵ isoform
	<i>PPP2R6A</i>	Striatin 1, PP2A regulatory B	subunit B, B''' α isoform
	<i>PPP2R6B</i>	Striatin 3, PP2A regulatory B	subunit B, B''' β isoform
	<i>PPP2R6C</i>	Striatin 4, PP2A regulatory B	subunit B, B''' γ isoform
Catalytic subunit C	<i>PPP2CA</i>	PP2A catalytic subunit α isoform	subunit C, α isoform
	<i>PPP2CB</i>	PP2A catalytic subunit β isoform	subunit C, β isoform

1.3.2 The role of oncoprotein I2PP2A/SET in cancers

I2PP2A, also known as SET, is an endogenous inhibitor of PP2A, has been recently found to be upregulated or amplified in various tumors, including B cell chronic lymphocytic leukemia (CLL), head and neck squamous cell carcinoma (HNSCC), and prostate cancers (83-85). I2PP2A was first identified in acute undifferentiated leukemia, where the *SET-CAN* fused gene was shown to promote overexpression of *CAN*, encoding NVP214, a nuclear pore complex protein (86). Preliminary data showed upregulated I2PP2A protein but not mRNA levels in tumors from *NeuroD2: SmoA1* mouse models (data in Chapter 3), which is a SHH medulloblastoma mouse model that recapitulates patient SHH medulloblastoma in histology and expression profiles (87, 88).

As illustrated in **Figure 1.6**, I2PP2A is a 39kDa protein with a serine-rich N terminus, acidic C terminus, and central nucleosome assembly protein (NAP) region. According to I2PP2A investigations in mammalian cell lines, serine residues at the N terminus can be phosphorylated, and the phosphorylated N terminus has been shown to get involved in the cellular localization and the stabilization of I2PP2A in mammalian cells (89). Residues ¹⁶⁸KRSSQTQNKASRKR¹⁸¹ within the NAP region have been designated as the nuclear localization signal sequence (90). The acidic C terminus of I2PP2A has been demonstrated to be critical in its binding affinity with other proteins such as PP2A, Rac1 and NME1(89). I2PP2A has multiple isoforms in mouse and human cells, but the most abundant versions are isoform 1 and isoform 2, which share >90% homology and are also the isoforms we detected and focused on for our research.

I2PP2A/SET has been demonstrated to be a multifunctional protein located both in the nucleus and the cytoplasm. I2PP2A is a very potent and selective PP2A suppressor, with an EC₅₀ of 2nM, which does not affect other serine/threonine phosphatases like PP1 or PP2B (91). Other researchers have demonstrated that both full-length and truncated forms with either N-terminal or C-terminal can

suppress PP2A at nanomolar levels (92, 93). I2PP2A performs its function primarily through suppressing PP2A. For example, I2PP2A cooperates with PP2A temporally to regulate oocyte meiosis (94). In meiosis I, PP2A dephosphorylates Rec8, a component of the Cohesin complex, to protect the sister chromatid from separation; whereas in meiosis II, I2PP2A suppresses PP2A function, when sister chromatids can be successfully separated. Secondly, cytoplasmic accumulation of I2PP2A was shown in Alzheimer's disease to suppress PP2A and thus lead to hyperphosphorylation of Tau proteins (92, 93). Furthermore, I2PP2A trans-localized to the plasma membrane can suppress PP2A's function on RAC1, which maintains the activity of RAC1-MAPK signaling in mediating cell migration. PP2A also dephosphorylates RB protein and CDKs during the cell cycle, whereas I2PP2A might suppress PP2A to switch off the function of these proteins (95, 96).

In addition to suppressing PP2A, I2PP2A can also function in a PP2A-independent manner. Fan *et al.* showed that I2PP2A could be cleaved by Granzyme A and released from NME1 (non-metastatic marker 1), which can induce cellular death of target cells, suggesting the possible role of I2PP2A in inhibiting cell death caused by cytotoxic T-cells (97). NME1 is a DNA exonuclease and can enter the nucleus and cause DNA damages and subsequent caspase-independent cellular death once released from I2PP2A. I2PP2A, in a complex called Inhibitor of Histone Acetylase (INHAT) also containing I1PP2A, was shown to inhibit histone acetylation by directly binding and masking histone tails, which are otherwise exposed to p300/CBP acetyltransferases for subsequent transcriptional activation (98). In another report, I2PP2A can destabilize the genome by retaining KAP1 and HP1 at the DNA damage site, which compacts the chromatin and prevents DNA damage repair or homologous recombination from happening correctly (99).

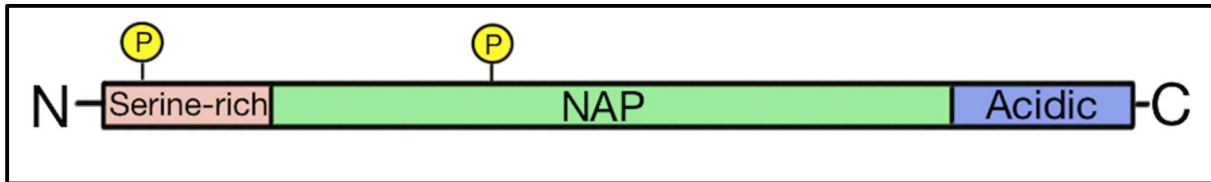


Figure 1.6. Identification and characterization of I2PP2A in SHH medulloblastoma. schematic view of I2PP2A protein, which contains a serine-rich N terminal, an acidic C terminal, and NAP (nucleosome assembly protein) homology region. Phosphorylation at Ser9 or Ser45 were putative modifications that activate I2PP2A's function in suppressing PP2A (100).

1.3.3 Hypothesis: I2PP2A compromises wildtype p53 in SHH medulloblastoma

As I2PP2A shows multiple roles in mammalian cells, the dysregulation of I2PP2A in SHH medulloblastoma might contribute to tumor initiation or progression in many ways. However, as p53 function has been demonstrated to play critical roles in this specific tumor, we were intrigued to ask if the upregulated I2PP2A protein compromises p53 function by suppressing PP2A. Though not previously tested in medulloblastoma cells, PP2A was shown to dephosphorylate MDM2 at Ser166, which is an activating modification of MDM2 protein. MDM2, as the central negative regulator of wildtype p53, has not been reported as frequently amplified in SHH medulloblastomas, suggesting other mechanisms might exist to compromise p53 function. Therefore, we **hypothesized** that upregulated I2PP2A might suppress PP2A's dephosphorylation of pMDM2^{S166}, which result in hyper-active MDM2, thereby suppressing wildtype p53 activity in SHH medulloblastoma.

As discussed earlier in section 1.2, the classic *Ptch*^{+/-} SHH medulloblastoma mouse model developed spontaneous *Trp53* mutations or *p16*^{ink4a} inactivation in more than one-third of advanced tumor mice, rendering it unsuitable to investigate wildtype p53 activity. Therefore, we utilized the *NeuroD2:SmO.A1* mouse model to test the hypothesis mentioned above, in which no somatic p53 mutations have been reported. *NeuroD2: SmO.A1* mice constitutively express an activated Smoothed in early cerebellum development, which corresponds to *SmOM2*, a mutated gene resulting in tryptophan-to-leucine transition at residue 539 identified in human SHH medulloblastoma patients (101). As shown in **Figure 1.7 d**, heterozygous mice showed a tumor incidence of ~50%, peaking at 5-6 months (87). Tumors from these mice recapitulate the histology and expression profiles of patient SHH medulloblastomas. The same research group generated homozygous *NeuroD2: SmO.A1* mice in 2008, with a higher incidence of ~90%, most of which happen between 4-6 months (88). Most of the research in Chapter 3 to test the hypothesis mentioned above was performed using homozygous *NeuroD2: SmO.A1* mice.

In addition to mouse models, we also utilized patient-derived SHH medulloblastoma cell lines in our research, including DAOY, ONS76 and UW228 cells. As these patient-derived cell lines have been passaged in cultures for quite a while, rapidly-dividing cells with various mutations were selected out after many passages (102). These cells thus are not considered optimal for detailed mechanism studies although they overexpress molecules involved in SHH signaling pathway. Therefore, we started to test our hypothesis in primary MBCs derived from *NeuroD2:SmoA1* mice, and then validated our hypothesis in these patient-derived cell lines.

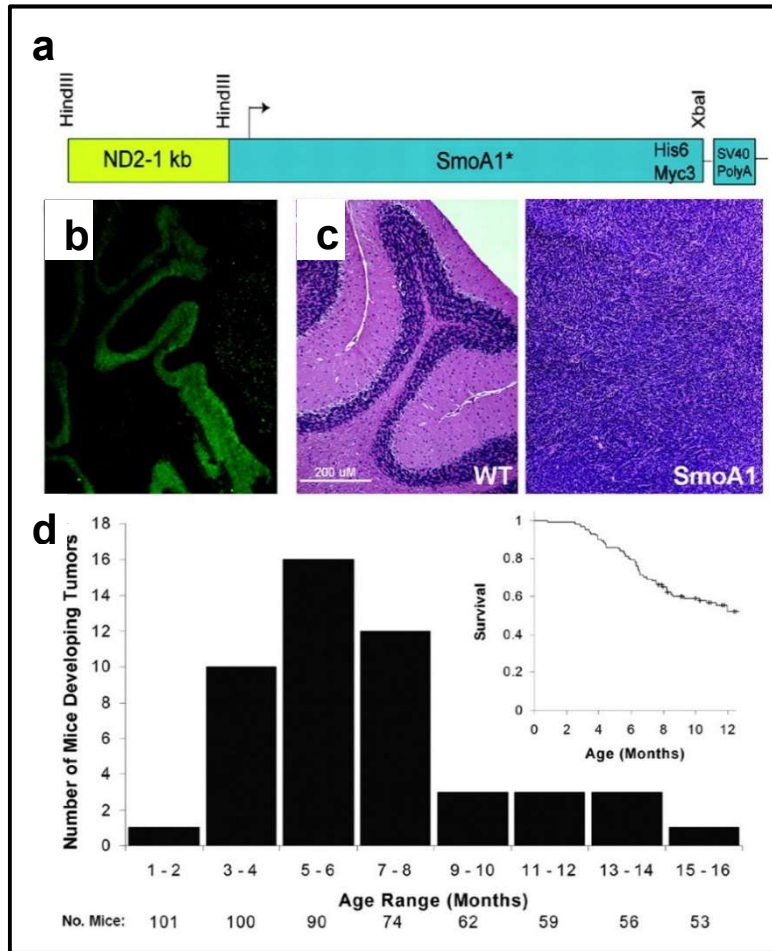


Figure 1.7. Heterozygous *NeuroD2: SmoA1SHH* medulloblastoma mouse model. Taken from (87) with permission. **a**, transgenic construct containing NeuroD2 1kb as promoter region, activated Smoothed encoding SmoM2 (W539L), tagged with His6 and Myc3. **b**, immunostaining of His6 in adult cerebellum of *NeuroD2: SmoA1* mouse. **c**, comparison of HE staining between wildtype adult cerebellum (*left*) and SmoA1 medulloblastoma tissue (*right*). Tumor tissue displayed compacted cells with small “blue” nuclei, representing the classic histology of SHH medulloblastoma. **d**, number of *SmoA1* mice developing tumors in the range of 16 months. Kaplan-Meier survival curve was generated and shown in the *Inset*.

1.4 Dissertation goals

1.4.1 Untangling the tumor heterogeneity of SHH medulloblastoma

As discussed in section 1.1.3, challenges in current standard treatment are compounded by a lack of tumor heterogeneity research integration into stratification or therapeutic systems. Even within SHH medulloblastoma patients, intra-subgroup heterogeneity contributes to the failure of targeted therapy such as the Smoothened inhibitor vismodegib. This underscores the importance of understanding the cellular, genetic and molecular attributes of tumor initiation and progression of SHH medulloblastomas. SHH medulloblastomas display intra-subgroup heterogeneity in demographics (age or sex distribution), cytogenetics (chromosome aberrations), histological features and cell compositions of the tumor microenvironment. Furthermore, a myriad of cell types comprises the tumor microenvironment of SHH medulloblastomas; these include immune cells such as brain-residing microglia and bone-marrow-derived macrophages. Various signaling pathways are implicated in SHH medulloblastomas that are critical for tumor cell proliferation and survival. Understanding these pathways and the possible interaction among different signals would help identify potential novel therapeutic targets for SHH medulloblastoma patients. Of note, alterations in epigenetics have been recently shown to be implicated in the tumor development of all subgroups of medulloblastomas, with moderate presentations in the SHH subgroup. The wealth of recent discoveries about the tumor microenvironment in CNS tumors should be beneficial in multiple ways, such as improving drug delivery efficacy or devising novel therapeutic strategies. For example, with better knowledge, we potentially can re-educate immune cells to target medulloblastoma cells, which otherwise have evaded the supervision by native and infiltrating immune cells. Therefore, our first goal is to untangle this tumor heterogeneity with the hope of providing clues for future personalized or precision medicine, which will be further discussed in Chapter 2.

1.4.2 Investigating the interaction of I2PP2A-p53 in SHH medulloblastoma

Our second goal is to interrogate the possible interaction between increased I2PP2A protein and wildtype p53 by utilizing the *NeuroD2: SmoA1* transgenic mouse model. As discussed earlier, I2PP2A has been proposed to be a good target in other tumor types; but whether it is targetable in SHH medulloblastoma remains to be elucidated. Importantly, we need to evaluate whether I2PP2A promotes tumor growth or not in the SHH medulloblastomas. Moreover, if yes, understanding how the upregulated I2PP2A protein functions in the tumor development of SHH MBs would enable us to target it better. On the other hand, considering the critical roles of p53 function in suppressing SHH subgroup tumors, whether p53 is suppressed through mechanisms other than mutation is still unknown. The mechanistic study of possible p53 upstream suppressors would provide novel therapeutic targets considering the challenges in re-introducing a tumor suppressor with current treatment modalities. If we could test the hypothesis that I2PP2A acts as a negative regulator of p53, it would be ideal to find ways to target I2PP2A in SHH medulloblastoma patients. Interestingly, the drug FTY720, which is proposed to target I2PP2A (103), has been FDA-approved in treating refractory multiple sclerosis (MS) patients. Furthermore, FTY720 has been shown to penetrate the blood brain barrier in these MS patients and may be of clinical value in treating SHH *TP53*-wildtype medulloblastoma patients as well. Therefore, as presented in Chapter 3, we set out to test the hypothesis that I2PP2A compromises p53 in SHH medulloblastomas utilizing the *NeuroD2:SmoA1* mouse model. We later validated our findings in patient-derived medulloblastoma cells. Future studies (Chapter 4) include the investigation of whether the cellular killing effects resulted from I2PP2A targeting in primary MBCs could delay tumor growth and increase survival rates in our *in vivo* allograft model.

Chapter 2. Untangling tumor heterogeneity in Sonic Hedgehog medulloblastomas

Yun Wei^{1,2}, Hope Robinson^{1,2}, Anna Marie Kenney^{1,2}

Affiliations:

¹Department of Pediatrics Oncology, Emory University, Atlanta, GA 30322, USA

²Winship Cancer Institute, Atlanta, GA 30322, USA

This work was adapted from the unpublished review paper titled “Untangling tumor heterogeneity in Sonic Hedgehog medulloblastomas” in preparation for Annual Reviews of Pathology: Mechanisms in Disease.

Abstract

Medulloblastoma is the most common malignant pediatric brain tumor, which can be classified into at least four molecular subgroups, namely WNT-activated, SHH-activated *TP53*-wildtype, SHH-activated *TP53*-mutant, non-SHH/WNT subgroup (also known as Group 3 and Group 4). SHH medulloblastomas account for ~30% of all medulloblastoma cases and display intra-subgroup heterogeneity regarding clinical features/histology, cytogenetics, expression profiles, demographics in age, as well as prognosis post-treatment. Molecular presentations such as *TP53* mutations, *PTCH* mutations, signaling crosstalk, and epigenetic alterations might contribute to the intra-subgroup heterogeneity of SHH medulloblastomas. Additionally, cellular components of the tumor microenvironment of SHH medulloblastomas are distinct from other solid tumors or other medulloblastoma subgroups. In this review, we aim to understand these molecular aberrations and cellular components of SHH medulloblastomas in detail, with the hope to provide implications for future clinical trials, pertaining to diagnosis, potential therapeutic target, and novel treatment strategies.

2.1 Introduction

Surpassed only by blood malignancies in children, central nervous system (CNS) tumors account for 26% of all pediatric cancers in the United States according to Cancer Statistics, 2017 (104). The most common pediatric CNS tumor, medulloblastoma was first described and histologically characterized by Bailey and Cushing in 1925 (4). This first-ever histological classification revolutionized the way neurosurgeons treated these tumors, which also set the foundation for medulloblastoma research (105). In 2016, the World Health Organization (WHO) designated four molecular subgroups of medulloblastoma, namely WNT-activated, SHH-activated TP53-mutant, SHH-activated TP53-wildtype, and non-SHH/WNT (previously called Group 3 and Group 4) (34). The newly established classification underscores the importance of understanding the molecular and cellular context for medulloblastoma development.

SHH (Sonic Hedgehog) activated medulloblastomas, accounting for ~30% of all medulloblastoma cases, are best studied utilizing different systems, including transgenic mouse models, patient-derived murine xenografts, patient-derived cancer cell lines, and clinical samples (6, 8, 18, 38, 87, 88, 102, 106). This subgroup was first identified by its connection with Gorlin syndrome; patients with nevoid basal cell carcinoma harboring germline mutation in *PTCH*, a suppressor of SHH signaling, were predisposed to medulloblastomas (24, 27). Sonic Hedgehog is a mitogen/morphogen critical for embryonic development, especially for the patterning of the nervous system (31, 107-109). Mutations or aberrant expression of any signaling molecule in the SHH pathway during development can lead to malformations or disease such as cerebellar hypoplasia, basal cell carcinoma, and medulloblastoma.

The current standard therapy for medulloblastoma patients includes surgery, craniospinal irradiation, and chemotherapy, based on risk-group stratification at diagnosis, which secures a ~70% 5-year overall survival. However, the improvement in cure rates plateaued over the past decade, necessitating

the search for new therapeutic modalities (110). As Smoothed is a SHH signaling activator, targeted therapy using a Smoothed inhibitor, vismodegib, was proposed to treat SHH medulloblastoma patients. This proposal exhibited several limitations, including the scarcity of mutations of/upstream of Smoothed granting *a priori* resistance, the bone toxicity of this drug, and acquired resistance to the inhibitor (32, 33, 44, 45). Moreover, the molecular and cellular heterogeneity of SHH medulloblastoma makes it challenging to cure all patients with the same therapy, leading to over-treatment of average-risk groups and inadequacy of therapy for some high-risk patients. Even worse, recurrent tumors, which are proposed to evolve from a small population of the primary tumors not eradicated by the first line of treatment, are always lethal. In order to understand where we are in our efforts to treat SHH medulloblastoma, in this review we will discuss intra-subgroup heterogeneity of SHH medulloblastoma, focusing on aberrant signaling crosstalk, the tumor microenvironment, and epigenetic changes, as well as the implications of these discoveries in guiding future personalized/precision medicine.

2.2 Intra-subgroup heterogeneity of SHH medulloblastoma

Researchers at the Boston SNO meeting in 2010 came to a consensus that MB can be classified into four molecular subgroups, namely SHH, WNT, Group 3, and Group 4 (6-9). Transcriptomic and genomic studies of patient samples combined with subgroup-specific demographics and clinical features were reported separately, but most of the resulting data has been uploaded to the R2 website (<http://r2.amc.nl>) providing researchers with a powerful tool for large-scale comparisons. SHH medulloblastomas (MB) have been increasingly acknowledged as cancer composed of heterogeneous tumors presenting different genetic mutations, expression profiles, histological features, cytogenic markers, and distinct clinical outcomes. More than 80% of patient samples from SHH subgroup harbored aberrations in known genes of the SHH signaling pathway, such as mutually exclusive mutations in *PTCH*, *SMO*, *SUFU*, or amplifications in *GLIs*, *MYCN*, *E2Fs*, and *YAP1* (24, 26, 32, 111, 112). SHH MBs represent the histological heterogeneity of medulloblastomas, including classic, desmoplastic, large cell anaplastic (LCA), and medulloblastoma with extensive nodularity (MBEN) (5). Cytogenic markers of SHH MBs feature chromosome changes including 3q gain or losses of 9q or 10q (6, 9). The clinical outcome of SHH MBs is intermediate partly because metastasis is not seen as frequently as in Group 3 or Group 4 tumors (6, 7, 9). Recurrent SHH MBs are still affiliated with the SHH subgroup based on expression profiles but present with increased mutational load and high-risk features as compared to primary tumors (57, 113, 114).

Multiple factors may be responsible for the poor prognosis for recurrent SHH medulloblastoma, including *NMYC* and *GLI2* amplifications, LCA histology, *TP53* mutation, PI3K/AKT pathway activation, age/metastasis at diagnosis, and possible complications like hydrocephalus (3, 9). Metastasis and LCA have been integrated into the stratification criteria for “high-risk” patients of all medulloblastoma cases (3, 115). SHH MBs display a bimodal distribution in age demographics, with patients predominantly infants (≤ 3 years old) and adults (≥ 16 years old), pediatric cases comprising

less than 30% of all SHH cases (7, 9, 116). In 2011, Northcott *et al.* proposed pediatric and adult SHH MBs were clinically and molecularly distinct based on transcriptome and clinical outcomes (116). Kool *et al.* further showed that infant patients are separate from children or adult SHH MB patients (32). The current standard of care for pediatric and adult SHH MB patients follows the same protocol, with slight modifications in infant patient treatment, as craniospinal irradiation is contraindicated in these patients (3).

Infant SHH medulloblastomas

The cure rate of infant medulloblastoma patients is less than optimal as they are deferred to radiotherapy post-operation due to the likelihood of neurocognitive sequelae caused by radiation (3, 117, 118). Approximately 35% of SHH MB patients are infants, while 65% of infant MB cases belong to SHH subgroup (116, 119). Mutations of both SHH signal repressor genes, *PTCH* and *SUFU*, are detected in infant SHH MBs, but not the *SMO* mutation (32). *PTCH* mutations are almost equally distributed among all age groups. *SUFU* mutation or PTEN deletions is exclusively found in this age group, and some of these patients have inherited germline *SUFU* mutations (32, 119). Some upregulated genes in infant SHH MBs are critical for neuronal development, such as *ID2*, *ZIC5*, and *ZIC2*, as well as *MYCN* (116). Metastatic tumors were detected in the infant group and are non-statistically significant in predicting prognosis of overall survival (9, 119).

Pediatric SHH medulloblastomas

A combination of surgery, radiation, and chemotherapy with cytotoxic regimens brings up the survival rates of “average-risk” patients to 85% and “high-risk” patients to 60% or more in children with medulloblastomas (3). This might not represent the statistics in SHH medulloblastoma well because pediatric patients predominantly fall in the WNT subgroup. SHH cases only account for ~15% of all pediatric medulloblastoma cases, and approximately 30% of all SHH MBs belong to this age group





(116, 119). Pediatric SHH MBs showed much greater genomic instability compared with infant or adult groups, mainly due to the prevalence of *TP53* mutations in this subgroup (32, 58). 9q, 10q, and 17p loss, or *NMYC*, *GLI2* and *PPM1D* amplifications are frequently seen in childhood SHH MBs, possibly caused by chromothripsis, catastrophic chromosome rearrangements due to p53 deficiency (32, 68). Metastasis in this age group is seen as frequently as in the infant group, but more than that in adult SHH MBs.

Adult SHH medulloblastomas

Clinical trials in adult medulloblastomas are relatively limited because there are fewer adult cases; however, adult patients show less chemotherapy tolerance as compared to younger groups (3, 120). SHH medulloblastomas account for approximately 70% of all adult MB cases, and more than 35% of SHH MBs are adult tumors (116, 119). *SMO* mutations are exclusively found in adult SHH MBs (32). Similarly, *TERT* promoter mutation and hypermethylation are exclusively detected in this group, found in 43 out of 44 patients in a 2014 report from Kool et al. (32, 121). PI3K signaling activation by aberrations in pathway components such as *PIK3CA*, *PI3KC2G* mutations, or *PTEN* loss, is frequently detected in adult SHH MBs, but less so in infant SHH MB cases, nearly non-existent in pediatric SHH MB and is in most cases associated with poor prognosis(32).

Cavalli et al. in 2017 analyzed the expression and methylation data of 763 medulloblastoma patient samples, which include 223 SHH samples, and provided evidence of further subclassification of SHH medulloblastomas into SHH α (pediatric), SHH β (infant), SHH γ (infant), and SHH δ (adult) subtypes (119). The demographics, clinical features, and genetics are summarized among subtypes as illustrated in **Table 2.1**.

Table 2.1. Subtypes of SHH medulloblastoma.

SHH Medulloblastoma				
Shh signaling activation: <i>PTCH/SMO</i> mutation; uncommonly metastatic; intermediate prognosis				
COMMON FEATURES	SHH α	SHH β	SHH γ	SHH δ
SUBTYPES	29.1%	15.7%	21.1%	34.1%
DEMOGRAPHICS				
Age				
Gender	♀:♂ ~1:1	♀:♂ ~1:1	♀:♂ ~1:1	♀:♂♂ ~1:2
CLINICAL FEATURES				
Histology	LCA Desmoplastic	Desmoplastic	MBEN Desmoplastic	Desmoplastic
Metastasis	20%	33%	8.9%	9.4%
5-year Survival	69.8%	67.3%	88%	88.5%
GENETICS				
Broad	9q-,10q-,17p-			
Focal	<i>MYCN/GLI2/YAPI</i> amplification, <i>TP53</i> mutations	<i>PTEN</i> loss		10q22-,11q23.3-, <i>PIK3CA</i> mutations <i>TERT</i> promoter

2.3 Aberrant signaling crosstalk

Patient genomics, gene expression, and methylation studies suggest that a few signaling pathways are critically involved in SHH MBs. SHH signaling is the primary driver for MB initiation and development, and PI3K and/or p53 may facilitate tumor progression to malignancy. Detailed mechanistic studies of how the signaling patterns were first identified, and how it could affect SHH medulloblastoma development were performed in model systems such as *Drosophila*, human cancer cell lines, and mouse models. Crosstalk among signaling pathways are briefly illustrated in **Figure 2.1**, and further discussed below.

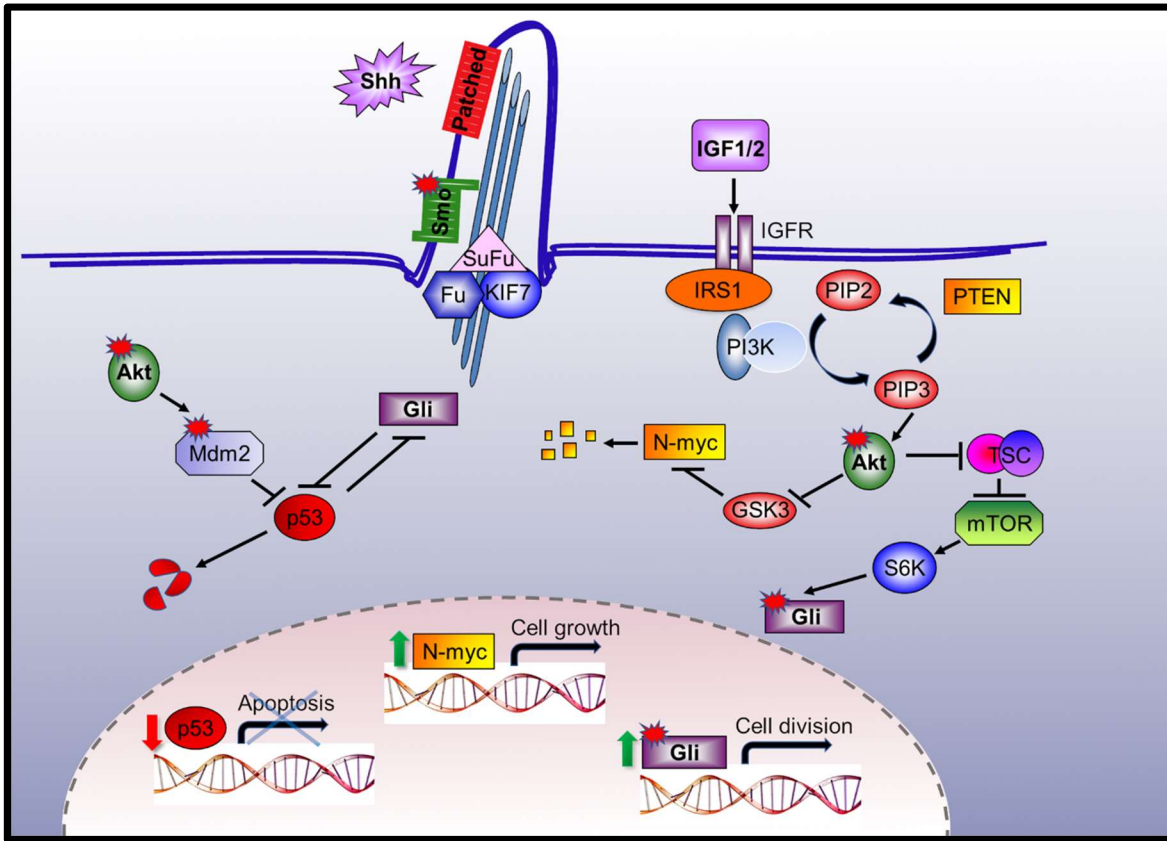


Figure 2.1. Signaling crosstalk in SHH medulloblastoma cells. The Sonic Hedgehog (SHH) molecule dissociates Patched, a 12-transmembrane protein from Smoothed. The activation of smoothed requires phosphorylation to release GLI transcriptional factors from the SUFU suppressor complex containing Suppressor of Fused, Fused, and KIF7. NMYC could also be activated and stabilized by SHH signaling and promote cell proliferation and growth. IGF/PI3K signaling interacts with SHH signaling in two ways: the p-AKT mediated suppression of GSK3 stabilizes NMYC protein by inhibiting its degradation, and the activation of mTOR which activates S6K to phosphorylate and activate GLI. Released and phosphorylated GLI could then enter the nucleus and trigger expression of cell cycle regulating genes, such as CCND1 and CCND2 and CDK6. p53 as a tumor suppressor could also suppress GLI function. And MDM2, which is the central negative regulator of p53, could be activated and stabilized through phosphorylation mediated by p-AKT.

Mutations, deletions or amplifications of genes involved in all three signaling pathway were observed in individual SHH medulloblastoma patients and might contribute to the tumor initiation and development.

SHH signaling as the proliferative driver

The Sonic Hedgehog (SHH) Signaling pathway was primarily illustrated in *Drosophila melanogaster* studies, where researchers discovered that the interference of each hedgehog (hh) component could disrupt normal segmental development, as reviewed by Robbins *et al.*(43). Homologs of these hh components were found in vertebrates and mammals and proved to be conserved in amino acid sequences and function in embryonal and CNS development. SHH, is produced by Purkinje cells and processed into a lipid-modified truncated ~19kDa molecule, which functions in an autocrine or paracrine fashion. Patched (PTCH), which is a 12-transmembrane receptor on cerebellum neuron precursor cells (CGNPs), is the receptor for SHH and acts by constitutively suppressing Smoothed (SMO). This suppression is released when SHH binds to PTCH. Additionally, *PTCH* is a transcriptional target of SHH signaling. Besides PTCH, co-receptors for SHH molecules include CDO/BOC, which is required for SHH signaling transduction in mammalian cells. The binding of SHH with PTCH and other co-receptors then triggers the translocation of SMO to the primary cilia of mammalian cells. Primary cilia extend beyond the cell surface and are supported by microtubules, which also present the KIF7 (Costal2) complex, including supporting molecules KIF7 and GLI, Fused, and SUFU. Upon arrival of Smoothed, GLI as a transcription factor is released from SUFU and activates downstream genes. The GLI protein family contains three zinc finger proteins, including SHH activators GLI1 and GLI2, and a repressor GLI3. Post-translational modifications of some SHH components proves to be critical; phosphorylation of Smoothed mediates its activation, while phosphorylation of GLI1 at Ser84 mediates its translocation into the nucleus and subsequent transcriptional activity.

Dysregulation in SHH pathway includes mutations in *PTCH*, *SMO*, *SUFU*, or amplification of *GLI2*, *YAP1*, *E2F* family members, and *MYCN*, which have been identified by several groups using mouse

model (21, 26, 38, 111, 122-126). Most of these aberrations have been identified or validated in patient samples using techniques such as tissue microarray or genomic studies (25, 127, 128).

The interplay between Shh signaling and RTK-PI3K-AKT-mTOR pathway

Insulin-like growth factor 2 (IGF2) and its receptor IGF1R were shown to be required for SHH medulloblastoma growth in *Ptch*^{+/-} mice, the proliferation of *in vitro* CGNPs, and in the patient-derived medulloblastoma cell line DAOY (129-132). However, it was not until later when patients acquired resistance to the Smoothed inhibitor vismodegib that researchers postulated that combination therapy targeting both SHH and IGF/PI3K (phosphoinositide 3-kinase) signaling would benefit SHH medulloblastoma patients. Buonamici *et al.* detected aberrantly activated IGF-1R, PIP3 and AKT pathways in Smoothed inhibitor LDE225 resistant tumors as compared to primary tumors using SHH mouse models, and combination therapy targeting both SHH and PI3K pathways significantly increased mouse survival and tumor regression (47). Aberrant PI3K signaling promotes cancer cell growth and survival and thus has been investigated and is widely-accepted as oncogenic. PI3K pathway abnormalities have been detected in primary SHH medulloblastoma tumors such as mutations in *PIK3CA* and *PIK3C2G* (32). Mutations or promoter methylation of PTEN, the suppressor of the pathway, have also been identified in this subgroup (133, 134). Additionally, active PI3K signaling has been proposed to drive recurrence in radiation or drug-resistant tumors (135). Researchers showed that p-Akt and p-S6, downstream targets of the PI3K pathway were enriched at the perivascular niche (PVN) and co-stained with stem-like cell marker nestin hours post-irradiation in a SHH medulloblastoma mouse model.

During normal development, SHH signaling is active in undifferentiated and proliferative cells while AKT-mTOR pathway activation is associated with differentiation and cell aging (136, 137). However, dysregulated SHH signaling and the PI3K pathway synergize in cancer cells at multiple levels in

amplifying the proliferative and survival signals. For example, IRS1 is a post-transcriptional target of SHH signaling in CGNPs, as cyclopamine inhibition of SHH facilitates IRS1 protein decrease, but not its mRNA level change (138). Research has discovered that GLI can be activated in a SMO-independent way; one proposed mechanism is that accumulated p-AKT in cancer cells phosphorylates and inhibits GSK3 β and PKA, both kinases that mediate phosphorylation and inactivation of GLI (139-142). A third example was evidenced in esophageal adenocarcinoma cells where the mTOR target S6K1 also directly phosphorylates and activates GLI, releasing it from SUFU suppression (143). Another critical downstream effector of SHH signaling N-myc was also found to be destabilized by GSK3 β mediated phosphorylation in CGNPs(112). The synergy between SHH signaling and PI3K/mTOR pathway warrants the future evaluation of combination therapy targeting these two pathways in SHH medulloblastoma patients, especially for the adult group where the PI3K signaling showed significant prognostic value (32).

***TP53* mutation as a prognostic marker in SHH MB**

Patients with Li-Fraumeni Syndrome harboring germline mutations of the p53 allele predispose a few of them to medulloblastomas (28). However, the prognostic value of a *TP53* mutation has been controversial; some researchers reported that p53 mutations in MB were associated with a poorer prognosis while others did not observe a connection between p53 status and patient survival (50, 52-57). In 2013, Zhukov *et al.* analyzed two different cohorts in a subgroup-dependent manner and concluded that *TP53* mutation has prognostic value in the SHH subgroup, but not in WNT MBs, where p53 mutations were only detected in subsets of SHH and WNT MBs but not in Group 3, and rarely seen in Group 4 patients (58).

p53, as a gatekeeper for cell division and growth, has a short half-life (~30min) in mammalian cells under normal conditions (51). However, when cells are exposed to stress, such as DNA strand breaks

caused by UV light, radiation, or oncogenic proliferative signaling, p53 is stabilized and activated to either arrest cell cycles and check for DNA repair or facilitate apoptosis/senescence of these healthy cells. Utilizing SHH MB mouse models, researchers observed that the deficiency of p53 accelerates tumor growth and increases the tumor incidence. For example, p53 loss in both alleles of *Ptch*^{+/-} mice increased the tumor incidence from 14% without p53 loss up to 95%, all of which succumb to SHH MBs within 12 weeks (59). In 2016, Tamayo-Orrego *et al.* illustrated in *Ptch*^{+/-} mice, that p53 deficiency occurs after the LOH (Loss of Heterozygosity) in Patched and is a necessary step for preneoplastic cells to evade senescence before progression to advanced SHH medulloblastomas (63). Interestingly, some researchers generated mice with SHH medulloblastoma without aberration in SHH pathway, instead of with constitutional *Lig4* loss (DNA ligase IV, a protein critical for non-homologous end joining), and *Trp53* deficiency (60, 61). Medulloblastoma from these mice showed overexpression of *Matb1* and *Gli1*, features of SHH medulloblastomas. Consistent with this finding, Rausch *et al.* identified chromothripsis in a subset of SHH MB patients, where they proposed acute shattering of chromosomes (chromothripsis) in granule precursor cells with constitutional or early somatic *TP53* mutations predisposed patients to SHH MBs, but not other subgroups of MBs (68). The mutation of *TP53* sometimes co-occurs with *MYCN* amplification in metastatic or relapsed patients with SHH MBs, which define a rapidly progressive disease with a dismal outcome for SHH, but not WNT subgroup patients (52, 53, 55, 57). Other than *TP53* mutations, amplification of p53 suppressors, such as MDM2 or WIP1, may also contribute to the deficiency of p53 function (49, 72, 73, 77). Furthermore, some *in vivo* and cell line studies indicated that GLI1 and p53 form an inhibitory loop where GLI1 suppresses p53 function by preventing its entry into the nucleus and *vice versa* (74, 75, 144).

As reviewed by Ramaswamy, the role of p53 in medulloblastomas was controversial and gradually has been accepted as a prognostic marker in SHH MBs in WHO 2016 Classification of Tumors of the Central Nervous System(34, 145). WHO subdivided SHH MBs into *TP53 wildtype* and *TP53 mutant*,

based on the finding that the 5-year overall survival (OS) of SHH medulloblastoma patients with wildtype *TP53* is ~80%, while the 5-year OS of patients with mutant *TP53* is ~40% (58, 62, 63).

2.4 Epigenetics

As in other pediatric cancers, the mutational load of SHH MB is very low, and efforts to target these few mutations have met with limited success. Epigenetics, heritable changes in gene expression without changes to the DNA sequence, control the availability of the genome to the transcriptional machinery. These changes can result in very different phenotypical outcomes for cells that are genetically identical, and many of these changes have been identified in cancers including SHH medulloblastoma (146).

Chromatin is the complex of proteins and DNA that allow dense packaging of eukaryotic DNA into the higher order structure of chromosomes. The basic unit of chromatin is the nucleosome, an octamer of histones with ~147 base pairs of DNA wrapped around it (147). Epigenetic changes are made by covalent modifications to components of chromatin, DNA or histones, which change whether it is available for further modification or transcription (148).

The most often discussed DNA modification is methylation of the pyrimidine base cytosine, especially in childhood cancers (146). Hypomethylation of DNA may activate transcription of oncogenes and contribute to genome instability (149). Hypermethylation, particularly of CpG islands in the promoters of genes, may result in gene silencing, a phenomenon seen in TSGs, which may act as the “second hit” in Knudson’s hypothesis (149). Resolution of cytosine methylation, specifically 5-methylcytosine, can be accomplished through oxidation via TET (ten-eleven translocations) family enzymes (149). However, spontaneous hydrolytic deamination of 5mc to thymine also occurs, thereby creating a point mutation (148). 50% of the mutations found in p53 are at cytosine methylation sites, mutations of which are found in 20% of SHH medulloblastoma cases (149).

In SHH MB, differential DNA methylation has been described in multiple published reports (119, 150-152). Genome-wide methylation arrays have confirmed that the four major subgroups have

specific DNA methylation patterns (119, 151). Hypermethylation as a mechanism for gene silencing was not found to be a critical regulatory feature in a study of 34 human medulloblastoma samples (150). However, there are a few genes with critical roles in controlling cell proliferation whose methylation state positively or negatively corresponds with gene expression. Hypomethylation of the gene for VAV1 leads to elevated expression of VAV1 in mouse and human SHH MB and is associated with poor outcomes (153). Hypermethylation of specific CpG sites upstream of the transcription start site for TERT was reported in 36% of SHH MB tumors (121). SHH tumors in infants and children showed hypermethylation at this site while adult MB tumors displayed more frequent mutations of the *TERT* gene. A more recent study noted that hypermethylation was more prominent in children when compared to infants (151). This group corresponds to the SHH- α group which is also known to have a higher proportion of cases with p53 mutations and a worse prognosis (119).

Histones are foundational to the structure of chromatin. Each histone has a tail comprised mainly of lysine and arginine residues that are prone to modification. These modifications, primarily methylation and acetylation, alter the affinity of DNA for the histone octamer, thereby determining the level of compaction of the chromatin (154). Many of the gene mutations in medulloblastoma are found in enzymes that add “write”, “erase”, or “read” these marks on histones (155). Mutations of histone lysine methyltransferases and demethylases have been identified across subgroups of medulloblastoma without identified subgroup affiliation (17, 156, 157). Mutation of histone acetyltransferases (HATs) or upregulation of histone deacetylases (HDACs) has also been described in medulloblastoma (158). One study from 2013 showed that SHH signaling regulates activation of HDACs and that this activation is required for CGNP proliferation (155, 159). In a study using SHH MB stem-like cell cultures and a xenograft tumor model, inhibition of the methyltransferase EZH2 reduced H3K27me3 levels which reduced cell proliferation, induced cellular apoptosis and delayed tumor growth (160). The histone demethylase KDM1A, also called LSD1, is upregulated in human and mouse models of

SHH MB (161). When authors knocked down KDM1A, they observed inhibition of migratory capacity in addition to reduced proliferation and increased apoptosis of these cells (161). Depletion of the histone acetyltransferase PCAF/KAT2B in SHH MB cell lines also decreased proliferation and increased apoptosis (162).

Aside from covalent modifications to DNA or histones, another method of epigenetic control is chromatin remodeling. This process involves molecular machinery that utilizes the energy of ATP hydrolysis to disrupt DNA histone interactions, altering the position of nucleosomes, or exchanging histone protein variants (163). There are four families of mammalian chromatin-remodeling ATPases that are differentiated based on the binding domains that enable function. These ATPases work in large complexes along with enzymes described above that modify DNA and histone tails. One good example is N-CoR complex, nuclear receptor co-repressor, mutations in three members of which were found in SHH MB, namely BCL6 co-repressor (*BCOR*), LIM-domain binding 1 (*LDB1*), and G-protein pathway suppressor 2 (*GPS2*) (16, 164). As suggested by the name of the complex, it is believed to act as a repressor to gene transcription possibly via HDAC activity and mutations in components of the complex likely results in aberrant transcription (16, 164). BMI1, a member of the polycomb repressive complex 1 (PRC1), is overexpressed in SHH MB and its transcription is driven in part by GLI family members (165). Inhibition of the BET bromodomain proteins with JQ1 in transgenic mouse models and patient-derived SHH tumors resulted in decreased tumor cell proliferation even in tumors resistant to SMO inhibitors (166). The authors found that GLI1 and GLI2 transcription are subject to epigenetic control by BET proteins and modulation of these downstream effectors of SHH holds promise, particularly for patients with primary or secondary resistance to SMO inhibitors (166). In another study using a SMO mouse model, the chromatin remodeler BRG1 was shown to coordinate genetic and epigenetic networks in mouse cerebellar development and murine SHH medulloblastoma (167).

Lastly, RNA interference by non-coding RNAs called microRNAs (miRNAs) can alter the expression of genes without changing the underlying DNA sequence in SHH MBs as reviewed by Wang *et al.* in 2017. The importance of alterations in the normal epigenetic regulation of transcription is becoming increasingly clear. In pediatric cancers, epigenetics may be the path to targeted treatments in tumors that typically have few genetic mutations. Importantly, epigenetic regulation can be modulated, which increases the likelihood that research in this area can lead to targeted therapeutics. Our understanding of these factors and how they function is still a work in progress, but the next few years hold promise for exciting discoveries that will likely change our understanding of cancer and how to treat it.

2.5 Tumor microenvironment

The importance of the tumor microenvironment (TME) for cancer development has been appreciated since the 1980s, where researchers proposed that the TME provides the oxygen and nutrient supply for rapidly proliferating tumor cells (168). Though the most abundant cell population of SHH medulloblastoma is tumor cells putatively derived from CGNPs, various other cell types play roles in tumor development, maintenance and progression. SHH MBs display histological heterogeneity, suggesting the diversity of cell types found in the TME (169-171). As depicted in **Figure 2.2**, the TME of SHH MB is comprised of residing microglia, astrocytes, infiltrating immune cells, and stem-like cells, as well as the vasculature formed by endothelial cells (172-175). These various cell populations, and the communication among different cell types via cytokines, membrane receptors, secreted factors, physical contact, and the subsequent signaling activation contributes to the specific TME of medulloblastomas (176). The TME of SHH medulloblastoma is different from other brain tumors, as the blood brain barrier is almost intact in this subgroup of medulloblastomas, but not in WNT medulloblastomas (177). Understanding the TME of SHH MBs can help us better decode the tumor heterogeneity with the hope of devising novel targeting strategies to treat this specific disease.

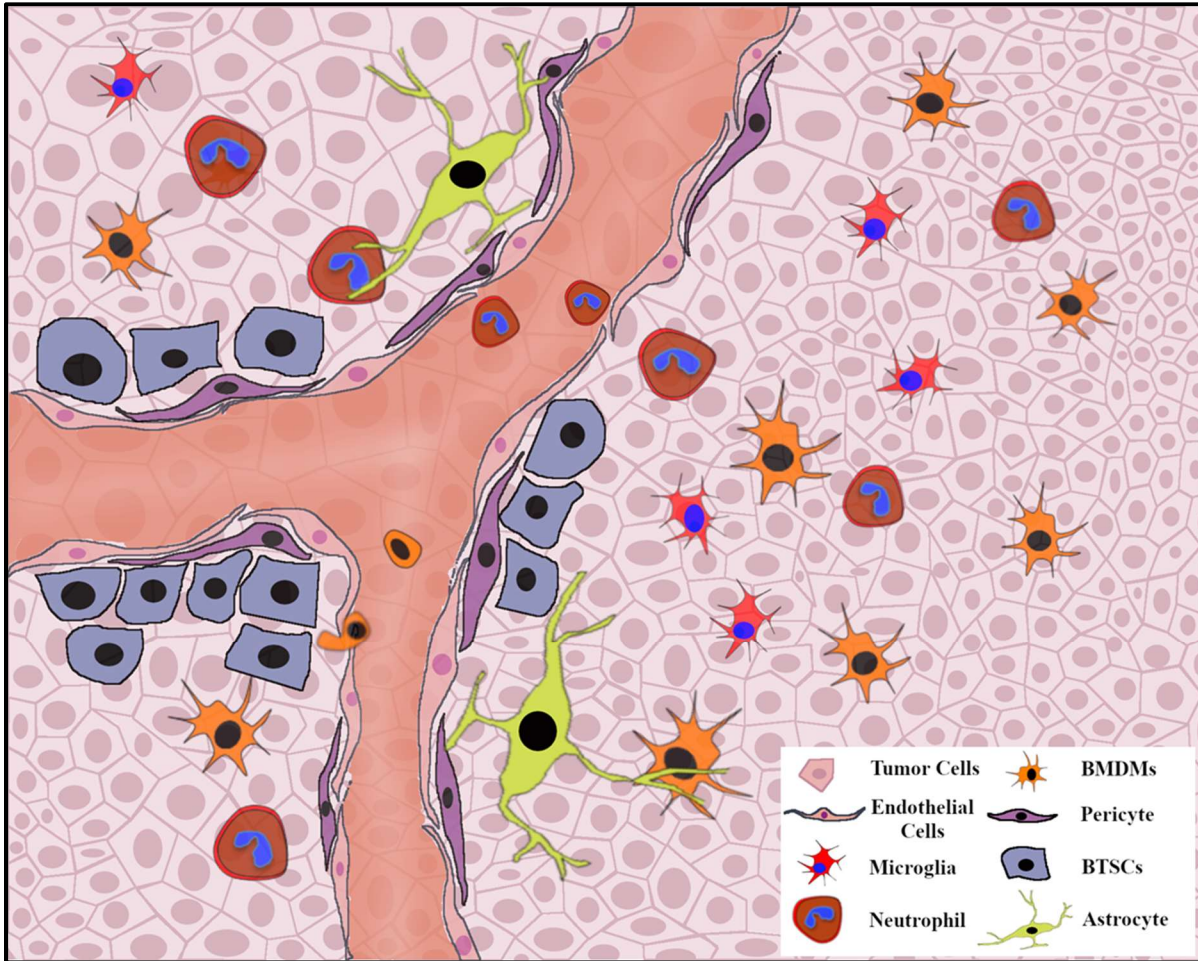


Figure 2.2. Various cell populations in the tumor microenvironment (TME) of SHH medulloblastoma. As noted on the bottom right, various cell types compose the TME of SHH medulloblastoma near the perivascular niche (PVN). Endfeet of astrocytes ensheath the vasculature formed by endothelial cells and pericytes, comprising the blood brain barrier. Infiltrating bone-marrow derived macrophages and neutrophils are distributed both near the vessels and in the tumor parenchyma. Microglia are resident immune cells which are activated, together with activated astroglia distributed in the TME, which provides neurotrophic support and act as “stroma” to these tumor cells. Brain tumor stem cells (BTSCs) are located near the PVN, which show positive PI3K signaling and contribute to cell repopulation post irradiation.

Cells of origin for SHH MB

As reviewed by Martirosian, the early onset of medulloblastomas underscores the importance of the interdisciplinary understanding of both neuronal development and cancer progression (176). SHH MBs, different from other subtypes, is proposed to be caused by dysregulated SHH signaling, which promotes the aberrant growth of cerebellar granule neuron precursors from the external granule layers, putatively originated from rhombic lip (19, 178, 179). During cerebellar development, the timely coordinated interaction among granule precursors, Purkinje cells, and Bergmann glial cells ensures the regular foliation and layering of the cerebellum, which properly regulates an individual's voluntary movements through motor neurons upon maturity (175, 180-183).

Resident microglia and astrocytes

Other than undifferentiated tumor cells with neuronal markers, the second most abundant populations are microglia and astrocytes in the TME of SHH MBs. Astrocytes have glial cell markers such as GFAP or S100 β and act as “stroma”, which provides neurotrophic support to neurons through direct contact or as yet unidentified secreted factors, and functions in synaptic pruning, synaptogenesis, maturation and maintenance through their phagocytic activity (184-186). Astrocyte also contributes to blood brain barrier (BBB) through the ensheathing of blood vessels by their endfeet (187). In pathological conditions, such as medulloblastoma, astrocytes can be activated to either protect (A1 subtype) or destroy (A2) neurons with different expression profiles (188, 189).

As CNS tissue-specific macrophages, microglia are not derived from the neuron stem cell lineage like other glial cells; instead, they are primitive immune cells which originate from the yolk sac before the BBB forms (190, 191). CSF1R, macrophage colony stimulating factor 1 receptor, is essential for the homing of microglia in the CNS during embryonic development (192, 193). Microglia provide innate immune surveillance through their mobile protrusions and assist in neurogenesis, synaptic pruning,

myelinogenesis, and programmed cell death of neurons during development (194-197). If disease-associated inflammation or injury occurs, microglia can be activated through Toll-like receptors 2 and 4 and function through phagocytosis or factors that are pro-inflammatory (198, 199). In medulloblastomas, an increase in reactive amoeboid microglia has been observed although their function in tumor development or maintenance is still unclear. Investigations of resident astrocytes or microglia in SHH MBs are quite limited due to the difficulty in isolating and culturing single cell populations. As progress has been made in coping with these challenges, it would be interesting to study how they function in tumor progression and maintenance and whether they can be re-educated to target tumor cells, which might lead to a less aggressive way for treating young SHH medulloblastoma patients (184, 200).

Infiltrating immune cells

CNS tumors were at first considered to be immunologically privileged because of the blood brain barrier, which prohibits the entry or exit of myeloid or lymphoid immune cells. However, the expression profiles of tumor-associated macrophages in MB proved the existence of at least the infiltrating macrophages in the TME of SHH MBs (201). T-helper cells were found in medulloblastoma patients by several groups and proposed to correlate with better patient survival in one study (202-204). Modeling in a SHH mouse model, researchers also found infiltrating myeloid-derived suppressor cells, dendritic cells, and tumor-associated macrophages in the TME (205). As analyzed by Maximov *et al.* (*unpublished*), bone-marrow-derived macrophages and neutrophils compose the most abundant infiltrating immune populations, followed by dendritic cells in the TME of SHH MB mice. However, whether these cells are tumor-promoting or suppressing in SHH MBs in patients has not been determined. CD163, a marker for tumor-associated macrophages, didn't show statistically significant prognostic value in a cohort of SHH MB patients (201). In contrast, Maximov

et al. indicated that macrophages suppressed tumor growth in a SHH mouse model and that high expression of *AIF1* (a macrophage marker) correlated with better survival, particularly in the SHH α subtype.

Cancer stem-like cells/ brain tumor-initiating cells

Though considered as undifferentiated embryonal tumors, SHH medulloblastomas display a hierarchy of stemness. In 2003, CD133 positive cells from patients' primary medulloblastomas were initially identified and shown to repopulate neurospheres or tumors in a xenograft mouse model (206), indicating CD133 positive population might represent stem-like cells or tumor-initiating cells for medulloblastoma. Interestingly, two other groups proposed that CD15⁺ cells were the tumor-initiating cells in *Ptch*^{+/-} mouse models and that "CD15 positive" expression profiles in medulloblastoma patients correlates with poorer overall survival (207, 208). Most recently, Vanner *et al.* proposed that a rare population (5% of all tumor cells) with Sox2 expression are the primary stem cells in the TME of *Ptch*^{+/-} medulloblastoma (209). Importantly, they suggested the hierarchy of stemness in the tumor bulk of SHH MBs: Sox2⁺ population as stem cells, quiescent and self-renewing but with the most significant differentiation potential, Doublecortin⁺ cells as precursors, rapidly proliferating cells, and finally the differentiated NeuN⁺ cells, which exit the cell cycle, and some even show apoptotic markers. Different molecules have been proposed to regulate stemness in SHH MBs, including hypoxia induced factor HIF1 α , PI3K signaling at the perivascular niche, a component of polycomb complex that regulates differentiation BMI-1, and p53 (135, 144, 165, 210, 211).

Angiogenesis, metastasis, and recurrence of SHH MBs

As compared to glioblastoma, the angiogenesis of medulloblastoma is subtle. Angiogenesis is induced when rapidly growing tumor cells need more oxygen or nutrients (212). For example, new vessels can be induced by low levels of oxygen. HIF1 α , hypoxia-induced factor, transactivates the expression of

VEGF (vascular endothelial growth factor), which can increase the permeability of endothelial cell membranes to metabolites and assist in the degradation of stroma or supporting fibers in the TME, thus promoting the vessel formation. However, quite limited data exists in studying angiogenesis in SHH MBs. Functional VEGF and its receptors were found to be expressed on SHH patient-derived medulloblastoma cell line DAOY (213).

Local (mostly leptomeningeal) spread and distant metastases are seen in rare cases of medulloblastomas patients at primary diagnosis or recurrence. Of all the metastases, the most frequent site is bone, around 70% in both adults and children, followed by lymph nodes (214). Distant metastases were observed in 7.1% of all medulloblastoma cases. Though metastatic tumors have been proposed to remain stable with subgroup affiliations, the expression profiles of metastases are entirely different from primary tumors, featuring upregulated signals such as PDGFR and MAPK pathways, as well as MET kinase (215-217). Metastases might undergo EMT (epidermal to mesenchymal transition) based on studies of patient-derived cell lines (218). E-cadherin is a marker of EMT. The function loss of E-cadherin was found to be associated with poor prognosis in medulloblastoma patients (17). Recurrent tumors might come from residual tumor left from primary surgery, or from tumors evolved from a rare population at primary treatment, or from metastases not detected at diagnosis. Metastasis and recurrence in medulloblastoma patients are associated with dismal prognosis, but with limited investigations so far.

2.6 Conclusions

As the best-studied medulloblastoma subgroup, SHH medulloblastoma displays heterogeneity in histology, genetics, epigenetics, tumor microenvironment components, and signaling pathways involved during tumor development. A comprehensive understanding from different perspectives not only reveals the intra-subgroup heterogeneity of this tumor but also provides insights into future therapeutic strategy. The current failure of targeted therapy in treating SHH MB patients by merely inhibiting Smoothed, irrespective of their detailed molecular profiles, suggests that we need to know more than just subgroup affiliations.

SHH medulloblastomas are different from other cancer types primarily in two aspects: the blood brain barrier makes it relatively immune-privileged, and with the lower mutational burden as pediatric tumors. The unique TME of SHH medulloblastoma prohibits effective immune therapy such as checkpoint inhibitor PD-1, which activates cytotoxic T cells or natural killer cells in treating other types of cancers. However, the abundant pro-inflammatory microglia or infiltrating bone-marrow-derived macrophages may provide novel therapeutic strategies if we can understand them better in the context of SHH medulloblastomas. Additionally, connecting aberrant signaling with different cell populations in the TME will also benefit targeted therapy. Dwelling within these tumors are stem-like or tumor-propagating cells which contribute to the repopulation of fatal, recurrent tumors. The presence of these cells provides opportunities for targeted therapy. One example is to employ nanoparticles conjugated with antibodies to target stem-like cells expressing surface markers such as CD133 in SHH MBs. SHH medulloblastoma, along with other subgroups, are primarily defined as undifferentiated embryonal tumors. Recently, advancements in epigenetic studies have correlated epigenetic marks with cell differentiation status. Epigenetic research in SHH medulloblastoma might also suggest novel treatment strategies, such as reverting these tumor cells into a more differentiated state by altering the epigenetic marks on the chromosomes of tumor cells.

In summary, as precision medicine gains more attention nowadays, therapeutic strategies employing combination regimens to target known dysregulated signaling pathways, epigenetic modulators, and stem cells can be tailored to individual patients with various subtypes of SHH medulloblastomas, even beyond the Cavalli subtyping scope. These strategies hold promise for not only increasing the cure rate but may also save young patients from severe lifelong side effects as more tailored therapy are applied. Furthermore, if we can understand how SHH medulloblastoma first initiates in a context-dependent manner, we might be able to prevent or diagnose SHH medulloblastoma at an earlier stage.

Chapter 3. p53 Function is Compromised by Inhibitor 2 of Phosphatase 2A in Sonic Hedgehog Medulloblastoma

Yun Wei^{1,2}, Victor Maximov¹, Sorana A. Morrissy³, Michael D. Taylor⁴, David C. Pallas^{2,5},
Anna Marie Kenney^{1,2}

Affiliations:

¹Department of Pediatrics Oncology, Emory University, Atlanta, GA 30322, USA

²Winship Cancer Institute, Atlanta, GA 30322, USA

³Department of Biochemistry & Molecular Biology, Cumming School of Medicine, University of Calgary, 2500 University Dr. NW Calgary, Alberta, T2N 1N4, Canada,

⁴The Hospital for Sick Children (SickKids), University of Toronto, Toronto, Ontario M5G 1X8, Canada

⁵Department of Biochemistry, Emory University, Atlanta, GA 30322, USA

This work was adapted from the research accepted by Molecular Cancer Research.

Abstract

Medulloblastomas, the most common malignant pediatric brain tumors, have been genetically defined into four subclasses, namely WNT-activated, sonic hedgehog (SHH)-activated, Group 3 and Group 4. Approximately 30% of medulloblastomas have aberrant SHH signaling and thus are referred to as SHH-activated medulloblastoma. The tumor suppressor gene *TP53* has been recently recognized as a prognostic marker for SHH-activated medulloblastoma patients; patients with mutant *TP53* have a significantly worse outcome than those with wild-type *TP53*. It remains unknown whether p53 activity is impaired in SHH-activated, wild-type *TP53* medulloblastoma which is about 80% of SHH-activated medulloblastomas. Utilizing the homozygous *NeuroD2:SmcA1* mouse model with wild-type *Trp53*, which recapitulates human SHH-activated medulloblastoma, it was discovered that the endogenous Inhibitor 2 of Protein Phosphatase 2A (SET/I2PP2A) suppresses p53 function by promoting accumulation of phospho-MDM2 (S166), an active form of MDM2 that negatively regulates p53. Knockdown of I2PP2A in *SmcA1* primary medulloblastoma cells reduced viability and proliferation in a p53-dependent manner, indicating the oncogenic role of I2PP2A. Importantly, this mechanism is conserved in the human medulloblastoma cell line ONS76 with wild-type *TP53*. Taken together, these findings indicate that p53 activity is inhibited by I2PP2A upstream of PP2A in wild-type *TP53*, SHH-activated medulloblastomas.

3.1 Introduction

Medulloblastoma is the most common malignant pediatric Central Nervous System (CNS) tumor and are a leading cause of cancer-related childhood mortality. Currently, the standard therapy comprising surgery, craniospinal radiation, and chemotherapy “cures” approximately 70% of medulloblastoma patients. However, these conventional therapeutic modalities cause long-term developmental, psychosocial, neurocognition and neuroendocrine problems, severely compromising survivors’ quality of life (219-222). Medulloblastoma has been divided into four molecular subgroups, namely WNT-activated, SHH (Sonic Hedgehog)-activated, Group 3, and Group 4, based on the gene expression profiling of patient samples (6, 7, 9). The SHH-activated subgroup comprises approximately 30% of all medulloblastoma cases. This subtype, putatively originating from malignant transformation of granule neuron progenitors during early cerebellar development, is defined by either mutation/amplification of SHH signaling activators such as *SMO* (*Smoothened*), *MYCN*, *YAP*, *E2F*, *GLI1*, *GLI2*, or deficiency/loss of SHH signaling suppressors including *PTCH* and *SUFU* (21, 24, 111, 223). The smoothened inhibitor vismodegib has been tested in clinical trials (44, 45), but its use remains controversial for several reasons, including the low percentage of tumors with *Ptch/Smoo* mutations, bone developmental toxicity of the drug, and acquired resistance post-treatment of these patients (32, 33). The detrimental outcome from standard treatment and the scarcity of effective target therapies necessitate improved understanding of tumor progression in SHH-activated medulloblastoma.

The tumor suppressor gene *TP53* has recently been recognized as a prognostic marker for SHH-activated medulloblastoma patients and a critical player in transforming precancerous lesions into advanced medulloblastoma (34, 58). WHO reclassified the SHH-activated subgroup into *TP53*-wildtype and *TP53*-mutant in 2016 (34), based on the observation that five-year overall survival of patients with *TP53*-wildtype tumors was ~ 80% while *TP53*-mutant tumor patient survival rate was ~

40% (58). Utilizing the *Ptcb*^{+/-} mouse model, which develops SHH medulloblastoma with the incidence of 14%, researchers have illustrated that homozygous deficient *Trp53* facilitates tumor formation, raising the incidence to 95% and largely reducing the latency period (59). Furthermore, Tamayo-Orrego *et al.* have shown that *Trp53* mutation or *Cdkn2a* inactivation hardwires tumor cells to evade senescence, a necessary step for advanced medulloblastoma formation in the *ptcb*^{+/-} mouse model (63). However, approximately 80% of SHH-activated, 85% of Wnt-activated, and all of group 3 and group 4 medulloblastoma patients harbor wildtype *TP53* at diagnosis, and all of these patients receive the harsh standard of treatment described above. Due to the critical role of p53 in suppressing tumor progression in SHH-activated medulloblastoma, we proposed that p53 function is compromised in medulloblastoma patients with wildtype p53. Understanding the upstream negative regulation of p53 may help identify novel therapeutic targets to treat these *TP53* wildtype patients with less aggressive modalities.

As *TP53* is not mutated in the majority of medulloblastomas, we wished to investigate whether its product p53 protein is post-translationally impaired, utilizing the homozygous genetically engineered *NeuroD2:SmoA1* (*SmoA1*) mouse model. More than 90% of *SmoA1* mice develop medulloblastoma within nine months and these tumors recapitulate human SHH-activated medulloblastoma in pathology, etiology, and molecular profiles (23, 24), with no p53 mutation reported. In mammalian cells, *wildtype* p53 is shown to exhibit a short half-life (~15min) under normal conditions due to MDM2-mediated proteasomal degradation. MDM2 (mouse double minute 2) is a p53 transcriptional target which facilitates p53 degradation by ligating ubiquitin to p53 (71). MDM2 can be stabilized and activated by an AKT-mediated phosphorylation at serine residue 166 (p-MDM2^{S166}) (76, 224, 225). This mechanism is proposed to be employed by cancer cells with aberrant PI3K/AKT signaling to sustain survival especially when these cells are exposed to external stress such as hypoxia, or intrinsic oncogenic stress. In addition to AKT-mediated phosphorylation, p-MDM2^{S166} can also be regulated

by dephosphorylation by Protein Phosphatase type 2A (PP2A). Okamoto et al. showed that PP2A dephosphorylates MDM2 at serine residues 186 and 166 in the non-small cell lung carcinoma cell line H1299 (81). However, whether PP2A dephosphorylates p-MDM2^{S166} in the context of medulloblastoma remains unknown.

PP2A is the major serine-threonine phosphatase in mammalian cells, composed of structural A, regulatory B, and catalytic C subunits. PP2A holoenzyme dephosphorylates a wide range of substrates which mediate oncogenic signaling, such as p-AKT, p-ERK, and thus has been proposed to be a tumor suppressor (226). Inactivation by viral oncoproteins, mutations in various regulatory B subunits, or the overexpression of its endogenous inhibitors contributes to the dysregulation of PP2A, thus facilitating tumor development and maintenance. As no mutation of PP2A subunits has been associated with SHH medulloblastoma to date ([r2.amc.nl](https://doi.org/10.1002/ajmg.b.32401)), we determined to investigate its endogenous inhibitors including Inhibitor 1 of PP2A (I1PP2A), Inhibitor 2 of PP2A (I2PP2A). I1PP2A and I2PP2A are non-competitive inhibitors of PP2A. I2PP2A, a product of the *Set* gene, has been shown to be elevated in cancers, such as leukemia, prostate cancer, and head and neck small cell carcinoma (83-85, 103, 227, 228). However, whether any of these endogenous inhibitors is upregulated and whether the upregulated inhibitor could interfere with p53 signaling in medulloblastoma has not been addressed.

Utilizing the *NeuroD2:SmoA1* mouse model, we first validated that p53 is functional in this mouse SHH-activated medulloblastoma. When we treated primary medulloblastoma cells derived from these *SmoA1* mice with Nutlin-3a, which disrupts the interaction between p53 and MDM2, thus suppressing MDM2 function, we observed a dose-dependent stabilization of p53, upregulated expression of p53's transcriptional targets, and induced apoptosis. Next, we observed increased protein levels of I2PP2A and upregulated phosphorylation of p-MDM2^{S166}, implying I2PP2A could suppress p53 function

mediated through p-MDM2^{S166}. We tested this possibility using pharmacological suppression and lentiviral knockdown of I2PP2A in these cells; I2PP2A suppression caused PP2A activation, lower levels of p-MDM2^{S166}, and increased p53 in an AKT-independent manner; I2PP2A knockdown reduced p-MDM2 levels, and reactivated p53 function. Importantly, this mechanism is conserved in patient-derived SHH-activated and *TP53*-wildtype medulloblastoma cell line ONS76. Taken together, our findings indicate that in SHH-activated p53-wildtype medulloblastoma, upregulated endogenous I2PP2A suppresses p53 activity through promoting accumulation of p-MDM2^{S166}. Moreover, our studies raise the possibility of targeting I2PP2A as novel therapeutic approach to preserve p53 activity, thereby promoting improved response to therapy and perhaps indicating a de-escalation of radiation and chemotherapy.

3.2 Materials and Methods

Animal studies

NeuroD2:Sm α 1 (87, 88) mice were obtained from Jackson Research Laboratories. Breeding, maintenance, and tumor harvest were carried out in compliance with the Emory University Institutional Animal Care and Use Committee guidelines. Active *Sm α 1* in these mice corresponds to patient mutant form SmoM2.

Medulloblastoma primary cell culture

Medulloblastoma cells (MBCs) were isolated from *NeuroD2:Sm α 1* mouse tumors and cultured as described in (31, 229). Cells were seeded on poly-D-lysine (SIGMA) and geltrex (Gibco) coated plates with Neurobasal medium containing Pen/Strep, 1mM Sodium Pyruvate, 1X B27 supplement, and 2mM L-Glutamine. Primary MBCs were cultured for 24hours before drug or lentivirus treatment. Lysates or RNA from MBCs were prepared following drug treatment or virus infection.

Patient data analysis

Patient data analyzed for I2PP2A expression is available. A total of 97 patients samples were subgrouped into WNT-activated, SHH-activated, Group 3 and Group 4 medulloblastomas. Control samples include 5 adult cerebella samples, and 4 fetal cerebella samples. RNA sequencing data is available via the European Genome-phenome Archive (EGA; <https://www.ebi.ac.uk/ega/home>) accession number EGAD00001001899. Fastq files were processed using the STAR alignment tool (Dobin et al., 2013) and normalized using the RSEM package (Li and Dewey, 2011) based upon the hg19 reference genome and the GENCODE v19 gene annotation set. Gene transcript level expression was quantified in units of TPM and gene-level expression was quantified in units of FPKM. Differential expression of SET/I2PP2A was analyzed statistically using the Wilcoxon Rank Sum test.

PP2A subunit isoforms interrogation was performed through R2 website (r2.amc.nl), which provides the database of a cohort named Medulloblastoma 500. After login to R2 website, on the left panel, one can navigate through “Change Data Scope>Paper>Medulloblastoma 500”. Then after clicking on “Goto Medulloblastoma 500 home”, one can search through Genome Browser to interrogate whether mutations were detected of a specific gene from the Pfister 167 cohort genome profiles. Two isoforms of structural A subunit (PPP2R1A, PPP2R1B), twelve isoforms of regulatory B (PPP2R2B, PPP2R2C, PPP2R2D, PPP2R3A, PPP2R3B, PPP2R3C, PPP2R4, PPP2R5A, PPP2R5B, PPP2R5C, PPP2R5D, PPP2R5E), two isoforms of catalytic C (PPP2CA, PPP2CB) were subjected to mutation analysis through the Genome Browser mentioned above.

Human medulloblastoma cell lines

Daoy (ATCC Cat# HTB-186, RRID: CVCL_1167), UW228 (RRID: CVCL_8585) and ONS76 (JCRB Cat# IFO50355, RRID: CVCL_1624) cell lines were gifted by Tobey J. MacDonald, Emory University (230-232). Cells were cultured as described previously (233). Cells were infected with lentiviruses 24 hours post seeding and lysates or RNA were prepared 72 hours post infection.

Drugs and Peptide

Nutlin-3a (Selleck Chemicals-S8059) was resuspended in ethanol (234), with final concentrations of 2.5uM, 5uM, and 10uM administered as indicated. COG112 (Biotin-RQIKIWFQNRRMKWKKCLRVRLASHLRKLRKRL-amide) was obtained from NeoBiolab and resuspended in water, with final concentration of 200nM. Pifithrin (TOCRIS) and Wortmannin (SIGMA-W1628) were reconstituted in DMSO and used at 200nM.

Antibodies

The following primary antibodies were used for western blot: β -tubulin (SIGMA, T4026, RRID:AB_477577), β -actin (CST #4970, RRID:AB_2223172), I2PP2A (sc-5655, RRID:AB_650246), I2PP2A (described below), I1PP2A (ab5991, RRID:AB_2056306), PP2A C subunit (CST #2038, RRID:AB_10693604), p19^{ARF} (sc-1665), Nmyc (sc-56729, RRID:AB_2266882), CyclinD2 (sc-593, RRID:AB_2070794), p-MDM2^{S166} (CST #3521, RRID:AB_2143550), MDM2 (ab16895, RRID:AB_2143534), p53 (CST #2524, RRID:AB_331743), Akt (CST #9272, RRID:AB_329827), p-AKT Ser473 (CST #9271, RRID:AB_329825), p-AKT T308 (CST #4056, RRID:AB_331163).

Rabbit polyclonal I2PP2A antisera was generated using keyhole limpet hemocyanin (KLH)-conjugated peptide DP51 as the immunogen. Peptide DP51 (TKRSSQTQNKASRKRQHEEPESC) corresponds to the first 22 residues of mouse/human/rat I2PP2A variants, with an additional carboxyl-terminal cysteine for coupling to KLH. Peptides were conjugated to KLH using the KLH conjugation kit (Pierce) according to the manufacturer's instructions.

Primary antibodies for immunofluorescence staining include I2PP2A (described above), PCNA (Calbiochem, NA03, RRID: AB_213111), turboGFP (OriGene TA150041, RRID: AB_2622256) and BrdU (ab6326, RRID: AB_305426).

HRP-conjugated secondary antibodies for western blot include: Goat anti- Rabbit IgG HRP (ThermoFisher Scientific, 31460, RRID: AB_228341), Rabbit anti-Goat IgG HRP (ThermoFisher, Cat# 31402, RRID: AB_228395), and Peroxidase AffiniPure Fragment Donkey Anti-Mouse IgG (cat# 715-036-150, RRID: AB_2340773). Alexa Fluorophore conjugated secondary antibodies for immunofluorescence staining: Donkey anti- Rabbit Alexa 594 (ThermoFisher, A21207, RRID: AB_141637), Donkey anti- Mouse Alexa 488 (ThermoFisher, A21202, RRID: AB_141607), Donkey anti- Mouse Alexa 594 (ThermoFisher, A21203, RRID: AB_2535789) and Donkey anti- Rabbit Alexa 488 (ThermoFisher, A21206, RRID: AB_2535792)

Virus production and infection

Lentiviruses and retroviruses were produced in 293RTV packaging cells as described in (21). 293RTV cells were co-transfected with VSVg, Delta 8.9 and pLKO.1-CMV-TurboGFP-shRNA (SIGMA) to produce lentivirus, or with MSCV-ires-GFP (MiG), MSCV-ires-DDp53-GFP (MiG-DDp53), MSCV-ires-DNp53-GFP (MiG-DNp53) and pCL-Eco (gifted by Christopher C. Porter) to produce retroviruses (235, 236). TRCN0000077183 and TRCN0000433634 (indicated as #1 and #5 respectively) shRNA targeting I2PP2A demonstrated the most efficacy and were used in both primary MBCs and patient-derived SHH medulloblastoma cells. PLKO.1-CMV-turboGFP-scrambled shRNA (SHC003) was used as a control, while MiG was the retroviral control. Virus supernatants from these 293RTV cells were pooled and concentrated. Cells were exposed to viruses for 3hrs and collected 72hrs post-infection.

Protein preparation and western blot

Protein lysates were prepared from mouse tumor, neighboring cerebellum, primary *SmoA1* cell cultures, or human medulloblastoma cell lines. Tissues were homogenized and lysed in lysis buffer comprised of 50mM HEPES, 150mM NaCl, 1mM EDTA, 2.5mM EGTA, 1% Tween 20, 10% Glycerol, 1mM DTT, and a protease inhibitors cocktail, and phosphatase inhibitors. 15-30 μ g of each sample was denatured and separated in 10-12% polyacrylamide gels, then transferred to immobilon-P membranes (Millipore)(237). The same amount of each sample was loaded to different gels in parallel, to avoid unequal loading. For quantification purposes, chemiluminescent signals were normalized to that of β -actin/ β -tubulin on the same blot.

RNA extraction and real-time PCR

RNA was isolated using QIAGEN RNAsasy kit. Quantitative real time PCR was performed as described in (238). Primers for *Gusb*, *Actb*, *Mycn*, *Ccnd2*, *Gli1*, *Gli2*, *Trp53*, and *Mdm2* were purchased

from Bio-rad. Primers for *Bax* (Forward: CTCAAGGCCCTGTGCACTA Reverse: AGCCACCCTGGTCTTGGAT), *Bid* (Forward: AAACCTTTGCCTTAGCCCGT Reverse: AGCAGGTCTGTGATGTGCTC), *Plk2* (Forward: ACAGTGGCAAGAGTCCTTCG Reverse: AGCCCCGTTGTTGAAAAGGA), *Cdkn1a* (Forward: CCAAGCCATTCCATAGGCGT Reverse: GCCAAGGGGAAGGACATCAT), *Bbc3* (Forward: ACCATCTCAGGAAAGGCTGC Reverse: GCTAGTGGTCAGGTTTGGCT), and *Set* (Forward: GCCAAAGCCAGTAAAAAGGAG Reverse: AAAATGGTTGGCGGAGTTTGT), were designed using Primer-BLAST from NCBI and acquired through Eurofins Scientific. Primers from Eurofins were validated by analyzing PCR products on agarose gels. *Gusb* and *Actb* mRNAs were used as internal controls.

Flow Cytometry

Primary MBCs were dissociated by Accutase (STEMCELL Technologies), fixed in 70% ethanol, treated with RNase (100ug/mL), and then stained by Propidium Iodide (50ug/mL). Interrogation was performed using CytoFLEX platform (Beckman Coulter) with CytExpert software. Analysis of data was performed using FlowJo software.

HE and immunofluorescence staining

Hematoxylin and Eosin (HE) staining were performed as described previously in (135). Mice were euthanized and perfused with 4% paraformaldehyde solution. Paraffin embedding and processing were performed at Winship Pathology Core of Emory University. 5 μ m sections were prepared using a LEICA microtome and stained following the standard immunostaining protocol. The I2PP2A antibody produced in this study and PCNA antibody were used as the primary antibodies for immunofluorescence (IF). Alexa-fluorophore-conjugated secondary antibody was used. Whole slide scanning of *SmoA1* mouse cerebellum and tumor was performed through Winship Pathology Core of

Emory University using Hamamatsu's Nanozoomer, with 40X objective. Images were analyzed using ImageScope.

PP2A C Activity Assay

PP2A C activity assay was performed using Millipore PP2A Immunoprecipitation Phosphatase Assay Kit (# 17-313) and following the manufacturer's protocol. The PP2A C subunit from cell lysates was immunoprecipitated by the PP2A C antibody and then exposed to the substrate containing threonine phosphopeptide. Free phosphates were produced from threonine phosphopeptide by catalysis of precipitated PP2A C. Absorbance at 650nm wavelength indicating free phosphates concentrations was measured by a plate reader. Relative activity was calculated based on the standard curve.

MTT Viability Assay

MTT (3-(4,5-dimethylthiazol-2-yl)2,5-diphenyltetrazolium bromide) reagent (#1758430) was purchased from Thermo Fisher and used according to the manufacturer's instructions. Briefly, 12mM MTT was added to medulloblastoma cells in a 96-well plate with various experimental treatments. 10%SDS and 0.01M HCl were then added to dissolve formazan generated by viable medulloblastoma cells. Absorbance at 570 nm indicating formazan concentration was measured using a plate reader.

BrdU Incorporation Assay

MBCs were cultured on coverslips (Thermo Fisher #1) and infected with lentiviruses or retroviruses. 72hrs later, cells were pulsed with 10ug/ml BrdU reagent (Fisher) for 2hrs before 4% paraformaldehyde fixation. Then MBCs were exposed to 2N HCl for 30min, followed by standard immunofluorescence staining procedures. Immunofluorescence images of BrdU assay were captured by a fluorescence microscope Leica DM2500 with the software Leica LAS X. Positive staining was quantified using CellProfiler.

Statistical Analysis

All data shown were generated from independent experiments as indicated by *n*. G-power analysis was used to determine the sample size for all experiments. *SmoA1* mice were randomized for experiments, in respect of sex, age and body weight. One representative western blot result was shown from at least three replicates. Representative immunofluorescence images from at least 4 fields were shown. Statistical analysis was performed using student's t-test, one-way, or two-way *ANOVA* for data comparisons among different groups. Human patient expression data comparison were performed using Kruskal-Wallis Sum test. Graphs and p-values were generated using GraphPad Prism. Differences between groups were identified as statistically significant at levels indicated by p-values (asterisks).

3.3 Results

p-MDM2^{S166} is upregulated in *Trp53*-wildtype SHH-activated medulloblastoma.

We wished to determine whether p53 function is compromised in SHH-activated medulloblastoma using the *Trp53*-wildtype *SmoA1* mouse model. We first validated that p53 can be activated in *SmoA1* mouse tumor tissues. Primary medulloblastoma cells from four individual *SmoA1* mice were challenged with the MDM2 inhibitor Nutlin-3a. As illustrated in **Figure 3.1 a**, we observed a dose-dependent stabilization of p53 4 hours post Nutlin-3a treatment, indicating that MDM2 is a major negative regulator of p53 protein levels in *SmoA1* SHH medulloblastoma cells. To confirm that the stabilization of p53 led to the restoration of p53 transcriptional activity, we measured the expression of p53 downstream target genes *Bax*, *Bbc3*, *Bid*, *Bid*, which can promote cellular death, as well as *Cdkn1a*, which promotes cell cycle arrest. As shown in **Figure 3.1 b**, p53 targets *Mdm2*, *Bax*, *Cdkn1a*, and *Bbc3* were significantly upregulated 24 hours after Nutlin-3a treatment in a dose-dependent manner, suggesting that the wildtype function of p53, namely transcriptional activation of pro-cell death and growth-arresting markers, is conserved in these *SmoA1* tumors. Furthermore, we performed MTT assays and found that medulloblastoma cell viability was reduced 48 hours after p53 activation by Nutlin-3a in a dose-dependent manner (**Fig. 3.1 c**). The reduced viability resulted from induced apoptosis and cell cycle arrest as illustrated by Supplemental Figure 1, where we observed induced cleaved caspase 3 (Supplemental **Fig. S3.2 b**), more sub-G1 phase cell populations (**Fig. S3.1 a**), and decreased G2 phase cells (**Fig. S3.1 c**), which could be facilitated by activated p53 transcriptional targets.

It has been shown that SHH signaling inhibits p53 activity and that p53 suppresses the SHH-driven mitogenic activity mediated by Gli transcription factors, forming an inhibitory loop to regulate

stemness of cancer cells and thus control cell numbers (75, 144). Abe et al. showed that activated smoothed SmoM1, SmoM2 in Saos-2 cells drives accumulation of p-MDM2^{S166} and promotes rapid degradation of p53 (75). Consistent with this, Malek et al. proposed that Sonic hedgehog promotes p-MDM2^{S166} and the stabilization of MDM2, while MDM2 deficiency deactivates SHH downstream targets such as *Gli1*, *Nmyc* and *Cnd2* (74). Moreover, Stecca and Ruiz demonstrated that the GLI-p53 inhibitory loop controls neural precursor cell numbers (144). Thus, we analyzed the expression of SHH downstream targets (*Gli1*, *Gli2*, *Mycn* and *Cnd2*) to determine if SHH signaling was impacted by p53 reactivation. We observed that SHH target mRNAs including *Gli1*, *Gli2*, and *Mycn*, but not *Cnd2*, were reduced when MDM2 was inhibited by Nutlin-3a (**Fig. 3.1 d**), supporting that p53 stabilization leads to SHH signaling activity decrease.

Though Malek et al. showed that exogenous SHH upregulated p-MDM2^{S166} and MDM2 in cerebellar granule neuron precursors, the proposed cells-of-origin for SHH medulloblastoma, whether SHH medulloblastoma tissues feature elevated p-MDM2^{S166} or MDM2 remains unknown. We analyzed MDM2 mRNA expression and protein levels in *SmoA1* tumor tissue. As shown in **Figure 3.1 e**, and **3.1 f**, MDM2 total mRNA and protein levels were reduced in *SmoA1* tumor (MB) as compared to neighboring cerebellum (CB). However, despite the reduced levels of total MDM2, we observed a substantial increase of MDM2 phosphorylation at the serine 166 residue in tumor tissue (**Fig. 3.1 f**). P-MDM2^{S166} has been shown to be stabilized and suppress p53 (75, 76). Oncogenic stress in SHH medulloblastoma could induce p53 in the tumor tissue, which may explain why we observed upregulated p53 expression in medulloblastoma tissue (**Fig. 3.1 e**). Both MDM2 and p-MDM2^{S166} proteins that we referred to were detected by westerns approximately at 90kDa (**Fig. S3.2**). However, a band between 102kDa and 150kDa was also considered positive and correlates positively with 90kDa band in all experiments described.

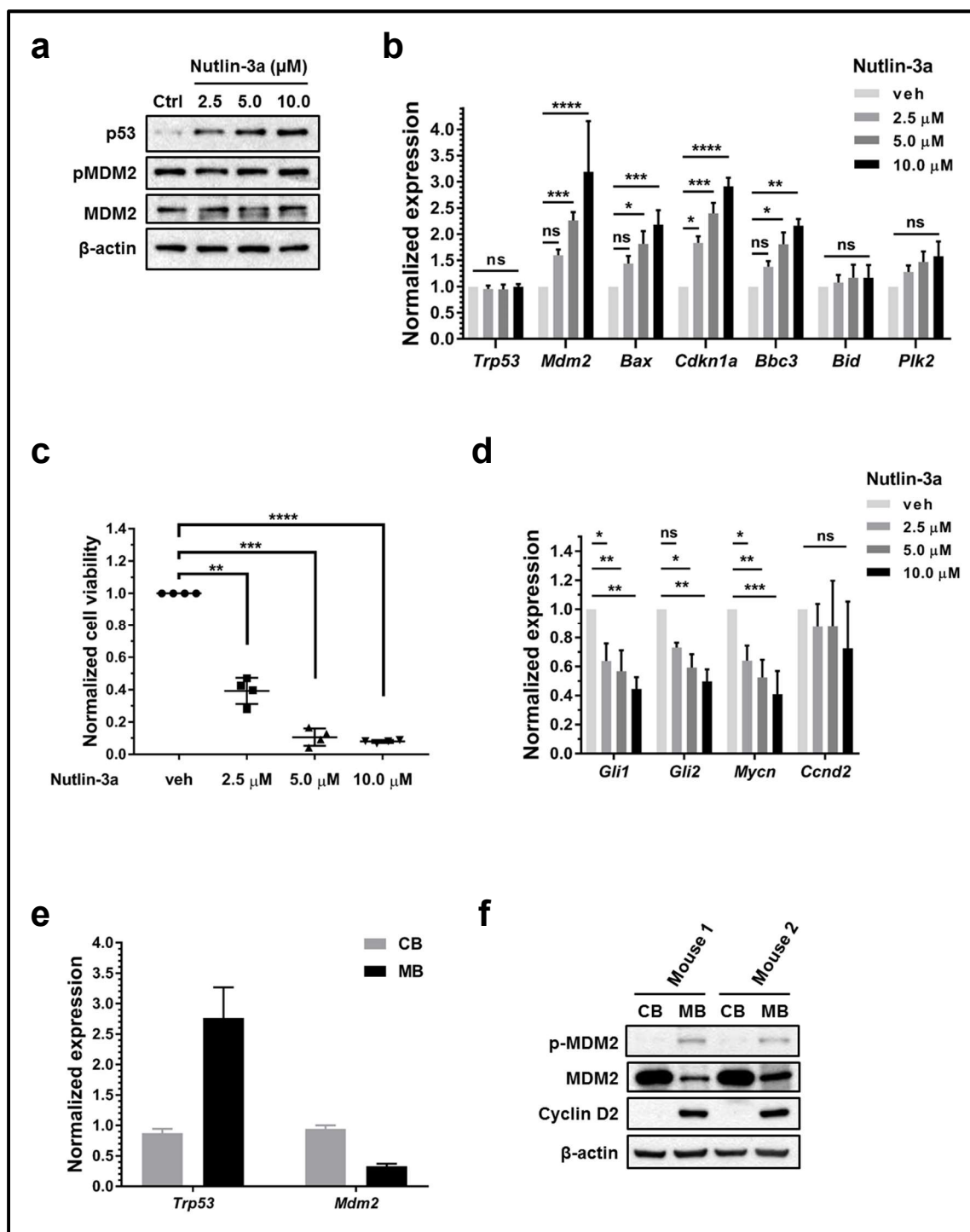


Figure 3.1. p-MDM2S166 is upregulated in Trp53-wildtype SHH-activated medulloblastoma.

a-d, Wildtype p53 can be reactivated in SmoA1 primary medulloblastoma cells. Nutlin-3a, an inhibitor

of MDM2, was added to primary medulloblastoma cells (MBCs) isolated from SmoA1 mice, at 2.5 nM, 5.0 nM, and 10.0 nM, ethanol as control vehicle. **a**, 4 hours later, cell lysates were collected, and western blots were performed to check p53, p-MDM2 and MDM2, n=3. **b** and **d**, 24 hours later, RNA from primary MBCS was purified and QPCR was performed to measure changes of p53 transcriptional target mRNA, and SHH signaling downstream target mRNA, mean \pm S.E.M., n=3, * $p<0.05$; ** $p<0.01$; *** $p<0.001$; **** $p<0.0001$. **c**, 48 hours later, MTT assay was performed to check viability of MBCs, mean \pm S.E.M., n=4, * $p<0.05$; ** $p<0.01$; *** $p<0.001$. **e**, Qualitative RT-PCR showed lower MDM2 mRNA and higher p53 mRNA in MB than that in CB tissues, mean \pm S.E.M., n=3. **f**, Western Blot showing upregulated p-MDM2 (Ser166) in medulloblastoma (MB) than neighboring cerebellum (CB). β -actin as loading control, CyclinD2 as positive control indicating good isolation of tumor tissue from neighboring cerebellum. Tissue lysates from four SmoA1 mice were analyzed, and representative images of two are shown.

Inhibitor 2 of Phosphatase 2A is elevated in SHH medulloblastoma.

Because PP2A is a serine/threonine phosphatase which can dephosphorylate MDM2 at Ser166 (81), we wished to determine whether PP2A activity is dysregulated in SHH medulloblastoma. We interrogated the most common PP2A subunit isoforms in the cohort named “Medulloblastoma 500” through the R2 (r2.amc.nl) genome browser and detected no mutations. As no mutation of PP2A subunits has been reported to date, we analyzed levels of its endogenous inhibitors I1PP2A, and I2PP2A, as well as the PP2A catalytic C subunit. As shown in **Figure 3.2 a-b**, we observed a significant ~100-fold increase of I2PP2A protein in comparison to adjacent non-tumor cerebellum tissue but no significant difference in the other PP2A inhibitor or PP2A C subunit (n=6). The relatively higher I2PP2A correlates positively with increase p-MDM2S¹⁶⁶ in tumor tissues (**Fig. 3.2 a**). When we examined I2PP2A localization, we observed intense I2PP2A staining in tumor cells (below dashed line) as compared to cells of the neighboring internal granule layer, where mature granule neurons reside (**Fig. 3.2 c**, n=4). In the tumor tissue (above dashed line), I2PP2A staining co-localizes with the proliferation marker PCNA, proliferating cell nuclear antigen, as shown in **Figure 3.2 d**.

Interestingly, we did not detect significantly higher I2PP2A (*Set*) mRNA in *SmoA1* tumors (**Fig. 3.2 e**). We analyzed patient SHH medulloblastoma gene expression data (n=50) (**Fig. S3.3**), and observed a slight I2PP2A mRNA increase (1.3 fold) relative to control samples (n=9), and this increase was marginally significant ($p=0.02759$, Wilcoxon Rank Sum test). The mRNA expression of I2PP2A in the SHH subgroup was on par with expression in the other medulloblastoma subtypes (1.37 in Group 3 vs controls (p value=0.003716; 1.25 in Group 4 vs controls (p value =0.016)). This implies that 1) I2PP2A may also show increased levels in other medulloblastoma subtypes with wildtype p53, and 2) the upregulation of I2PP2A in SHH subgroup is possibly caused by post-transcriptional stabilization. As I2PP2A has never been studied in SHH medulloblastomas, we characterized this

protein as shown in **Figure S3.4**. Because PP2A has been proven to suppress cellular proliferation in most of the research, overexpression of I2PP2A was proposed to be oncogenic in tumors mentioned above. As shown in **Figure S3.4 a and b**, both isoforms of I2PP2A protein were localized in both the nucleus and cytoplasm of tumor tissue, as well as primary medulloblastoma cells (MBCs), isolated from the NeuroD2:SmoA1 mice. The co-staining of I2PP2A with PP2A in the cytoplasm of primary medulloblastoma cells from NeuroD2:SmoA1 mice suggested the possible interaction between I2PP2A and PP2A. When we analyzed the patient mRNA expression data (in collaboration with Sorana Morrissy and Hamza Farooq, from Michael D. Taylor's Lab), we observed a slight upregulation of I2PP2A as compared to control samples (normal tissue from surgery of infant and adult patients) ($p=0.019$) as shown in **Figure S3.4 c**. Furthermore, the 5-year overall survival of I2PP2A-high ($n=7$) patients was only $\sim 40\%$, worse than $\sim 70\%$ observed in I2PP2A-low ($n=15$) SHH medulloblastoma patients, indicating that I2PP2A expression may have prognostic value. Brief characterization of I2PP2A in SHH medulloblastomas suggested this protein showed both nuclear and cytoplasmic distributions in medulloblastoma cells. Furthermore, the expression (mRNA) of I2PP2A showed an upregulation in all subgroups of medulloblastomas as compared to control samples. The colocalization of I2PP2A with PP2A in the cytosol of mouse SHH medulloblastoma cells suggests a possible interaction between these two proteins which needs further investigations. Importantly, although within a small cohort of SHH medulloblastoma patients, the high-I2PP2A expression group of patients showed worse 5-year overall survival as compared to patients with low-I2PP2A expression. In summary, we detected increased I2PP2A protein in SHH medulloblastoma tissue, which is not likely due to mRNA upregulation. The concomitant upregulation of p-MDM2 and I2PP2A protein in *SmoA1* tumor tissue we observed suggests that I2PP2A could be involved in upregulating p-MDM^{S166} in *SmoA1* tumors.

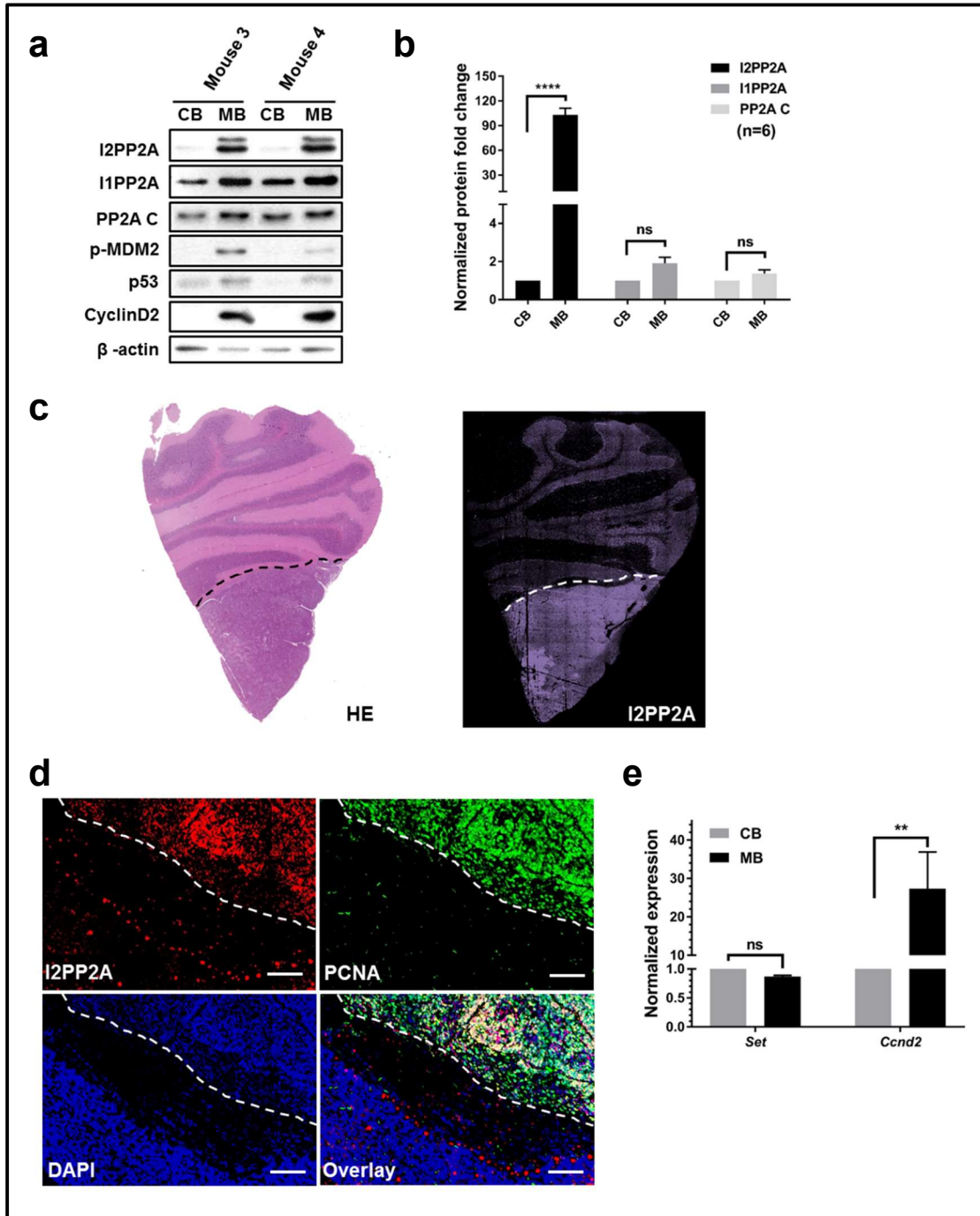


Figure 3.2. Inhibitor 2 of Phosphatase 2A is elevated in SHH medulloblastoma. **a-b**, western blot showing significant upregulation of I2PP2A, but not I1PP2A in SmoA1 medulloblastoma (MB) vs. neighboring cerebellum (CB). Tissue lysates from six SmoA1 mice were analyzed. **a**, representative

results. **b**, quantification and data analysis of western blot results (normalized), mean \pm S.E.M., n=6, **** $p < 0.0001$. **c**, Immunofluorescence staining of paraffin section shows elevated I2PP2A distributed in SmoA1 tumor tissue. Foliated tissue above dashed line represents normal cerebellum, while tumor tissue is below. SmoA1 mice (n=5) were sacrificed for sample analysis. One representative staining of a 5 μ m section of a horizontal plane is shown. Left, hematoxylin and eosin (HE) stained; right, immunostained with I2PP2A antibody. **d**, Co-localization of I2PP2A with proliferative marker PCNA by immunofluorescence staining on paraffin sections with tumor above the dashed line, and neighboring cerebellum below the dashed line. n=4, scale bar, 100 μ m. One representative image from four random fields were shown. **e**, Qualitative PCR indicating no significant increase of I2PP2A (Set) mRNA in MB than that of CB, Ccnd2 mRNA as positive control, mean \pm S.E.M., n=4, ** $p < 0.01$.

Pharmacological inhibition of I2PP2A results in MDM2 dephosphorylation and p53 stabilization.

To determine whether I2PP2A regulates p-MDM2^{S166}, we utilized COG112, a chimeric peptide shown to inhibit I2PP2A by disrupting the interaction between I2PP2A and PP2A (239). As shown in **Figure 3.3 a**, when primary medulloblastoma cells were challenged with COG112, we observed a reduction of p-MDM2^{S166} and total MDM2 as well as an increase of p53 protein in a time-dependent manner, indicating that I2PP2A regulates p-MDM2^{S166} to affect p53 levels in SHH medulloblastoma. Medulloblastoma cell viability/morphology were not affected significantly (**Fig. S3.5 a**) 8 hours post-COG112 treatment, indicating that the stabilization of p53 is not induced by off-target toxicity caused by COG112. To further validate the effects caused by COG112 are dependent on PP2A C activity, we employed a selective PP2A inhibitor, okadaic acid. As shown in **Figure 3.3 b**, reduced p-MDM2 levels in the presence of COG112 were rescued by okadaic acid, as were total MDM2 levels. We also observed destabilized p53 when we added okadaic acid. Consistent with COG112 blocking I2PP2A activity, we observed recovery of PP2A C activity after COG112 treatment, which was suppressed by concomitant okadaic acid treatment (**Fig. 3.3 c**).

The kinase AKT is also a substrate of PP2A and promotes p-MDM2^{S166} accumulation (240). We therefore asked whether the reduction of p-MDM2^{S166} is caused by PP2A-mediated impairment of p-AKT activity or directly by PP2A. Surprisingly, however, we observed increased p-AKT^{T308} and p-AKT^{S473} in a time-dependent manner as shown in Supplemental **Figure S3.5 b**, in the presence of COG112. Therefore, it is more likely that MDM2 dephosphorylation was caused by increased PP2A activity but not decreased p-AKT in this time frame post treatment. Upstream inhibition of the PI3K pathway resulted in reduced p-MDM2^{S166} and total MDM2 (**Fig. S3.5 c**), indicating the PI3K pathway also regulates p-MDM2 levels in SHH medulloblastoma; but in the COG112 treatment experiment, the effects caused by I2PP2A suppression are more dominant than the effects caused by PI3K/p-

AKT signaling. Taken together, our findings indicate that p-MDM2^{S166} negatively regulates p53 levels and is subject to the direct and indirect (via AKT) regulation by PP2A, and that PP2A activity was suppressed by upregulated I2PP2A in SHH medulloblastoma cells (**Fig. S3.5 d**).

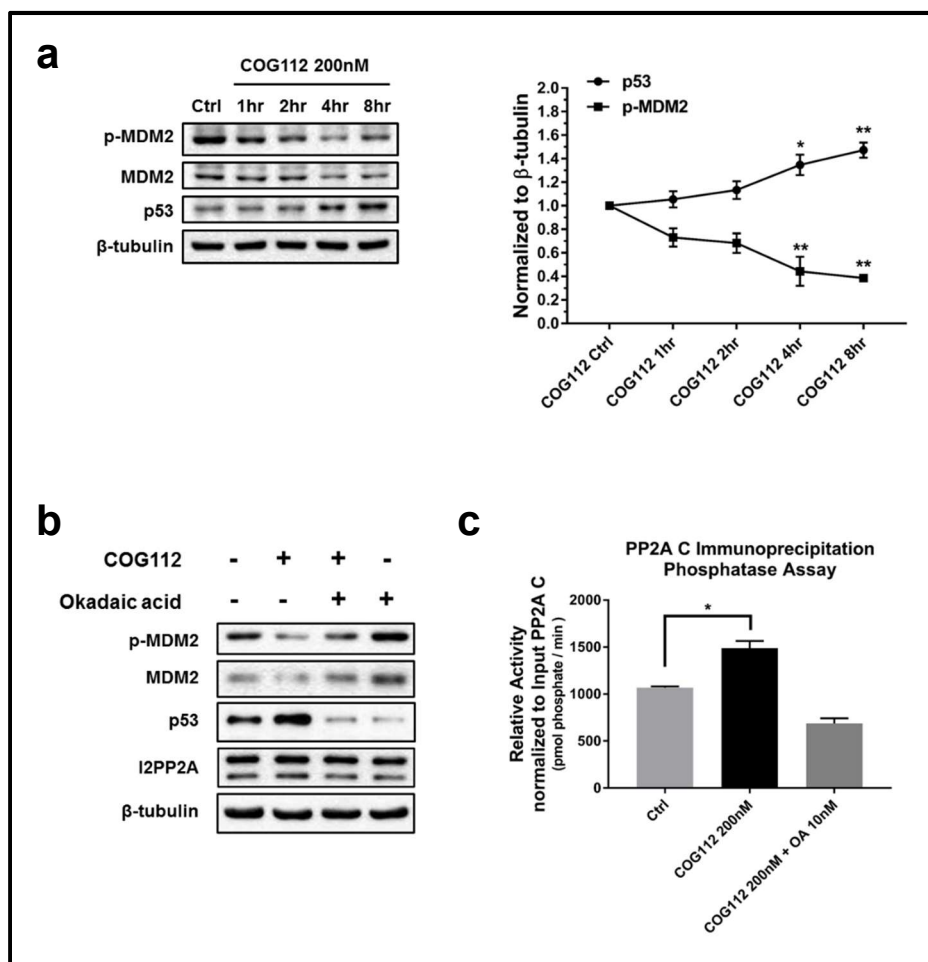


Figure 3.3. Pharmacological inhibition of I2PP2A results in MDM2 dephosphorylation and p53 stabilization. COG112, a peptide inhibitor of I2PP2A was used at 200nM to treat primary medulloblastoma cells from SmoA1 mice. **a**, cell lysates were prepared at different time points post drug treatment. Left, western blot showing a time-dependent decrease of p-MDM2, total MDM2, and time-dependent increase of p53 protein; right, quantification of p-MDM2 to β -tubulin, p53 to β -tubulin ratio, mean \pm S.E.M., $n=3$, * $p<0.05$; ** $p<0.01$. **b-c**, 200nM COG112 or 10uM okadaic acid was added independently or in combination to primary MBCs, 4 hours later, samples were collected for western or PP2A C activity assay, $n=4$. **b**, western blot showing decrease p-MDM2 and total MDM2 can be rescued in the presence of okadaic acid, $n=4$. **c**, PP2A activity assay showing that

PP2A C activity increase caused by COG112 could be reverted by okadaic acid treatment, okadaic acid only treatment values were subtracted, mean \pm S.E.M., n=4, ** $p < 0.01$.

I2PP2A knockdown decreases p-MDM2^{S166}, cell viability, and proliferation of *SmoA1* tumor cells.

As I2PP2A co-localizes with proliferating cells in SHH mouse medulloblastoma and compromises the tumor suppressor p53 through p-MDM2^{S166}, we wished to investigate whether I2PP2A is required for proliferation and survival of these cells. We therefore analyzed the proliferation rate and viability of these SHH primary medulloblastoma cells after I2PP2A abrogation. We utilized turbo-GFP tagged lentiviruses to knock down *I2pp2a/Set* in primary medulloblastoma cells and used scrambled shRNA turboGFP lentivirus-infected cells as a control. As shown in **Figure 3.4 a**, cells infected with scrambled, #1 I2PP2A shRNA or #5 shRNA containing lentiviruses showed comparable turboGFP expression. We also observed reduced p-MDM2, MDM2 and induced p53 in I2PP2A knockdown cells but not in scrambled-control medulloblastoma cells (**Fig. 3.4 a**), which is consistent with the results of I2PP2A inhibition by COG112.

Like the MDM2 inhibitor Nutlin-3a, I2PP2A knockdown reduced the viability of medulloblastoma cells, illustrated in **Figure 3.4 b**. Furthermore, I2PP2A knockdown significantly reduced cell proliferation as determined by BrdU incorporation (**Fig. 3.4 c**). To determine whether I2PP2A knockdown reactivated p53, we analyzed protein levels of p53 and its downstream target gene expression, and observed a stabilization of p53 and significant rescue of p53 targets (**Fig. 3.4 d**). Simultaneously, we detected significantly reduced SHH target gene expression in I2PP2A knockdown MBCs (**Fig. 3.4 e**). In summary, I2PP2A knockdown decreases p-MDM2 and MDM2, and reduces viability and proliferation rate of primary medulloblastoma cells, while rescuing p53 protein levels and its activity.

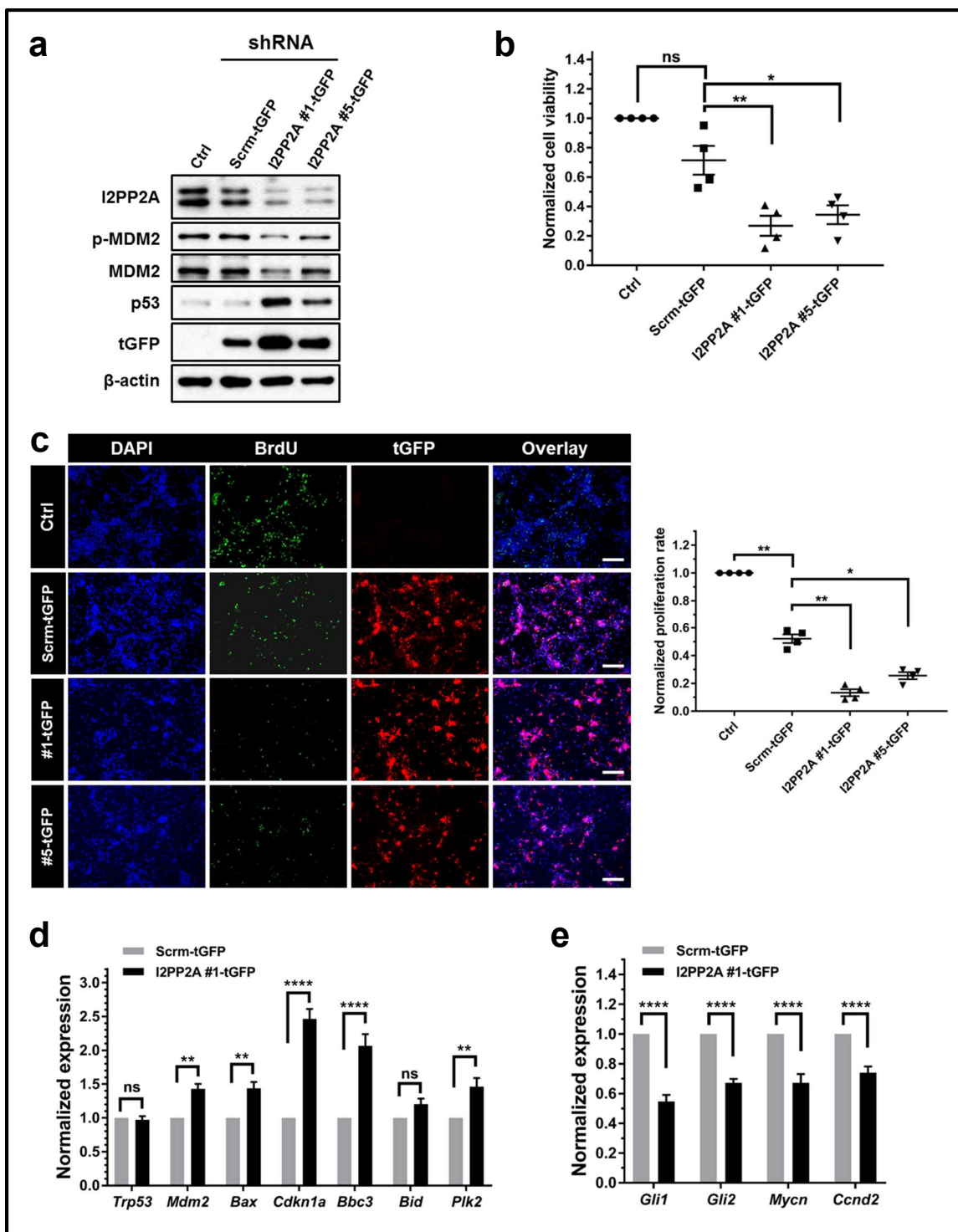


Figure 3.4. I2PP2A knock-down decreases p-MDM2S166, cell viability and proliferation of SmoA1 tumor cells. a, knockdown of I2PP2A reduced p-MDM2, total MDM2 and stabilized p53.

tGFP tagged lentiviruses containing scrambled shRNA or I2PP2A shRNA were added to primary MBCs for infection (MOI=8). Western blot for I2PP2A, p-MDM2, total MDM2 and turboGFP levels was performed 48 hours post-infection. tGFP levels show comparable infection efficiency of control scrambled and I2PP2A shRNA lentiviruses. Two different shRNAs targeting I2PP2A/Set gene were used as indicated by I2PP2A #1-tGFP and I2PP2A #5-tGFP. **b**, MTT assay indicated reduced viability in I2PP2A knockdown MBCs, mean \pm S.E.M., n=4, * $p<0.05$; ** $p<0.01$. **c**, BrdU incorporation assay in combination with tGFP staining showed lower proliferation rate in I2PP2A knockdown MBCs as compared to scrambled control cells. Left, representative images showing BrdU incorporation 48 hours post infection; green, BrdU; red, turboGFP. Right, statistical analysis of BrdU percentage from independent experiments; mean \pm S.E.M., n=4, * $p<0.05$; ** $p<0.01$. Scale bar, 100 μ m. **d-e**, p53 and its target mRNAs (**d**) or SHH signaling downstream mRNAs (**e**) in I2PP2A knockdown MBCs showed upregulation of p53 target gene expression and downregulation of SHH signaling targets, mean \pm S.E.M., n=3, * $p<0.05$; ** $p<0.01$; **** $p<0.0001$.

I2PP2A knockdown effects on SHH MBCs are dependent on p53.

To further investigate whether p53 activity is required for the effects caused by I2PP2A knockdown, we employed the p53 inhibitor pifithrin, or the retrovirus-mediated overexpression of two unique dominant-negative p53 proteins (designated as DDp53 and DNp53, GFP tagged), to block p53 function, concomitant with I2PP2A knockdown. As shown in **Figure S3.6 a and S3.6 b**, we performed successful lentiviral transduction in *SmoA1* MBCs in both the pifithrin treated cells and dominant negative p53 co-infected cells, as indicated by tGFP and GFP expressions. We found that pifithrin significantly abrogated the upregulation of p53 targets in I2PP2A knockdown cells but not in scrambled control cells (**Fig. 3.5 a**), and also reverted the reduction of SHH target gene expressions in I2PP2A knockdown cells (**Fig. 3.5 b**). When we overexpressed dominant-negative p53s, together with I2PP2A knockdown, we observed increased proliferation as compared to that of I2PP2A knockdown alone (**Fig. 3.5 c**). In addition, the introduction of dominant-negative p53 also reversed the effects on p53 and SHH downstream target gene expression caused by I2PP2A knockdown as shown in **Figure 3.5 d**.

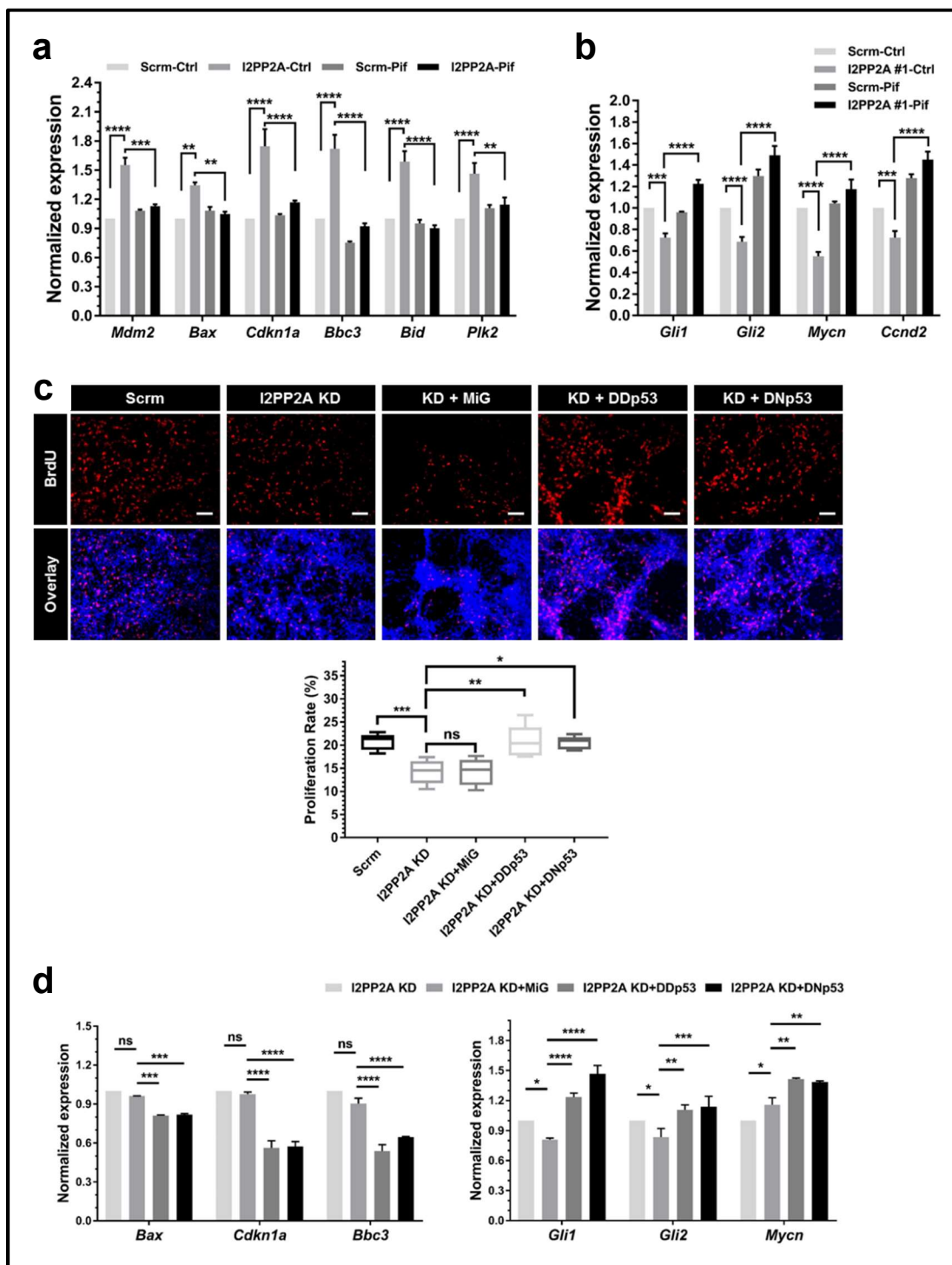


Figure 3.5. I2PP2A knock-down effects on SHH MBCs are dependent on p53. a-b, primary MBCs were seeded and transduced with lentiviruses, then 200nM p53 inhibitor pifithrin was added

24 hours before cell collection and RNA preparation. **a**, upregulation of p53 target gene expression in I2PP2A knockdown cells was reversed by pifithrin treatment, mean \pm S.E.M., n=3, ** $p<0.01$; *** $p<0.001$; **** $p<0.0001$. **b**, downregulation of SHH signaling target mRNAs in I2PP2A KD cells was rescued by pifithrin treatment, mean \pm S.E.M., n=3, *** $p<0.001$; **** $p<0.0001$. **c-d**, primary SmoA1 MBCs were either infected with lentivirus containing scrambled shRNA, I2PP2A shRNA alone, or co-infected with both lentivirus targeting I2PP2A and retrovirus overexpressing dominant-negative Trp53 -GFP (designated as DDp53, DNp53). MiG was used as vector control for retroviruses. **c**, BrdU incorporation assay indicates that decreased proliferation in SmoA1 MBCs caused by I2PP2A knockdown was rescued by overexpression of dominant-negative p53, but not by control vector, mean \pm S.E.M., n=5, * $p<0.05$; ** $p<0.01$; *** $p<0.001$. **d**, QPCR showing that upregulated p53 targets were reduced, while SHH signaling downstream targets were upregulated by dominant-negative p53 overexpression, mean \pm S.E.M., n=4, * $p<0.05$; ** $p<0.01$; *** $p<0.001$; **** $p<0.0001$.

I2PP2A knockdown-mediated loss of viability requires wildtype p53 in patient-derived medulloblastoma cells.

To further determine whether the signaling mediated through I2PP2A/PP2A-p-MDM2^{S166}-p53 in mouse tumor tissue is conserved in human medulloblastoma cells, we performed I2PP2A knockdown in Daoy, UW228 and ONS76 cells, which are patient-derived SHH-activated medulloblastoma cell lines. As shown in **Figure 3.6 a** and Supplemental Figure 6B, knockdown of I2PP2A reduced MDM2 and p-MDM2 in all three cell lines, indicating that I2PP2A's regulation of p-MDM2^{S166} is conserved in patient medulloblastoma cells. However, the upregulation of p21 protein, induction of p53 target gene *Mdm2* and *Cdkn1a*, and suppression of SHH target *Gli1* were only seen in ONS76 cells which harbor wildtype p53, but not in p53 mutant cell lines Daoy and UW228 (**Fig. 3.6 a, 3.6 b** and **Figure S3.7 a, S3.7 c, S3.7 d**). These findings further support that I2PP2A executes its tumorigenic function through suppression of wildtype p53. Moreover, when we performed viability assays (**Fig. 3.6 c**), we found that only ONS76 was susceptible to cell death when challenged with increasing lentivirus titers to knockdown I2PP2A. These findings indicate that the phenotypic effects caused by I2PP2A knockdown in medulloblastoma cells are dependent on p53 function and that I2PP2A compromises wildtype p53 activity in patient-derived SHH-activated medulloblastoma.

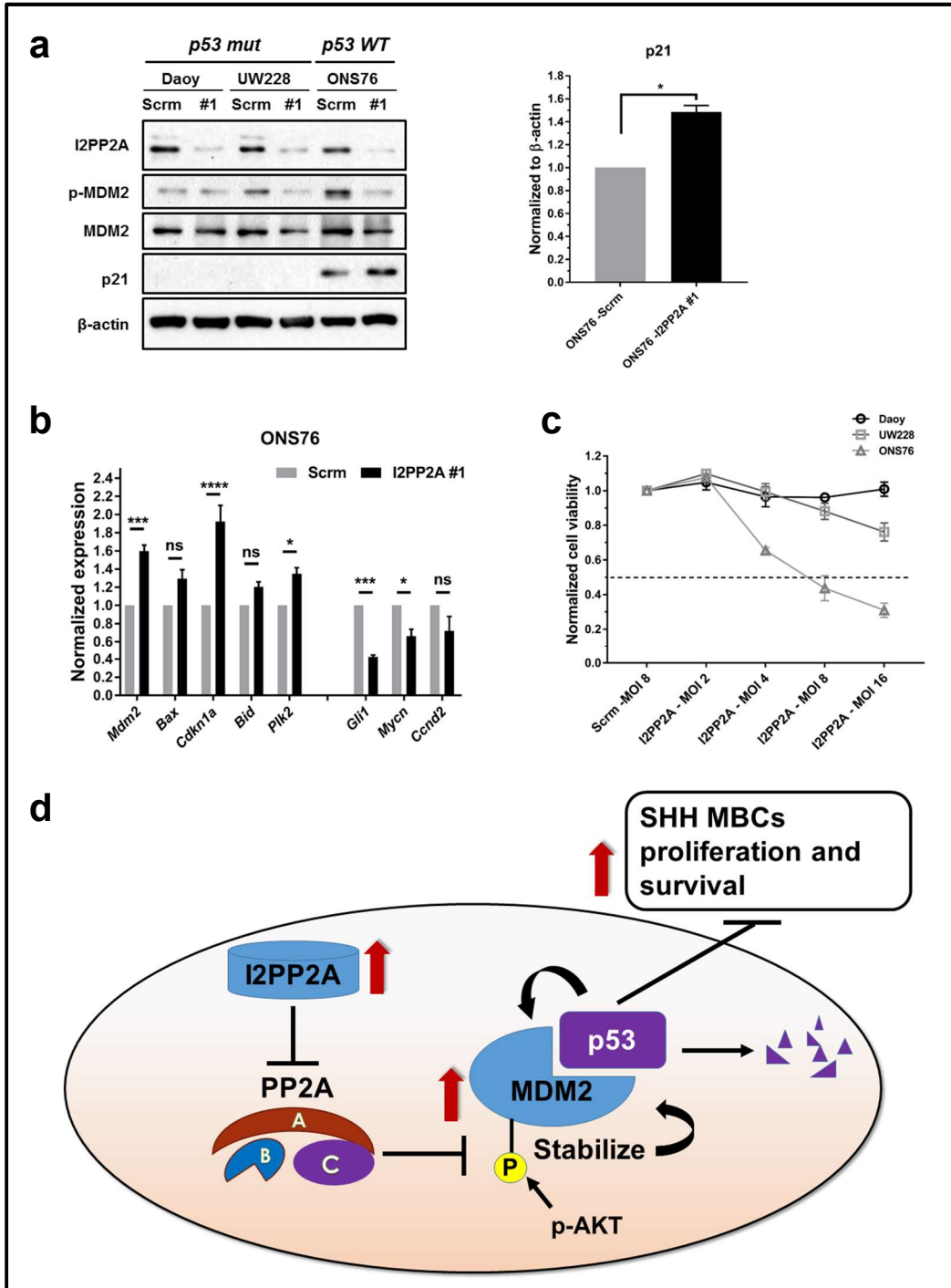


Figure 3.6. I2PP2A knockdown-mediated loss of viability requires wild-type p53 function in patient-derived medulloblastoma cells. **a**, patient-derived medulloblastoma cell lines Daoy, UW228, and ONS76 were cultured and infected. 72 hours later, cells were collected and lysed. Left,

western blot showing reduced p-MDM2 and total MDM2 in all three cell lines, but induced p21 only in p53 wildtype ONS76 cells; right, quantification of p21 protein induction in ONS76 cells after I2PP2A knockdown, mean \pm S.E.M., n=3, * $p < 0.05$. **b**, downstream target mRNAs of p53 and SHH signaling were analyzed 72 hours post-infection. **c**, MTT assay indicated lower survival curve of ONS76 cells after I2PP2A knockdown as compared to p53 mutant cell lines Daoy and UW228, mean \pm S.E.M., n=4. **d**, Increased I2PP2A suppresses PP2A activity, thus leading to less dephosphorylation of MDM2 at Ser166, which could then facilitate MDM2 to degrade p53 faster in SHH medulloblastoma cells. Upregulated I2PP2A could promote cell proliferation and survival by compromising wild type p53 function of SHH medulloblastoma.

3.4 Discussion

In many different cancers, the tumor suppressor p53 loses its function through mechanisms such as mutation, dysregulated post-translational modification, or amplification of its negative regulators. When exposed to extrinsic or intrinsic stress, cells with functional p53 undergo cell cycle arrest or cellular death, primarily by transcriptionally upregulating its target gene expression. In medulloblastoma, the most common malignant pediatric brain tumors, p53 mutations are not frequently detected, but confer a worse prognosis for patients when present. Knowing the critical role played by p53 in virtually all cancers and medulloblastoma, we hypothesized p53 function is compromised through mechanisms other than gene mutation in a p53 wild-type mouse model for SHH medulloblastoma, the *NeuroD2:SmoA1* (“*SmoA1*”) mouse. The aim of this research is to identify upstream regulators that suppress wild type p53 function in both mouse and human medulloblastoma cells, and as such could represent a novel therapeutic target in p53 wild type medulloblastoma patients. We observed upregulation of p53 in *SmoA1* tumor tissues compared to neighboring cerebellum. This p53 increase indicates that these medulloblastoma cells are under oncogenic stress which could sensitize them to p53-mediated cell death or cell cycle arrest. The E3 ubiquitin protein ligase MDM2 is a central negative regulator of p53 that targets it for degradation in unstressed cells. When exposed to stress, however, MDM2 is degraded while p53 in these cells is activated to arrest cell cycle or induce apoptosis. When cells bypass the apoptotic p53 signal, *Mdm2*, also a transcriptional target of p53, can be upregulated to suppress p53 again. MDM2 and p53 thus form a negative feedback loop in cells to safeguard and preserve the stability of genomes when cells are exposed to stress, including oncogenic stress. Interestingly, while we detected reduced total MDM2 protein in *SmoA1* medulloblastoma compared to adjacent non-tumor cerebellum, we observed significantly increased phosphorylation at serine residue 166 of MDM2 (p-MDM2^{S166}). It has been shown that p-MDM2^{S166} is an active and stable form of MDM2 that binds to and ubiquitinates p53. The upregulation of p-MDM2^{S166} suggests

this might be one mechanism utilized by medulloblastoma cells to compromise p53 function. Furthermore, MDM2 protein was only detected in ~20% of 86 medulloblastoma samples (77), consistent with our findings that MDM2 is at lower levels in SHH medulloblastoma, implying that other possible mechanisms may exist to compromise p53 function in p53 wild type medulloblastoma, such as aberrant activation of MDM2 by phosphorylation at Ser166.

To better understand the upstream regulation of p-MDM2^{S166}, we investigated protein phosphatase 2A, which has been shown to dephosphorylate MDM2^{S166} (81). Since no mutations of PP2A subunit have been reported in medulloblastoma to date (<http://r2.amc.nl>), we analyzed the levels of PP2A C and PP2A's endogenous inhibitors and found significantly increased I2PP2A protein levels. Utilizing a pharmacological inhibitor, COG112, to suppress I2PP2A in primary medulloblastoma cells isolated from *SmoA1* mice, we found that I2PP2A inhibition downregulates p-MDM2^{S166} and thus stabilizes p53 in these medulloblastoma cells through PP2A activity. Lentivirus-mediated knockdown of I2PP2A reduced p-MDM2^{S166}, as well as MDM2 levels, proliferation, and viability in *SmoA1* medulloblastoma cells, likely through p53 activation. Further experiments including treatment with the p53 inhibitor pifithrin and retroviral overexpression of dominant negative p53 rescued the effects caused by I2PP2A knockdown, suggesting the effects caused by I2PP2A abrogation are dependent on p53 activity. We also observed reduced viability and increased levels of the p53 target p21 in ONS76 cells, a patient-derived p53 wildtype SHH medulloblastoma cells, after I2PP2A abolishment, but not in p53 mutant Daoy and UW228 cells. These observations suggest that the I2PP2A-pMDM2-p53 pathway is conserved in human p53 wildtype SHH medulloblastoma, warranting further investigation of the I2PP2A-p53 axis in human samples. We propose that increased levels of I2PP2A protein inhibit PP2A activity and upregulate p-MDM2^{S166}, which leads to rapid degradation of wildtype p53, thus promoting tumor cell survival and proliferation during SHH medulloblastoma development (**Fig. 3.6 d**).

In recent years, I2PP2A has been proposed to play oncogenic roles through activating Akt, c-myc, nm23-H1 and Rac1 in various cancers. Here we reveal a novel tumor-promoting role of I2PP2A, compromising p53 function through p-MDM2^{S166} in the context of SHH medulloblastoma. I2PP2A disrupts the MDM2-p53 negative feedback loop, enabling medulloblastoma cells to survive or proliferate even under oncogenic stress. Our research is consistent with the finding that I2PP2A negatively regulates p53 transactivation in H1299, U2OS, MCF7, H460 and HCT116 cells (241). However, authors of that study suggest an alternative mechanism wherein I2PP2A directly binds to p53 and suppresses p300/CBP-mediated H3K18 and H3K27 acetylation on the p53 target promoter in the nucleus of unstressed cells. Our data suggests that in SHH medulloblastoma cells, I2PP2A regulates p-MDM2 levels independent of p53 as we observed reduced p-MDM2 and MDM2 proteins when we inhibit I2PP2A, not the other way around considering that *Mdm2* is a transcriptional target of p53.

The fact that it is difficult to re-introduce the functional tumor suppressor p53 with current therapeutic modalities underscores the importance of identifying its negative regulators. We have illustrated that I2PP2A promotes SHH medulloblastoma cell proliferation and survival by compromising p53 activity. However, future *in vivo* evaluation of the tumor-promoting function of I2PP2A is a necessary step to further demonstrate its therapeutic value. For example, I2PP2A can be targeted *in vivo* using an existing drug, FTY720 (83, 84, 103), which can bypass the blood brain barrier and is FDA-approved to treat relapsed multiple sclerosis patients. FTY720 has been shown to bind to I2PP2A directly and suppress its function by disrupting the I2PP2A-PP2A interaction. Currently, the lines of evidence in our studies elucidate a tumor-promoting signaling pathway mediated by I2PP2A-p-MDM2-p53 in p53 wildtype SHH medulloblastoma, and they warrant future investigation to evaluate the therapeutic value of modulating I2PP2A *in vivo* or in clinical trials, especially for patients suffering from current harsh treatments.

Supplemental Information

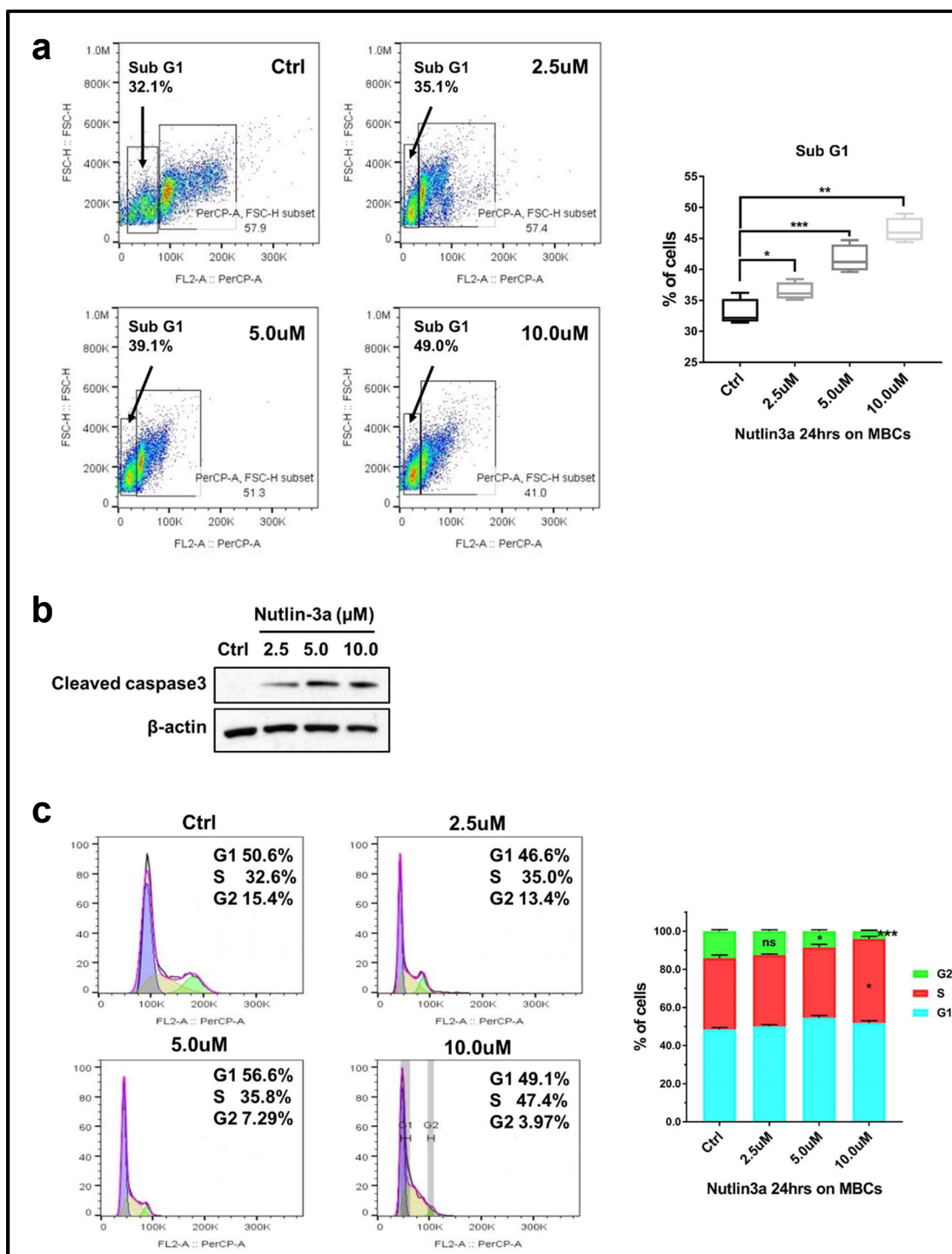


Figure S3.1. Nutlin-3a treatment caused apoptosis and cell cycle arrest. a-c, primary MBCs were treated with Nutlin-3a at different doses for 24 hours before cells were fixed for cell cycle analysis (a,

c) or lysed for western blot (**b**). **a**, fixed cells were stained with propidium iodide and sub-G1 phase cells were analyzed. Upregulated Sub G1 phase cells were observed, mean \pm S.E.M., n=4, * $p < 0.05$; ** $p < 0.01$; *** $p < 0.001$. **b**, western blots showed a dose-dependent induction of cleaved caspase 3 in Nutlin-3a treated cells. **c**, dose-dependent decrease of G2 phase cells were observed 24 hours post Nutlin-3a treatment, mean \pm S.E.M., n=4, * $p < 0.05$; *** $p < 0.001$.

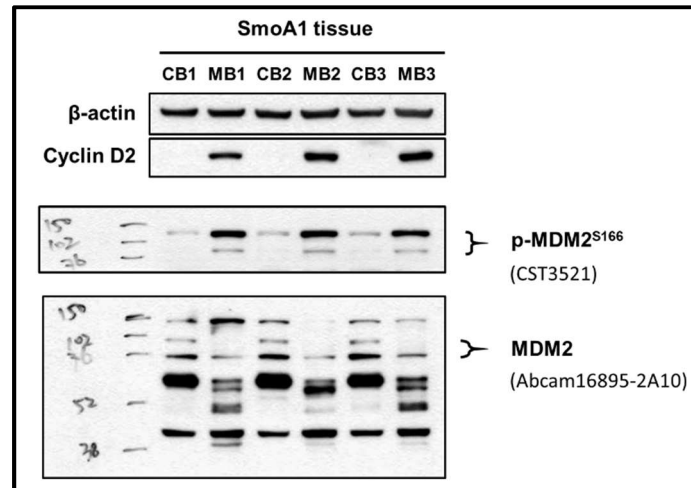


Figure S3.2. Whole blots of MDM2 and p-MDM2^{S166} in SmoA1 tumors. CB vs. MB three pairs were shown for quality control of MDM2 and p-MDM2^{S166} detection. Bands considered positive were indicated by right braces, and they showed positive correlated changes. Only lower band approximately at 90kDa was shown in later experiments. Antibodies used to detect MDM2 and p-MDM2^{S166} were indicated within parentheses.

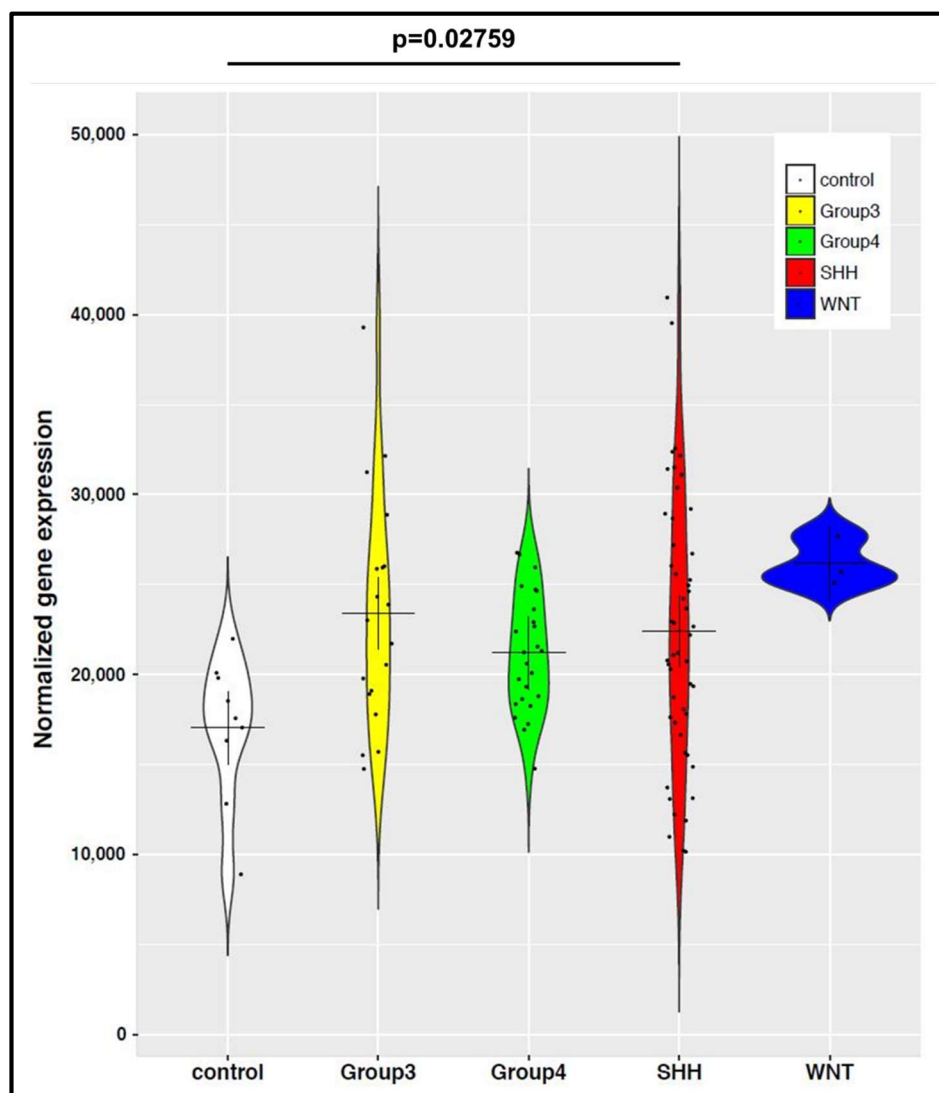


Figure S3.3. Normalized expression levels of I2PP2A mRNA in medulloblastoma patients showed a small difference between SHH medulloblastoma samples and cerebellar controls. Violin plots show expression levels of I2PP2A across four subgroups (WNT=3, SHH=50, Group 3=19, Group 4=25), and control samples (5 adult and 4 fetal cerebella samples). Wilcoxon Rank Sum test was used to test for significant differences between all distributions. Violin widths are scaled to the data distribution with wider areas containing more data points; crosses indicate median values; points represent individual patient values with added jitter in the x-direction for visibility.

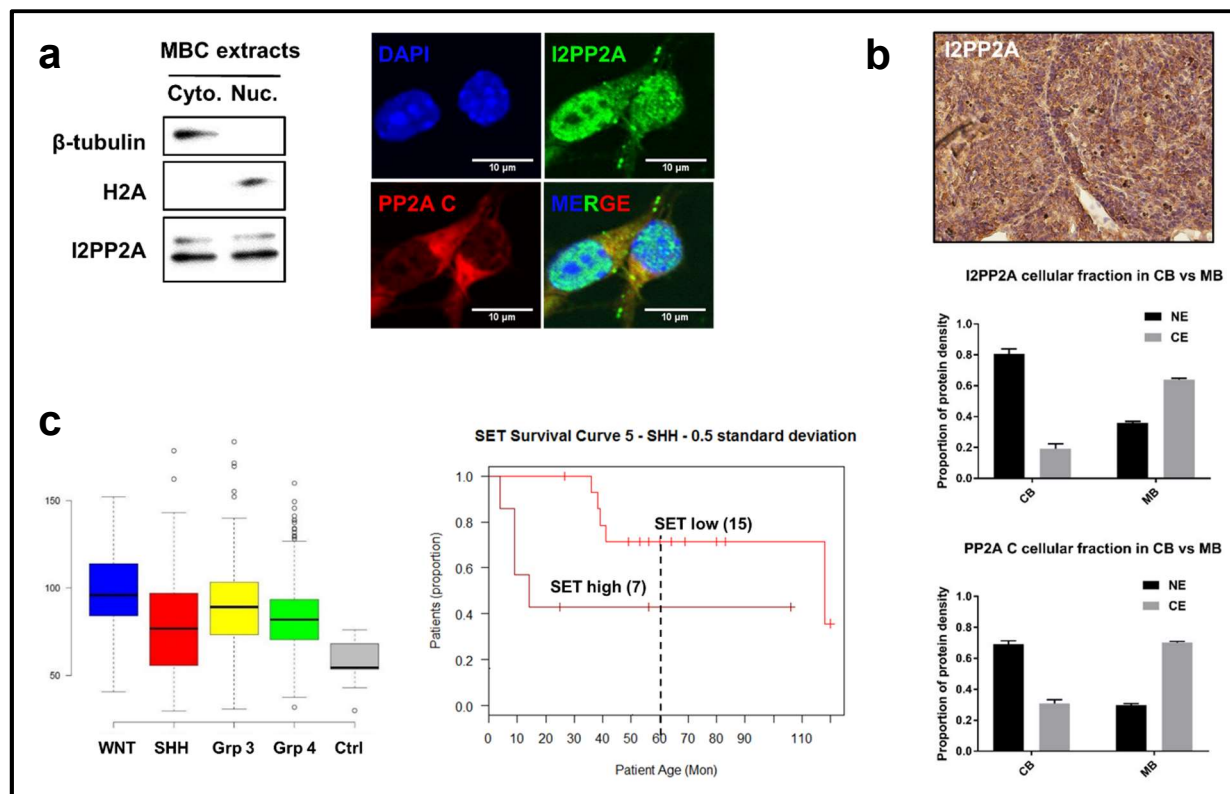


Figure S3.4. Brief characterization of I2PP2A in SHH medulloblastoma. **a**, in primary medulloblastoma cell culture, we either lysed the cells and checked the localization of I2PP2A (left panel), or stained cells with I2PP2A and PP2A to check their distribution in cellular compartments (right panel). I2PP2A protein was in the nucleus and cytoplasm, whereas PP2A was mainly in the cytoplasm (right panel). **b**, *in situ* IHC (immunohistochemistry) staining (upper panel) and tissue lysates extraction from medulloblastoma (bottom panel, n=3) and its normal neighboring cerebellum suggested both nuclear and cytoplasmic I2PP2A distribution. **c**, *left*, SHH subgroup showed slightly higher I2PP2A mRNA as compared to control group. Patient samples from WNT (n=66), SHH patients (279), Group 3 (n=192), and Group 4 (n=334) subgroups were compared with control group (n=9, five from infant and four from adult patients with normal tissue). Kruskal–Wallis Rank Sum test was performed for data analysis. *p* value is 0.019 for the comparison between SHH and control group. *Right*, survival curves of SHH medulloblastoma patients with either high (n=7) or low (n=15)

I2PP2A mRNA expression, with dashed line indicating the 5-year overall survival. Patients with higher I2PP2A mRNA displayed a lower 5-year overall survival rate as compared to that in I2PP2A-low group.

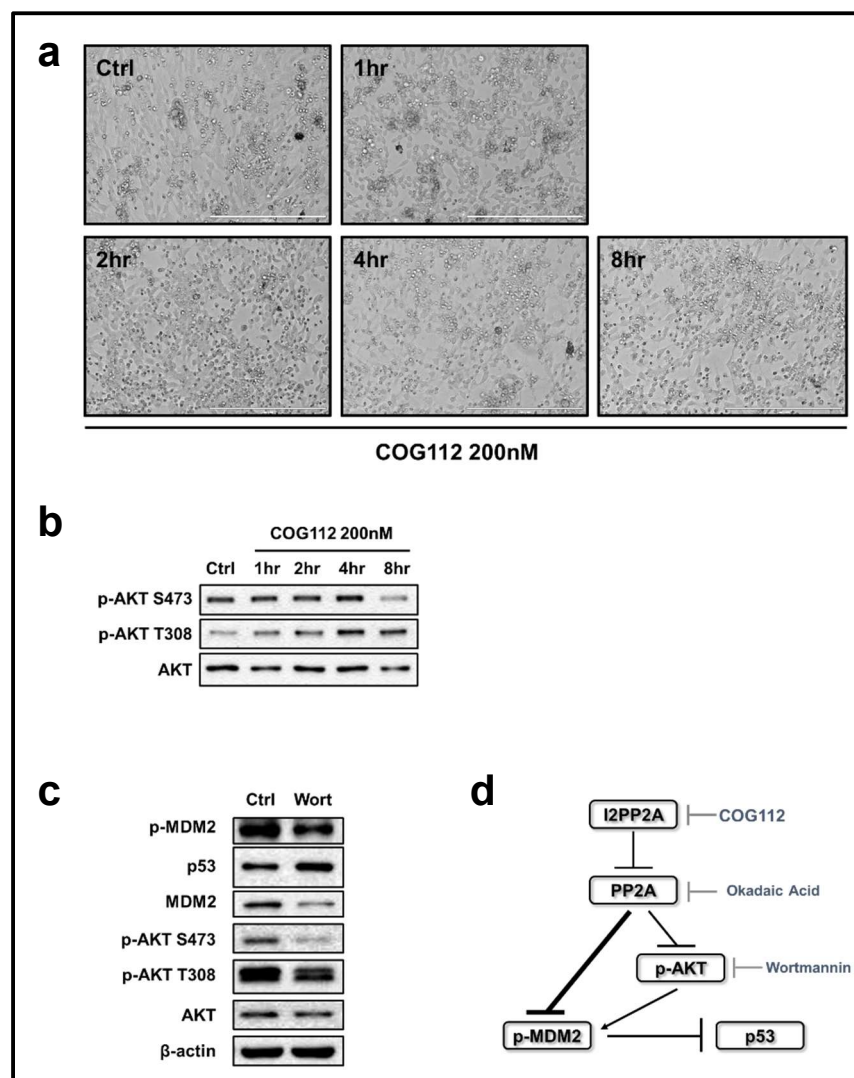


Figure S3.5. p-MDM2 is regulated by both PP2A and p-Akt. **a**, an inverted bright field light microscopy suggested no significant difference in cell viability/morphology within 8 hours of COG112 (200nM) treatment. Scale bar=200um. **b**, parallel check of p-Akt levels after COG112 treatment indicated PP2A regulates p-MDM2 directly. Western blot shows a time-dependent increase of p-Akt (T308) and no obvious difference of p-Akt (S473). **c**, wortmannin (200nM) alone reduces p-Akt and p-MDM2, indicating p-Akt is upstream of p-MDM2. **d**, schematic view of how p-MDM2 and p53 are regulated in SmoA1 medulloblastoma cells.

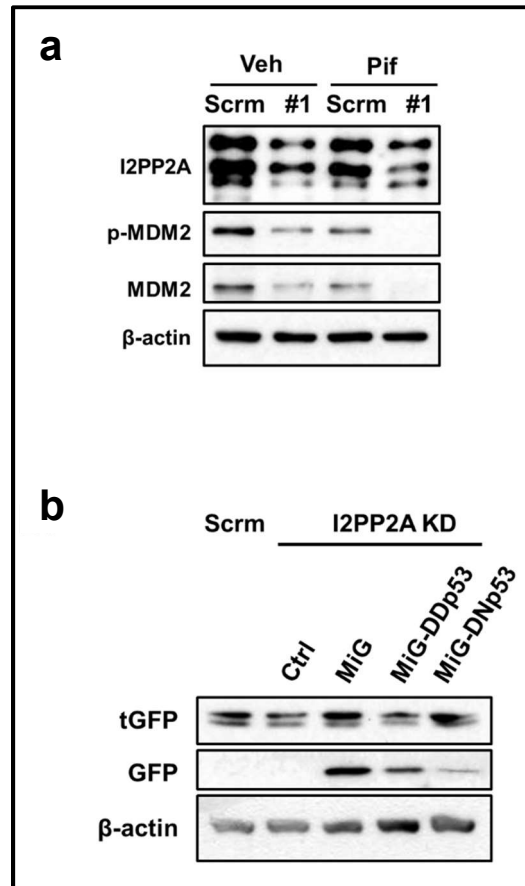


Figure S3.6. Lentivirus and retrovirus infection on SmoA1 MBCs are successful. **a**, in pifithrin treatment experiment, I2PP2A was successfully knocked down in both control and pifithrin treatment MBCs. **b**, in co-infection experiments, GFP was positive in MSCV-ires-GFP (MiG), MiG-DDp53 and MiG-DNp53 retrovirus infected MBCs; tGFP was positive in all pLKO.1-shRNA-tGFP lentivirus infected cells.

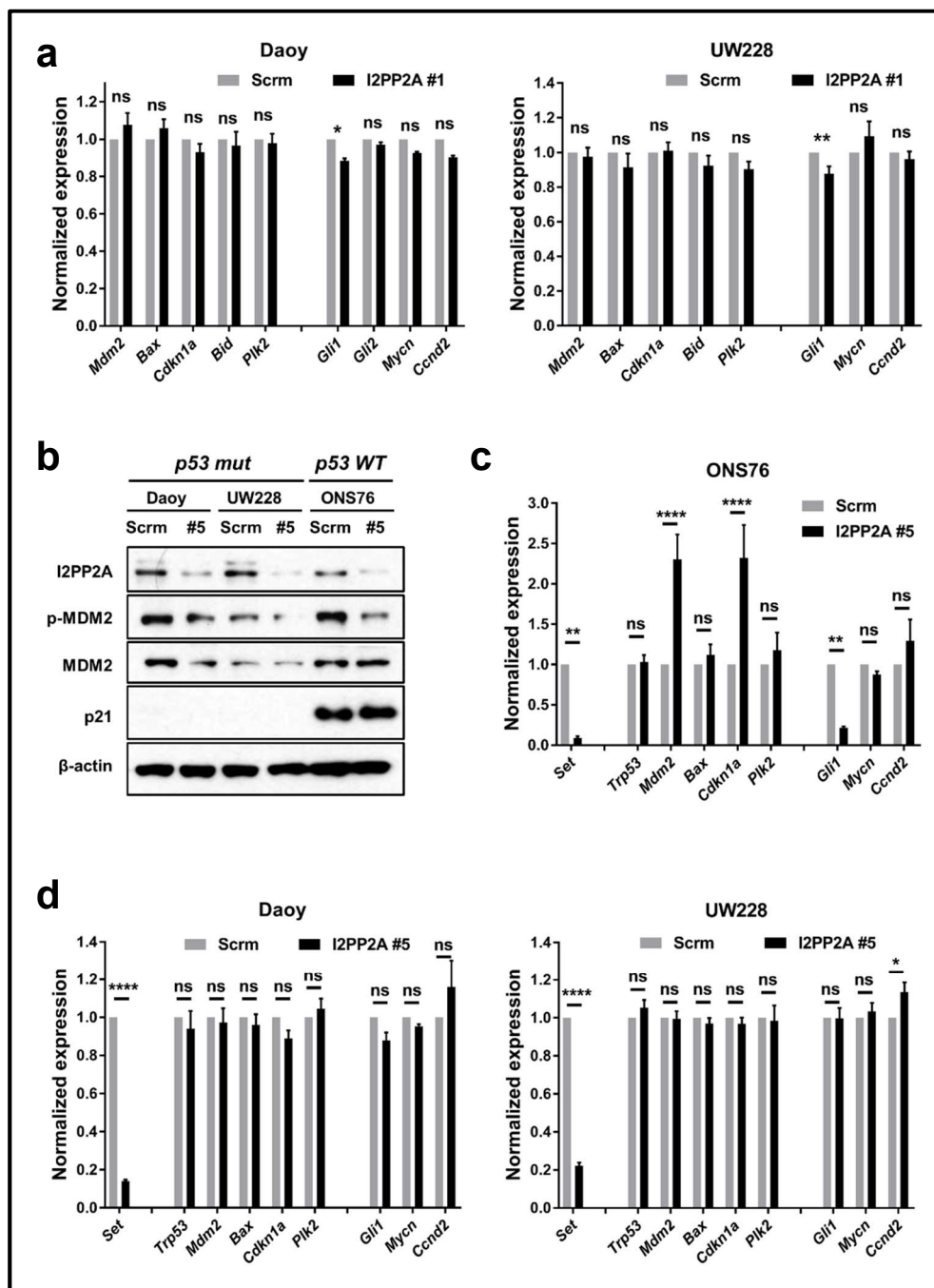


Figure S3.7. I2PP2A knockdown affected p53 targets and SHH signaling only in ONS76 cells.

a, RT-PCR of p53 targets and SHH signaling mRNAs showed no significant changes in Daoy and UW228 cells 72 hours after lentiviral mediated infection (I2PP2A shRNA #1), mean \pm S.E.M., $n=4$, * $p<0.05$; ** $p<0.01$. **b-d**, Daoy, UW228 and ONS76 cells were infected with lentiviruses containing

I2PP2A shRNA #5, and lysed 72 hours post-infection, mean \pm S.E.M., n=4, * $p < 0.05$; ** $p < 0.01$; *** $p < 0.0001$. **b**, western blot showed successful knockdown of I2PP2A in all three cells lines. **c** and **d**, RT-PCR results indicated the upregulation of p53 downstream targets and downregulation of SHH signaling only in ONS76 but not in Daoy or UW288 cells.

Chapter 4. Preliminary data of I2PP2A characterization

4.1 The oncogenic role of I2PP2A *in vivo*

The *in vitro* results in Chapter 3 suggest the possible oncogenic function of I2PP2A in primary medulloblastoma cells from mice and patient-derived cell lines. To further investigate if I2PP2A plays oncogenic roles in promoting SHH tumors *in vivo*, we injected the primary MBCs infected with lentiviruses containing either scrambled shRNA or shRNA targeting I2PP2A into postnatal day 2 C57BL/6J wildtype pups and generated an allograft model. As illustrated in **Figure 4.1 a**, primary MBCs 24 hours post-infection were exposed to fluorescence-activated cell sorting (FACS) to obtain viable and successfully transduced tGFP positive cells. Then 200,000 primary tGFP+ cells from each experimental group were injected to the hindbrain of C57BL/6J wildtype pups at postnatal day 2. Mice from two groups were monitored for symptoms of medulloblastoma for four months. Once they developed tumors and reached the clinical endpoint, indicated by severe symptoms such as head tilt, hunched postures, and less activity, sick mice were sacrificed. These mice were then immediately perfused with PBS; part of the tumor tissue was collected and frozen for protein lysates analysis, and the remaining whole brain was fixed in 4% PFA and embedded in paraffin for IHC/HE staining. As shown in **Figure 4.1 b**, 7 out of 9 mice injected with scrambled control MBCs succumbed to tumors within four months, whereas only 1 out of 9 mice injected with I2PP2A knockdown MBCs reached the endpoint. The survival rates from the two groups were statistically different with a *p*-value of 0.0033, indicating that I2PP2A knockdown delayed tumor growth as compared to the control group. When we analyzed tumor samples of one mouse from each group, we observed the lower protein levels of I2PP2A as indicated by **Figure 4.1 c**, and **Figure 4.1 d**. Consistent with *in vitro* findings, we also observed lower p-MDM2^{S166}, total MDM2, and less proliferation as indicated by lower Ki67

staining shown in **Figure 4.1 c-d**. We also observed the weak signal of tGFP retained in the tumor tissues. Interestingly, cleaved caspase 3 staining, which is a marker for apoptosis, was relatively lower in the I2PP2A KD tumor tissue as compared to the control tumor samples, possibly due to the quick turnover of these fast-proliferating cells in the control group. Another possible reason is that cells undergo apoptosis before the endpoint, making it difficult to capture the massive cell death at the collection date. We concluded that I2PP2A abrogation in MBCs delayed tumor growth in the *in vivo* allograft model. Detailed analysis of the tissue samples, such as quantification of the Ki67 staining, or cleaved caspase 3 staining, is needed to draw for further conclusions.

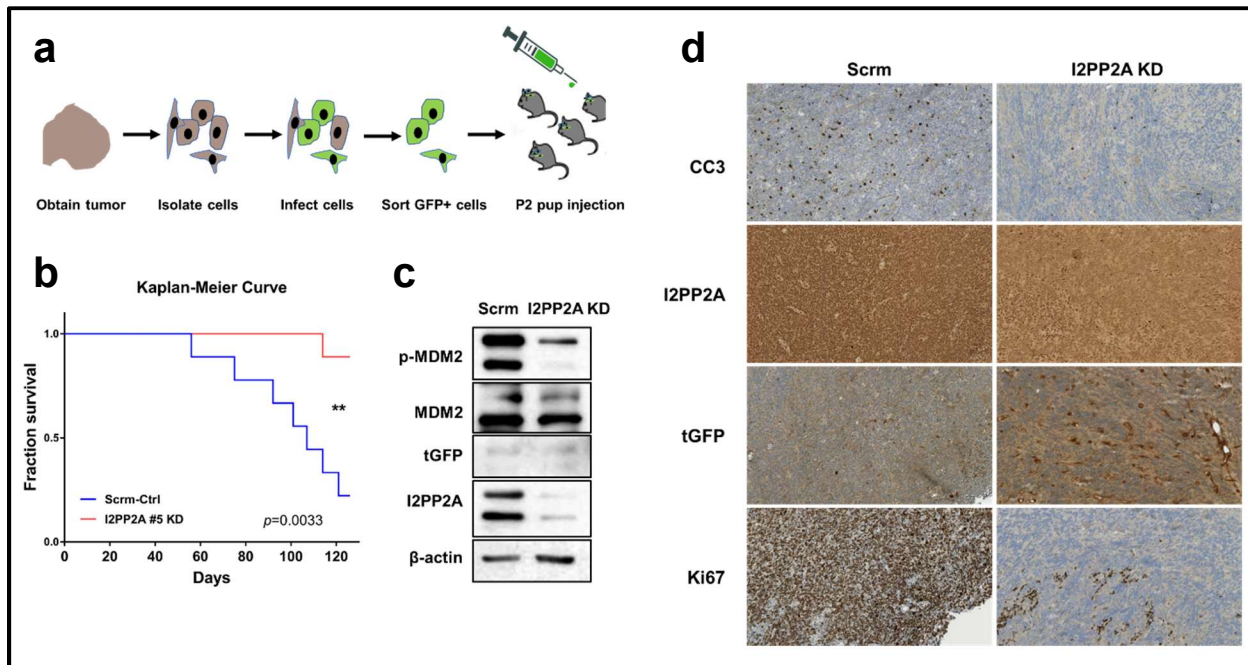


Figure 4.1. I2PP2A knockdown delayed tumor progression in an allograft model. **a**, schematic view of experimental design, primary MBCs were infected with lentiviruses containing shRNA-tGFP or scrambled-tGFP constructs. Successfully infected cells with positive tGFP were sorted out for injection into postnatal day 2 C57BL/6 wildtype pups. **b**, Survival curves of mice injected with either I2PP2A knockdown (red) or control MBCs (blue) indicated that I2PP2A knockdown delayed tumor growth *in vivo*, $n=8$ for each group, $**p<0.01$. **c**, western blot showing reduced I2PP2A, p-MDM2^{S166}, and total MDM2 proteins in I2PP2A KD tumors, though two groups showed comparable tGFP expression. **d**, IHC staining of cleaved caspase 3 (CC3), I2PP2A, tGFP and Ki67 on tumor tissues of one mouse from either group. I2PP2A KD tumors showed reduced I2PP2A and reduced Ki67 staining, but not tGFP or cleaved caspase 3 staining.

4.2 I2PP2A and MDM2 during cerebellar development

Although we have shown that the knockdown of I2PP2A delayed tumor growth with advanced medulloblastoma cells, it remains to be elucidated whether I2PP2A plays roles during normal cerebellar development or tumor initiation of SHH MBs. Acknowledging that SHH medulloblastomas present less-differentiated cells, it is critical to understand the tumor initiation step at the point where cells decide to differentiate or not. Therefore, it would be interesting to check I2PP2A and p-MDM2^{S166} levels during normal cerebellar development. As shown in **Figure 4.2**, I2PP2A and p-MDM2 showed decreased protein levels at later postnatal days of wildtype pups' cerebellum, whereas total MDM2 displayed an upregulation in the more differentiated cerebellum. The trend of all three protein level changes during differentiation at this point corroborates with the suggestion that medulloblastomas are less-differentiated neuronal cells, as we observed higher I2PP2A and p-MDM2, and lower total MDM2 proteins in advanced medulloblastomas as compared to its neighboring cerebellum based on NeuroD2:SmA1 mice studies. One possible connection between I2PP2A and differentiation status is that I2PP2A together with I1PP2A forms the INHAT complex, which masks histones and inhibits their acetylation (98). The chromatin will be in a more compact state with INHAT complex which prevents the active transcription of many genes, including differentiation-related genes. Interestingly, p53 is among the transcriptional factors that are subject to INHAT regulation (241). However, future investigation of whether I2PP2A regulates the stemness or if it is just a downstream indicator needs to be performed for any conclusion. A possible experiment would be to check I2PP2A expression at the so-called preneoplastic stage of the heterozygous *Patched* SHH MB mouse model mentioned in Chapter 1 to see if I2PP2A protein levels correlate negatively with senescence markers.

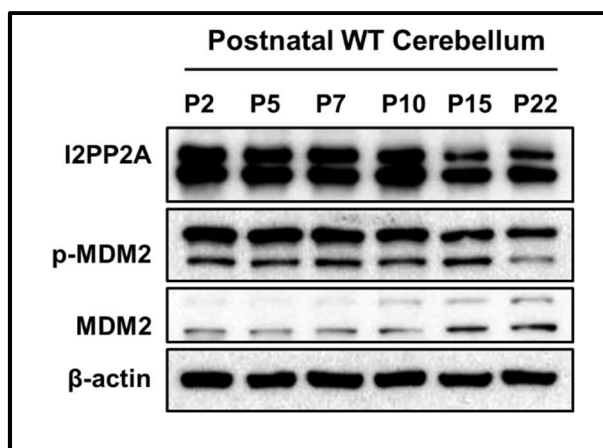


Figure 4.2. Expression of I2PP2A protein during postnatal cerebellar development of wildtype pups. Western blot showing I2PP2A, p-MDM2 and MDM2 protein levels in cerebellum from P2 (postnatal day 2) to P22. I2PP2A and p-MDM2 displayed a time-dependent decrease, indicating that these two proteins are more abundant in less differentiated state of cerebellum development.

4.3 The possible upstream regulator of I2PP2A protein stabilization

As demonstrated in Chapter 3, I2PP2A showed upregulation in protein but not mRNA levels in tumor tissue as compared to neighboring cerebellum. Even when we analyzed patient sample expression data, we observed a marginal difference in mRNA levels between this SHH subgroup and controls. Although further IHC analysis of the protein levels in patient samples is needed, this poses the question of how I2PP2A protein is stabilized in medulloblastoma tumor cells.

We checked I2PP2A protein levels in CGNPs with exogenous Sonic Hedgehog, in comparison with CGNPs exposed to vehicle control, and did not observe a significant increase of I2PP2A protein with Shh treatment (data not shown). This result suggests that SHH signaling might not be the direct upstream signaling to upregulate I2PP2A protein. We next questioned whether I2PP2A is rapidly transcribed or stabilized due to slow degradation. As shown in **Figure 4.3 a**, I2PP2A was quite stable in MBCs exposed to the proteasome inhibitor lactacystin or mTORC1 inhibitor Torin1. The insensitivity to Torin1 of I2PP2A suggests I2PP2A is not translated continuously in these primary MBCs; instead, the protein itself is quite stable once produced. I2PP2A can be degraded by the proteasome in MBCs as indicated by the changed level hours post lactacystin treatment. However, the extent of I2PP2A protein change was not as evident as the extent change of MYCN or CyclinD2, implying a relatively long half-life of I2PP2A. When we checked the localization of I2PP2A in primary MBCs, as shown in **Figure 1.6 b**, we observed a higher distribution in the nucleus than in the cytoplasm. We, therefore, speculated that I2PP2A is involved in various complexes and localized to different cellular compartments of the MBCs, all of which protect I2PP2A from degradation. As previously mentioned, I2PP2A might bind to proteins such as PP2A, NME1 or I1PP2A, forming the complexes which shield its residues from ubiquitination and subsequent degradation by proteasomes.

Furthermore, post-translational modifications of I2PP2A, such as phosphorylation, could also facilitate its binding to other proteins and thus stabilize it. For example, phosphorylation of I2PP2A at Ser9 has been demonstrated to promote its binding to RAC1, which recruits I2PP2A to the plasma membrane (89, 90). It will be intriguing to see if this serves as a mechanism to stabilize I2PP2A. In cardiac cells, the PI3K catalytic subunit p110 γ has been proposed to phosphorylate I2PP2A at Ser9 and activate its function in suppressing PP2A to sustain adrenergic receptor/PI3K signals (242). Therefore, we attempted to check if the suppression of PI3K activity could destabilize I2PP2A. In preliminary data shown in **Figure 4.3 b**, we treated primary MBCs with PI3K inhibitors LY294002 and AS252424 and observed reduced I2PP2A protein as compared to the vehicle control MBCs. This suggests PI3K might be one of the regulators that stabilize the I2PP2A protein. However, we had difficulty in detecting the phosphorylated I2PP2A in our system, rendering our system of primary MBC culture not optimal for the detailed mechanistic studies. An alternative system is the patient-derived cell line ONS76, which harbors wild-type *TP53* and can be passaged and efficiently transfected with plasmid constructs. With ONS76 cells, one potential experiment we can do is to check if mutagenesis at Ser9 to Alanine (A) or Glutamic Acid (E) would change the stability of I2PP2A in SHH medulloblastoma cell lines. Also, if we could prepare truncated forms of I2PP2A to modulate the nuclear-localization signal sequence at the NAP, we will be able to change the location of I2PP2A, and then investigate what procedures are affected by different localizations or levels of I2PP2A protein.

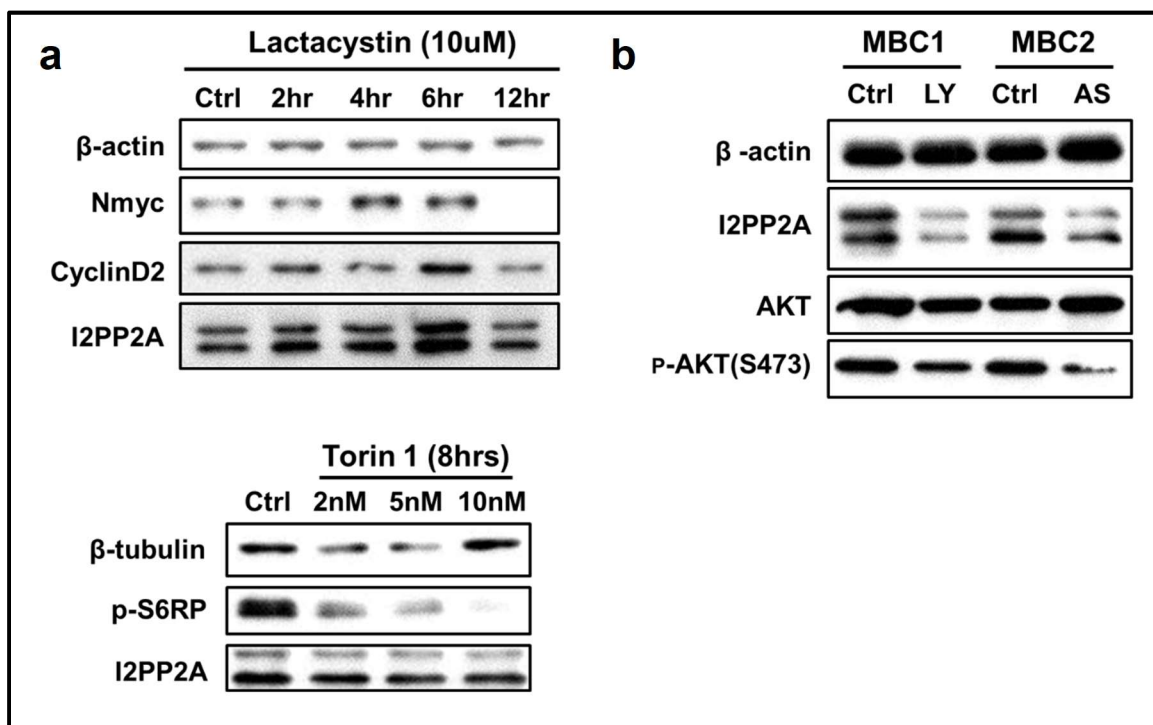


Figure 4.3. Preliminary data of I2PP2A protein stability. *a, upper*, time course treatment of lactacystin on primary MBCs at 10uM. All three proteins showed a time-dependent increase within 6 hours of treatment. 12 hours treatment might be toxic to primary MBCs and thus we did observe a rapid drop (even lower than control group) of MYCN and CyclinD2 proteins but not I2PP2A. *bottom*, mTORC1 inhibitor which decreases p-S6RP, a downstream indicator of mTORC1 signaling, in a dose-dependent manner, but not I2PP2A. These preliminary data suggest I2PP2A protein is quite stable and insensitive to stress in primary MBCs. *b*, I2PP2A showed reduced protein levels when primary MBCs were exposed to PI3K inhibitors. LY, LY294002, PI3K p110 α , β , δ inhibitor, IC₅₀=0.5uM, Treatment- 0.5uM for 4hrs, also can inhibit PI3K γ at a higher concentration; AS- AS252424, PI3K p110 γ inhibitor, IC₅₀=33nM, Treatment- 33nM for 1hr, also inhibit other PI3K isoforms at a much higher concentration. p-AKT (Ser473) was used as a positive control.

4.4 The role of p53 and p-AKT post-irradiation

As shown in **Figure 4.4**, p53 protein in *NeuroD2:SmoA1; Math1: GFP* mice (*NeuroD2:SmoA1* mice crossed with *Math1: GFP* mice, which can generate a homozygous progeny with GFP positive SHH tumors) was induced 3-6 hours post-irradiation treatment, followed by increased cleaved caspase 3, which is an indicator of cellular apoptosis. As the p53 induced apoptosis mediated by cleaved caspase 3 is conserved in mammalian cells, we postulate this mechanism also applies to SHH medulloblastoma patients with functional TP53. However, mutant TP53 loses the ability to induce apoptosis of medulloblastoma cells when they are exposed to radiation therapy. This offers a partial explanation for the worse prognosis of SHH *TP53* mutant patients, as TP53 mutations are exclusively seen in pediatric patients, an age group with irradiation as a standard treatment.

Additionally, consistent with the findings from Hambarzumyan *et al.*, cells with phosphorylated AKT are enriched 24 hours post-irradiation, suggesting that cells with positive PI3K signaling might survive the radiation therapy and might subsequently contribute to the repopulation of recurrent tumors. The upregulation of p-ERK was also observed 24 hours post-irradiation, which has never been reported. The enrichment of PI3K and MAPK signaling downstream effectors suggest their possible roles in contributing to cancer cell repopulation and tumor recurrence in patients. This provides implications for future combination therapy in the attempt to prevent tumor recurrence for SHH medulloblastoma patients.

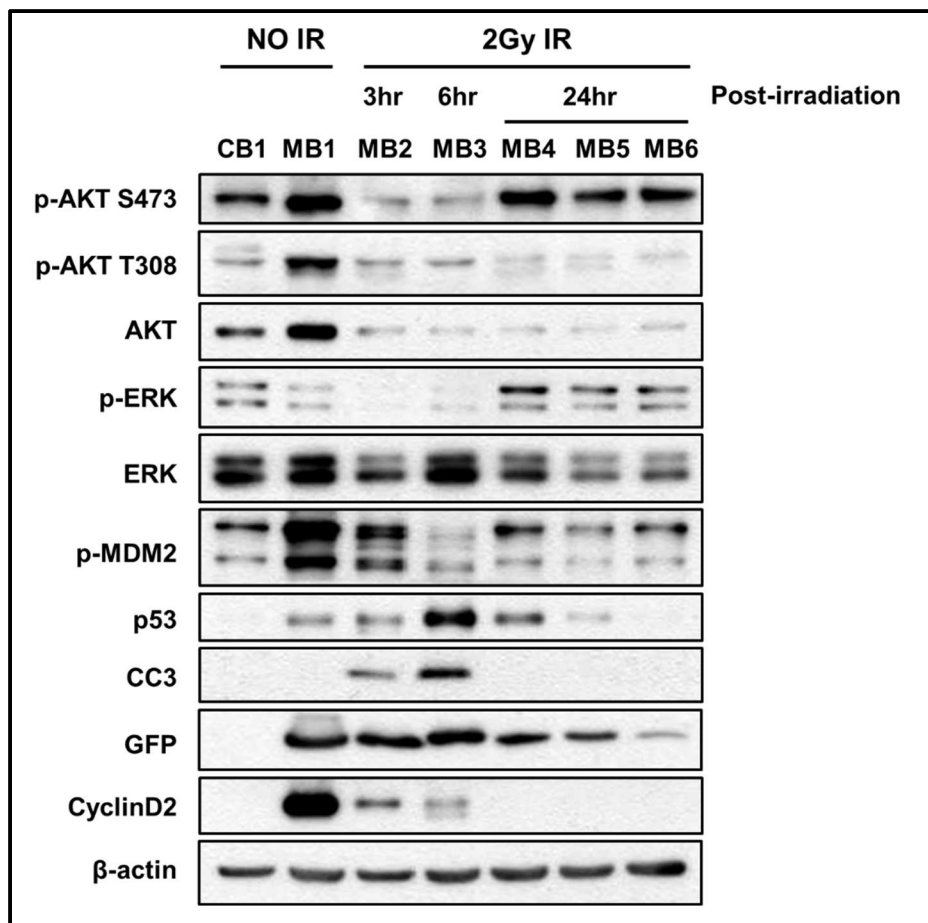


Figure 4.4. Reaction of tumor cells to radiation within 24 hours. Within 3 hours post irradiation (IR), tumor cells stop dividing as indicated by CyclinD2 expression drop. 3-6 hours post IR, p53 was stabilized, along with reduced p-MDM2, simultaneously, cellular apoptosis was induced as indicated by cleaved caspase 3 staining. 24 hours post IR, vast majority of tumor cells were dead suggested by the reduced GFP staining. Though total proteins of AKT or ERK showed a reduction at this point, p-AKT and p-ERK were enriched 24 hours post-treatment, suggesting cells with active PI3K and MAPK signaling might contribute to the following repopulation if recurrence happens post irradiation.

Chapter 5. Summary and Future Directions

5.1 Summary

5.1.1 Treatment options to target heterozygous SHH medulloblastomas

As discussed in Chapter 2, SHH medulloblastomas display heterogeneity in the TME cellular populations, driver or facilitator signaling pathways, and distinct genetics/epigenetics profiles in three age groups, rendering it challenging to find one specific target for all patients. Besides molecular and cellular heterogeneity, diverse clinical features also contribute to the complexity of treating this disease. For example, leptomeningeal spread or distant metastasis is an indicator of poor prognosis, and recurrent tumors are fatal in most cases. Furthermore, the old risk-group stratification is no longer ideal because survivors of SHH medulloblastoma or other subgroup patients who receive the same harsh treatment methods are beset with lifelong side effects, which may result in academic difficulty and future unemployment (110). Due to the under-appreciated tumor heterogeneity, the cure rate has reached a plateau with current non-specific treatment modalities, which necessitates the discovery of novel strategies to stratify and target individual SHH medulloblastoma patients based on a combination of clinical, pathological, and molecular features.

Even before the molecular subgrouping in 2010, researchers and clinicians had proposed a more refined risk-group stratification system for medulloblastoma patients than the existing one, which includes only average and high-risk groups. The average-risk group are patients older than three years, showing no or small residual tumors post-operation ($<1.5\text{cm}^2$ based on MRI), no metastases, and no LCA (Large cell/anaplastic) features, whereas all other patients are the high-risk group. In 2004, Gajjar *et al.* suggested that overexpressed ERBB2, a tyrosine receptor kinase which activates the PI3K or

MAPK pathway, should be considered a poor prognostic marker (243). The authors showed that the 5-year progression-free survival (PFS) rate of patients having ERBB2-negative tumors was ~72%, compared with only 42% for patients with ERBB2-expressing disease ($p = 0.019$). Furthermore, the combination of clinical/histopathological features such as metastasis/LCA, together with molecular markers like nuclear β -catenin, was proposed to be integrated into the new stratification system to replace the two-group classification (244). These authors suggested we should categorize medulloblastoma patients into three or even four risk-groups based on the presence of metastasis, LCA, *MYC* amplification or nuclear β -catenin as indicated in **Figure 5.1**. That patients in these four groups displayed significantly different PFS rates suggests the practical application of the more-refined stratification system. Moreover, this system shed lights on the future stratification of SHH medulloblastoma patients. The combination of mutant *TP53* and amplified *MYCN* has been shown to be a poor prognostic marker for SHH medulloblastoma patients thus the combination of LCA, metastasis, together with mutant *TP53*, and amplified *MYCN* could be used to stratify SHH medulloblastoma patients into more refined risk-groups. Moreover, SHH medulloblastoma cases are distributed in three age groups, with different survival rates and drug tolerance under current protocols. This adds another layer in the stratification, meaning that infant, pediatric, and adult SHH MB patients should be treated differently, aside from just excluding radiotherapy for infant patients. More evidence is needed to assess the newly-devised (2010) stratification system to see if it would help inform clinicians in performing tailored treatment protocols.

Besides fine-tuning the stratification system, the search for novel targeted therapy would also benefit from understanding the tumor heterogeneity of SHH MBs. For example, the activation of the PI3K pathway has been associated mainly with adult SHH medulloblastoma patients, more than so with any other prognostic marker (32). The combination therapy targeting both SHH signaling and the PI3K pathway has been tested by multiple groups, and showed promising treatment efficacy, especially for

recurrent tumors in SHH medulloblastoma mouse models. Clinical trials of combination therapy such as LDE225 (Smoothed inhibitor) with BKM120 (PI3K inhibitor) or with mTOR inhibitor RAD001 were proposed by these groups to treat SHH medulloblastoma patients with PI3K/mTOR activation signatures. We could foresee the beneficial roles of combination therapy of targeting SHH and PI3K pathways for specific subsets of SHH MB patients, particularly the adult group where PI3K activation is usually associated with a poor prognosis.

Additionally, a more comprehensive illumination of the tumor microenvironment (TME) will enable us to devise novel therapeutic strategies beyond targeting mutant or amplified proteins in SHH medulloblastoma patients. Three TME factors of the SHH MBs that are of interest include the cancer stem-like cells, immune cell populations, and the blood brain barrier. The cancer stem-like cells in the PVN of SHH medulloblastomas have been shown to be responsible for the repopulation of recurrent tumors post-irradiation. If we could find a way to target these stem-like cells, then we might be able to prevent recurrent fatal tumors. However, stem-like cells are generally quiescent, which renders most of the drugs unable to target them. Vanner *et al.* showed that mithramycin, an RNA synthesis inhibitor, had selective efficacy for suppressing the growth of *Sox2*⁺ cancer stem-like cells but no effect on other cell populations in the SHH medulloblastoma mouse model. This elicits the possibility of targeting cancer stem-like cells in the TME of medulloblastomas. Secondly, reactive astrocytes and microglia cells are the most abundant cell types other than neuronal tumor cells in the TME of SHH medulloblastomas. Although more research needs to be performed to investigate the communication between tumor cells and these surrounding reactive astrocytes or microglia, the re-education of these abundant cells in the TME might serve as a potential therapeutic strategy. Taking advantage of employing the local “self” cells could benefit younger patients particularly, who suffer from current harsh treatment modalities. A third example of targeting the TME is to increase the permeability of BBB in tumors of SHH medulloblastoma patients. This would allow the availability of the CNS tumors

to drugs in current standard therapy. As reviewed by Quail and Joyce, one possible reason for the good prognosis in WNT MB patients might be the compromised BBB in this subgroup whereas SHH MB patients usually have an intact BBB which prevents the entry of drugs (177). If we can find ways to increase the permeability of BBB locally in the TME, we probably can deliver drugs in a more efficient way for SHH medulloblastoma patients. One possible approach is to promote the angiogenesis of the TME for SHH medulloblastoma patients. According to the R2 platform, expressions of VEGFA and VEGFC, two factors that can promote angiogenesis, correlate with better survival for medulloblastoma patients. Further studies of the TME are needed as our knowledge about SHH medulloblastoma TME components, such as cancer stem-like cells, immune cells, astrocytes, and the angiogenesis or the communications and interactions between each component, is quite limited.

Epigenetic alterations, changes that affect gene expression or mRNA translation independently of the genome sequence, have drawn considerable attention in the field of stem cell and cancer research in recent years. These alterations include aberration in DNA methylation, histone methylation, acetylation or ubiquitination, as well as microRNA cluster copy number, all of which have been implicated in SHH medulloblastomas. Histone modification patterns have been shown to be distinct in stem-like and more differentiated mammalian cells. As medulloblastoma has been historically known as a tumor comprised of rapidly-dividing undifferentiated or embryonal neuron cells, there exists an intriguing possibility that epigenetics is extensively involved during medulloblastoma development. Epigenetic changes are more dominant in group 3 and group 4 tumors, which have no identified specific oncogenic drivers. Global histone methylation patterns are significantly different from those in normal cerebellum samples. Although detailed mechanisms not fully understood, mutations in chromatin remodelers, histone modifiers, as well as DNA methyltransferases have been gradually appreciated in SHH medulloblastoma patients. Some researchers proposed targeting

epigenetic regulators such as histone deacetylase in SHH medulloblastomas. In a report by Lee *et al.*, they showed that the administration of curcumin as an HDAC inhibitor attenuated cell proliferation *in vitro* of DAOY cells and delayed tumor growth *in vivo* in xenograft and homozygous *NeuroD2:SmcA1* mice (48). Detailed mechanistic studies of how these changes contribute to SHH medulloblastoma are needed for future development of novel therapies.

In summary, research in the prospering field of SHH medulloblastomas enables us to view the heterogeneity of SHH medulloblastomas comprehensively. With the advancement in clinical application of sequencing method, such as mRNA microarray, nanostring technique, we will be able to obtain better information from individual patients, which will further provide insights for future diagnosis, tailored treatment, and prognosis improvements for SHH medulloblastoma patients.

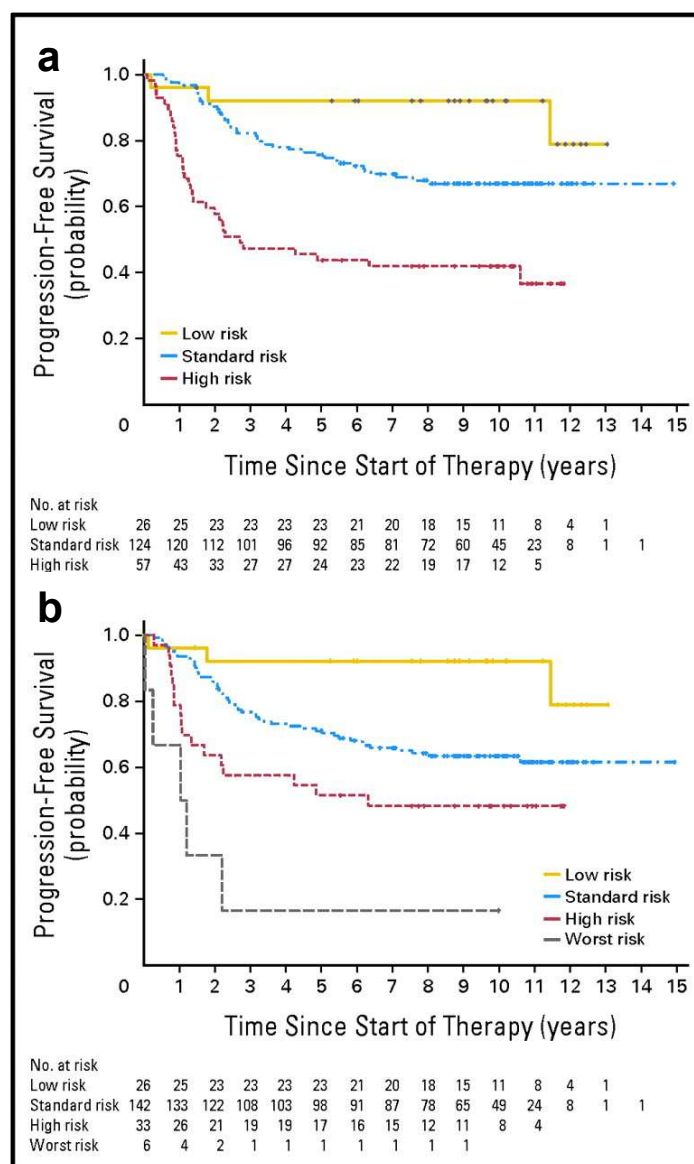


Figure 5.1. PFS curves for patients divided into (a) three or (b) four risk groups. Taken from (244) with permission. Low-risk group, nonmetastatic classic tumors without MYC amplification showing nuclear β -catenin positivity; high risk, LCA tumors or tumors with metastatic disease or MYC amplification; worst risk, LCA tumors plus metastatic disease or MYC amplification (only for **b**); standard risk, the remainder. Numbers along x-axis represent patients at risk of event; log-rank tests, both data sets, $p < .0001$.

5.1.2 I2PP2A as a possible target in TP53 wildtype SHH medulloblastoma patients

As discussed in Chapter 3 and Chapter 4, I2PP2A plays its oncogenic role primarily through stabilizing p-MDM2^{S166}, which is an active suppressor of wild-type p53 in *NeuroD2:SmcA1* mice as well as patient-derived ONS76 cells. Therefore, targeting I2PP2A could benefit patients with wild-type *TP53*, at least for SHH subgroup medulloblastoma patients. In combination with current subtyping of SHH medulloblastoma patients outlined in Chapter 2, *TP53* mutation is exclusively observed in pediatric patients (SHH α subtype). One speculation is that I2PP2A could be a good target for infant or adult medulloblastoma patients. Infant SHH medulloblastoma patients might benefit the most from targeted therapy like inhibiting I2PP2A because it is an age group deferred from craniospinal radiation, and additionally a group stratified into the high-risk category irrespective of its clinical or histopathological features. As infant patients are prone to adverse side effects of current treatment modalities, the identification of novel and effective therapeutic target is imperative for them. Though more detailed evaluation of I2PP2A inhibitors is needed, I2PP2A's suppression of wild-type p53 confers the potential for it to be a useful therapeutic target, especially for infant SHH medulloblastoma patients.

As discussed in Chapter 3, a distinct mechanism of how I2PP2A suppresses p53 activity in the nucleus was proposed by Wang *et al.* distinct from mechanism whereas I2PP2A destabilizes wildtype p53 in the cytoplasm that we have proposed (241). I2PP2A/SET has been known to be involved in the INHAT complex which inhibits histone acetylation mediated by p300/CBP. Wang *et al.* showed that negatively charged acidic C-terminal of I2PP2A could bind to the lysine-rich C-terminal domain (CTD) of p53; thus inhibiting p53's transactivation ability by prohibiting p300/CBP mediated acetylation of nearby histones. However, the acetylation on CTD of p53 induced by stress prevents the binding of I2PP2A to p53, thus p53 transactivation ability is restored, and its downstream genes are transcribed to cope with the cellular stress. If this mechanism also applies to granule neuron precursors, then the

increased I2PP2A in these “tumor-to-be” cells might compromise p53 function when cells are under stress, permitting error-prone DNA replication and genome instability in SHH medulloblastomas.

As demonstrated in lung tumor cells, sphingosine analog drug FTY720 was shown to bind I2PP2A directly through residues K209 and Y122 of I2PP2A, which result in tumor cell death (103). FTY720, which can permeate the BBB, has been FDA-approved to treat relapsed multiple sclerosis patients. The efficiency of FTY720 needs to be assessed in the future clinical trials. An alternative therapeutic strategy to restore wildtype p53 function in SHH medulloblastoma patients without mutant *TP53* would be the administration of Nutlin-3a, an MDM2 suppressor. As demonstrated by our lab and two other groups, Nutlin-3a has very potent cytotoxic effects on both mouse SHH medulloblastoma cells and patient-derived cell lines with wildtype p53 (77, 78). The administration of Nutlin-3a or FTY720 might also apply to other subgroups of medulloblastoma patients considering the rare mutation rate of *TP53*. For example, Garner *et al.* showed that FTY720 delayed medulloblastoma growth by inducing tumor cell apoptosis and cell cycle arrest in group 3 patient-derived-xenografts (245). Also, targeted therapy to restore p53 activity, adjuvant with craniospinal irradiation, might synergize as radiation causes cell death primarily through activating p53 and inducing cellular death. The beneficial role of either FTY720 or Nutlin-3a needs to be further evaluated in future clinical trials for SHH TP53-wildtype medulloblastoma patients.

5.2 Future directions

5.2.1 I2PP2A in SHH medulloblastoma patients

Although we have tested the interaction of I2PP2A-MDM2-p53 in the mouse model and patient-derived cell lines, it is necessary to check if I2PP2A show sufficient protein levels in patient samples. IHC staining of I2PP2A in patient samples tissue microarray would be recommended to check if I2PP2A is upregulated in protein levels in patient samples without *TP53* mutations. Another example of targeting I2PP2A would benefit SHH patients comes from the possible role of I2PP2A in facilitating tumor cell migration. Abundant I2PP2A in SHH medulloblastoma might also be a reservoir to promote tumor cell migration, which may contribute to metastasis. As extensively investigated in HeLa and Cos7 cell lines by the Hordijk group, phosphorylated I2PP2A (Ser9) can be recruited by active RAC1 onto the plasma membrane, where it promotes RAC1-PAK-MAPK signaling in cell migration and spreading (89, 90). They proposed that plasma membrane-localized I2PP2A might help sustain RAC1-MAPK signaling by suppressing PP2A, which has been demonstrated to dephosphorylate and inactivate p38 MAPK or ERK proteins. MacDonald *et al.* showed that PDGFR and RAS/MAPK signaling pathways were overexpressed in metastatic tumors from medulloblastoma patients, suggesting these signaling components are an excellent target to treat metastatic medulloblastomas (215). These findings suggest a possible function of abundant I2PP2A in SHH medulloblastomas, being a reservoir for promoting metastasis, which while uncommon in SHH medulloblastoma indicates a poor prognosis. As discussed in Chapter 2, metastasis remains a less-studied area in medulloblastoma research, and it would be very interesting to see if I2PP2A plays roles in tumor migration and thus metastasis of medulloblastomas.

Targeting I2PP2A in an earlier stage of treatment procedures might benefit SHH patients for several reasons. First, *TP53* mutations are more frequent in recurrent tumors, rendering I2PP2A inhibition pointless as no wildtype p53 is functional in inducing cancer cell death. Besides, early I2PP2A

suppression might help prevent further spread or metastasis of SHH medulloblastoma tumors considering the possible role of I2PP2A in facilitating cancer cell migration. To summarize, clinical trials of targeting I2PP2A by FTY720 in the early stage of SHH medulloblastoma treatment are suggested based on findings discussed above, especially for patients presumably harboring abundant I2PP2A proteins in their biopsies.

5.2.3 Implications of TP53 in radiation therapy for SHH medulloblastoma patients

The WHO has classified SHH medulloblastomas into *TP53* wildtype and *TP53* mutant subclasses due to the worse prognosis predicted by mutant *TP53*. Zhukov *et al.* proposed different treatment modalities should be administered to treat these two subclasses. As for SHH medulloblastoma patients with wildtype *TP53*, current irradiation protocols or possible future de-escalated irradiation would still benefit them because tumor shrinkage caused by radiation therapy is mainly due to p53-mediated tumor cell death.

Another concern for radiation therapy in this subclass of SHH MB patients is that the DNA damages caused by irradiation might predispose these patients to tumor recurrence or other malignancy, such as glioblastomas, in the future. Radiation kills tumor cells primarily through causing DNA damage which passes the threshold a tumor cell can tolerate. Tumor cells then trigger checkpoint system like the induction of p53 to induce cellular death. However, if a subpopulation of tumor cells harbors mutant *TP53*, these cells will bypass the stress checkpoint, and keep dividing into cells with various mutations accumulating. As mentioned previously, tumors with mutant *TP53* display higher mutational loads and genomic instability in LFS patients. A specific subpopulation of tumor cells with a proliferation advantage endowed by a specific combination of genetic mutations may be selected for and contribute to the tumor recurrence. Therefore, radiation therapy on SHH medulloblastoma patients with mutant *TP53* might increase the risk of tumor recurrence in these patients, which is fatal. Conversely, radiation therapy may also predispose patients to other malignancies, such as glioma, without giving them a curative advantage. If radiation is no longer an optimal choice, it would remain challenging to increase the cure rate for these patients before we can find better targets in SHH tumors with mutant *TP53*.

A realistic proposal to treat these patients is to integrate the combination therapy of SHH antagonists with a PI3K/MAPK inhibitor, which has been proposed by different groups to treat recurrent SHH medulloblastomas. *TP53* mutations were more frequently observed in recurrent tumors. As corroborated by **Figure 4.5**, p-AKT and p-ERK proteins were enriched 24 hours post irradiation (n=3), which were consistent with the finding that PI3K signaling at the PVN could contribute to tumor cell repopulation post radiation (135). Cells with active PI3K signaling in the PVN might be the reservoir of cancer stem-like cells, quiescent cells with the potential to proliferate or differentiate when exposed to the right environmental cues. Combination therapy of SHH antagonists with PI3K inhibitor might be a good future direction for clinical trials in treating the majority of SHH medulloblastoma patients, in regard of the status of *TP53* status.

References

1. Smoll, N.R. and K.J. Drummond, *The incidence of medulloblastomas and primitive neuroectodermal tumours in adults and children*. J Clin Neurosci, 2012. **19**(11): p. 1541-4.
2. Ostrom, Q.T., H. Gittleman, P. Liao, C. Rouse, Y. Chen, J. Dowling, et al., *CBTRUS statistical report: primary brain and central nervous system tumors diagnosed in the United States in 2007-2011*. Neuro Oncol, 2014. **16 Suppl 4**: p. iv1-63.
3. Packer, R.J. and G. Vezina, *Management of and prognosis with medulloblastoma: therapy at a crossroads*. Arch Neurol, 2008. **65**(11): p. 1419-24.
4. Bailey, P. and H. Cushing, *Medulloblastoma cerebelli - A common type of midcerebellar glioma of childhood*. Archives of Neurology and Psychiatry, 1925. **14**(2): p. 192-224.
5. Gilbertson, R.J. and D.W. Ellison, *The origins of medulloblastoma subtypes*. Annu Rev Pathol, 2008. **3**: p. 341-65.
6. Taylor, M.D., P.A. Northcott, A. Korshunov, M. Remke, Y.J. Cho, S.C. Clifford, et al., *Molecular subgroups of medulloblastoma: the current consensus*. Acta Neuropathol, 2012. **123**(4): p. 465-72.
7. Northcott, P.A., A. Korshunov, H. Witt, T. Hielscher, C.G. Eberhart, S. Mack, et al., *Medulloblastoma comprises four distinct molecular variants*. J Clin Oncol, 2011. **29**(11): p. 1408-14.
8. Ramaswamy, V., M. Remke, E. Bouffet, S. Bailey, S.C. Clifford, F. Doz, et al., *Risk stratification of childhood medulloblastoma in the molecular era: the current consensus*. Acta Neuropathol, 2016. **131**(6): p. 821-31.
9. Kool, M., A. Korshunov, M. Remke, D.T. Jones, M. Schlanstein, P.A. Northcott, et al., *Molecular subgroups of medulloblastoma: an international meta-analysis of transcriptome, genetic aberrations, and clinical data of WNT, SHH, Group 3, and Group 4 medulloblastomas*. Acta Neuropathol, 2012. **123**(4): p. 473-84.

10. Zurawel, R.H., S.A. Chiappa, C. Allen, and C. Raffel, *Sporadic medulloblastomas contain oncogenic beta-catenin mutations*. *Cancer Res*, 1998. **58**(5): p. 896-9.
11. Eberhart, C.G., T. Tihan, and P.C. Burger, *Nuclear localization and mutation of beta-catenin in medulloblastomas*. *J Neuropathol Exp Neurol*, 2000. **59**(4): p. 333-7.
12. Dahmen, R.P., A. Koch, D. Denkhaus, J.C. Tonn, N. Sorensen, F. Berthold, et al., *Deletions of AXIN1, a component of the WNT/wingless pathway, in sporadic medulloblastomas*. *Cancer Res*, 2001. **61**(19): p. 7039-43.
13. Baeza, N., J. Masuoka, P. Kleihues, and H. Ohgaki, *AXIN1 mutations but not deletions in cerebellar medulloblastomas*. *Oncogene*, 2003. **22**(4): p. 632-6.
14. Koch, A., A. Hrychyk, W. Hartmann, A. Waha, T. Mikeska, A. Waha, et al., *Mutations of the Wnt antagonist AXIN2 (Conductin) result in TCF-dependent transcription in medulloblastomas*. *Int J Cancer*, 2007. **121**(2): p. 284-91.
15. Hamilton, S.R., B. Liu, R.E. Parsons, N. Papadopoulos, J. Jen, S.M. Powell, et al., *The molecular basis of Turcot's syndrome*. *N Engl J Med*, 1995. **332**(13): p. 839-47.
16. Northcott, P.A., D.T. Jones, M. Kool, G.W. Robinson, R.J. Gilbertson, Y.J. Cho, et al., *Medulloblastomics: the end of the beginning*. *Nat Rev Cancer*, 2012. **12**(12): p. 818-34.
17. Robinson, G., M. Parker, T.A. Kranenburg, C. Lu, X. Chen, L. Ding, et al., *Novel mutations target distinct subgroups of medulloblastoma*. *Nature*, 2012. **488**(7409): p. 43-8.
18. Wu, X., P.A. Northcott, S. Croul, and M.D. Taylor, *Mouse models of medulloblastoma*. *Chin J Cancer*, 2011. **30**(7): p. 442-9.
19. Gibson, P., Y. Tong, G. Robinson, M.C. Thompson, D.S. Currel, C. Eden, et al., *Subtypes of medulloblastoma have distinct developmental origins*. *Nature*, 2010. **468**(7327): p. 1095-9.
20. Dai, P., H. Akimaru, Y. Tanaka, T. Maekawa, M. Nakafuku, and S. Ishii, *Sonic Hedgehog-induced activation of the Gli1 promoter is mediated by GLI3*. *J Biol Chem*, 1999. **274**(12): p. 8143-52.

21. Fernandez, L.A., P.A. Northcott, J. Dalton, C. Fraga, D. Ellison, S. Angers, et al., *YAP1 is amplified and up-regulated in hedgehog-associated medulloblastomas and mediates Sonic hedgehog-driven neural precursor proliferation*. Genes Dev, 2009. **23**(23): p. 2729-41.
22. Mill, P., R. Mo, H. Fu, M. Grachtchouk, P.C. Kim, A.A. Dlugosz, et al., *Sonic hedgehog-dependent activation of Gli2 is essential for embryonic hair follicle development*. Genes Dev, 2003. **17**(2): p. 282-94.
23. Wetmore, C., *Sonic hedgehog in normal and neoplastic proliferation: insight gained from human tumors and animal models*. Curr Opin Genet Dev, 2003. **13**(1): p. 34-42.
24. Raffel, C., R.B. Jenkins, L. Frederick, D. Hebrink, B. Alderete, D.W. Fults, et al., *Sporadic medulloblastomas contain PTCH mutations*. Cancer Res, 1997. **57**(5): p. 842-5.
25. Taylor, M.D., L. Liu, C. Raffel, C.C. Hui, T.G. Mainprize, X. Zhang, et al., *Mutations in SUFU predispose to medulloblastoma*. Nat Genet, 2002. **31**(3): p. 306-10.
26. Kenney, A.M., M.D. Cole, and D.H. Rowitch, *Nmyc upregulation by sonic hedgehog signaling promotes proliferation in developing cerebellar granule neuron precursors*. Development, 2003. **130**(1): p. 15-28.
27. Gorlin, R.J., *Nevoid basal cell carcinoma syndrome*. Dermatol Clin, 1995. **13**(1): p. 113-25.
28. Taylor, M.D., T.G. Mainprize, and J.T. Rutka, *Molecular insight into medulloblastoma and central nervous system primitive neuroectodermal tumor biology from hereditary syndromes: a review*. Neurosurgery, 2000. **47**(4): p. 888-901.
29. Oliver, T.G., T.A. Read, J.D. Kessler, A. Mehmeti, J.F. Wells, T.T. Huynh, et al., *Loss of patched and disruption of granule cell development in a pre-neoplastic stage of medulloblastoma*. Development, 2005. **132**(10): p. 2425-39.
30. Schuller, U., V.M. Heine, J. Mao, A.T. Kho, A.K. Dillon, Y.G. Han, et al., *Acquisition of granule neuron precursor identity is a critical determinant of progenitor cell competence to form Shh-induced medulloblastoma*. Cancer Cell, 2008. **14**(2): p. 123-34.

31. Wechsler-Reya, R.J. and M.P. Scott, *Control of neuronal precursor proliferation in the cerebellum by Sonic Hedgehog*. Neuron, 1999. **22**(1): p. 103-14.
32. Kool, M., D.T. Jones, N. Jager, P.A. Northcott, T.J. Pugh, V. Hovestadt, et al., *Genome sequencing of SHH medulloblastoma predicts genotype-related response to smoothed inhibition*. Cancer Cell, 2014. **25**(3): p. 393-405.
33. Yauch, R.L., G.J. Dijkgraaf, B. Alicke, T. Januario, C.P. Ahn, T. Holcomb, et al., *Smoothed mutation confers resistance to a Hedgehog pathway inhibitor in medulloblastoma*. Science, 2009. **326**(5952): p. 572-4.
34. Louis, D.N., A. Perry, G. Reifenberger, A. von Deimling, D. Figarella-Branger, W.K. Cavenee, et al., *The 2016 World Health Organization Classification of Tumors of the Central Nervous System: a summary*. Acta Neuropathol, 2016. **131**(6): p. 803-20.
35. Northcott, P.A., C. Lee, T. Zichner, A.M. Stutz, S. Erkek, D. Kawauchi, et al., *Enhancer hijacking activates GFII1 family oncogenes in medulloblastoma*. Nature, 2014. **511**(7510): p. 428-34.
36. Pei, Y., C.E. Moore, J. Wang, A.K. Tewari, A. Eroshkin, Y.J. Cho, et al., *An animal model of MYC-driven medulloblastoma*. Cancer Cell, 2012. **21**(2): p. 155-67.
37. Kawauchi, D., G. Robinson, T. Uziel, P. Gibson, J. Rehg, C. Gao, et al., *A mouse model of the most aggressive subgroup of human medulloblastoma*. Cancer Cell, 2012. **21**(2): p. 168-80.
38. Goodrich, L.V., L. Milenkovic, K.M. Higgins, and M.P. Scott, *Altered neural cell fates and medulloblastoma in mouse patched mutants*. Science, 1997. **277**(5329): p. 1109-13.
39. Knoepfler, P.S. and A.M. Kenney, *Neural precursor cycling at sonic speed: N-Myc pedals, GSK-3 brakes*. Cell Cycle, 2006. **5**(1): p. 47-52.
40. Corrales, J.D., S. Blaess, E.M. Mahoney, and A.L. Joyner, *The level of sonic hedgehog signaling regulates the complexity of cerebellar foliation*. Development, 2006. **133**(9): p. 1811-21.

41. Vaillant, C. and D. Monard, *SHH pathway and cerebellar development*. *Cerebellum*, 2009. **8**(3): p. 291-301.
42. Goodrich, L.V., R.L. Johnson, L. Milenkovic, J.A. McMahon, and M.P. Scott, *Conservation of the hedgehog/patched signaling pathway from flies to mice: induction of a mouse patched gene by Hedgehog*. *Genes Dev*, 1996. **10**(3): p. 301-12.
43. Robbins, D.J., D.L. Fei, and N.A. Riobo, *The Hedgehog signal transduction network*. *Sci Signal*, 2012. **5**(246): p. re6.
44. Gajjar, A., C.F. Stewart, D.W. Ellison, S. Kaste, L.E. Kun, R.J. Packer, et al., *Phase I study of vismodegib in children with recurrent or refractory medulloblastoma: a pediatric brain tumor consortium study*. *Clin Cancer Res*, 2013. **19**(22): p. 6305-12.
45. Robinson, G.W., B.A. Orr, G. Wu, S. Gururangan, T. Lin, I. Qaddoumi, et al., *Vismodegib Exerts Targeted Efficacy Against Recurrent Sonic Hedgehog-Subgroup Medulloblastoma: Results From Phase II Pediatric Brain Tumor Consortium Studies PBTC-025B and PBTC-032*. *J Clin Oncol*, 2015. **33**(24): p. 2646-54.
46. Low, J.A. and F.J. de Sauvage, *Clinical experience with Hedgehog pathway inhibitors*. *J Clin Oncol*, 2010. **28**(36): p. 5321-6.
47. Buonamici, S., J. Williams, M. Morrissey, A. Wang, R. Guo, A. Vattay, et al., *Interfering with resistance to smoothened antagonists by inhibition of the PI3K pathway in medulloblastoma*. *Sci Transl Med*, 2010. **2**(51): p. 51ra70.
48. Lee, S.J., C. Krauthauser, V. Maduskuie, P.T. Fawcett, J.M. Olson, and S.A. Rajasekaran, *Curcumin-induced HDAC inhibition and attenuation of medulloblastoma growth in vitro and in vivo*. *BMC Cancer*, 2011. **11**: p. 144.
49. Adesina, A.M., J. Nalbantoglu, and W.K. Cavenee, *p53 gene mutation and mdm2 gene amplification are uncommon in medulloblastoma*. *Cancer Res*, 1994. **54**(21): p. 5649-51.

50. Ohgaki, H., R.H. Eibl, O.D. Wiestler, M.G. Yasargil, E.W. Newcomb, and P. Kleihues, *p53 mutations in nonastrocytic human brain tumors*. *Cancer Res*, 1991. **51**(22): p. 6202-5.
51. Levine, A.J., *p53, the cellular gatekeeper for growth and division*. *Cell*, 1997. **88**(3): p. 323-31.
52. Gessi, M., A.O. von Bueren, S. Rutkowski, and T. Pietsch, *p53 expression predicts dismal outcome for medulloblastoma patients with metastatic disease*. *J Neurooncol*, 2012. **106**(1): p. 135-41.
53. Lindsey, J.C., R.M. Hill, H. Megahed, M.E. Lusher, E.C. Schwalbe, M. Cole, et al., *TP53 mutations in favorable-risk Wnt/Wingless-subtype medulloblastomas*. *J Clin Oncol*, 2011. **29**(12): p. e344-6; author reply e347-8.
54. Miralbell, R., M. Tolnay, S. Bieri, A. Probst, A.P. Sappino, W. Berchtold, et al., *Pediatric medulloblastoma: prognostic value of p53, bcl-2, Mib-1, and microvessel density*. *J Neurooncol*, 1999. **45**(2): p. 103-10.
55. Pfaff, E., M. Remke, D. Sturm, A. Benner, H. Witt, T. Milde, et al., *TP53 mutation is frequently associated with CTNNB1 mutation or MYCN amplification and is compatible with long-term survival in medulloblastoma*. *J Clin Oncol*, 2010. **28**(35): p. 5188-96.
56. Tabori, U., B. Baskin, M. Shago, N. Alon, M.D. Taylor, P.N. Ray, et al., *Universal poor survival in children with medulloblastoma harboring somatic TP53 mutations*. *J Clin Oncol*, 2010. **28**(8): p. 1345-50.
57. Hill, R.M., S. Kuijper, J.C. Lindsey, K. Petrie, E.C. Schwalbe, K. Barker, et al., *Combined MYC and P53 defects emerge at medulloblastoma relapse and define rapidly progressive, therapeutically targetable disease*. *Cancer Cell*, 2015. **27**(1): p. 72-84.
58. Zhukova, N., V. Ramaswamy, M. Remke, E. Pfaff, D.J. Shih, D.C. Martin, et al., *Subgroup-specific prognostic implications of TP53 mutation in medulloblastoma*. *J Clin Oncol*, 2013. **31**(23): p. 2927-35.
59. Wetmore, C., D.E. Eberhart, and T. Curran, *Loss of p53 but not ARF accelerates medulloblastoma in mice heterozygous for patched*. *Cancer Res*, 2001. **61**(2): p. 513-6.

60. Frank, K.M., N.E. Sharpless, Y. Gao, J.M. Sekiguchi, D.O. Ferguson, C. Zhu, et al., *DNA ligase IV deficiency in mice leads to defective neurogenesis and embryonic lethality via the p53 pathway*. Mol Cell, 2000. **5**(6): p. 993-1002.
61. Lee, Y. and P.J. McKinnon, *DNA ligase IV suppresses medulloblastoma formation*. Cancer Res, 2002. **62**(22): p. 6395-9.
62. Tamayo-Orrego, L., S.M. Swikert, and F. Charron, *Evasion of cell senescence in SHH medulloblastoma*. Cell Cycle, 2016. **15**(16): p. 2102-2107.
63. Tamayo-Orrego, L., C.L. Wu, N. Bouchard, A. Khedher, S.M. Swikert, M. Remke, et al., *Evasion of Cell Senescence Leads to Medulloblastoma Progression*. Cell Rep, 2016. **14**(12): p. 2925-37.
64. Corcoran, R.B. and M.P. Scott, *A mouse model for medulloblastoma and basal cell nevus syndrome*. J Neurooncol, 2001. **53**(3): p. 307-18.
65. Kim, J.Y., A.L. Nelson, S.A. Algon, O. Graves, L.M. Sturla, L.C. Goumnerova, et al., *Medulloblastoma tumorigenesis diverges from cerebellar granule cell differentiation in patched heterozygous mice*. Dev Biol, 2003. **263**(1): p. 50-66.
66. Kessler, J.D., H. Hasegawa, S.N. Brun, B.A. Emmenegger, Z.J. Yang, J.W. Dutton, et al., *N-myc alters the fate of preneoplastic cells in a mouse model of medulloblastoma*. Genes Dev, 2009. **23**(2): p. 157-70.
67. Parsons, D.W., M. Li, X. Zhang, S. Jones, R.J. Leary, J.C. Lin, et al., *The genetic landscape of the childhood cancer medulloblastoma*. Science, 2011. **331**(6016): p. 435-9.
68. Rausch, T., D.T. Jones, M. Zapatka, A.M. Stutz, T. Zichner, J. Weischenfeldt, et al., *Genome sequencing of pediatric medulloblastoma links catastrophic DNA rearrangements with TP53 mutations*. Cell, 2012. **148**(1-2): p. 59-71.

69. Bulavin, D.V., O.N. Demidov, S. Saito, P. Kauraniemi, C. Phillips, S.A. Amundson, et al., *Amplification of PPM1D in human tumors abrogates p53 tumor-suppressor activity*. Nat Genet, 2002. **31**(2): p. 210-5.
70. Lu, X., T.A. Nguyen, X. Zhang, and L.A. Donchower, *The Wip1 phosphatase and Mdm2: cracking the "Wip" on p53 stability*. Cell Cycle, 2008. **7**(2): p. 164-8.
71. Moll, U.M. and O. Petrenko, *The MDM2-p53 interaction*. Mol Cancer Res, 2003. **1**(14): p. 1001-8.
72. Castellino, R.C., M. De Bortoli, X. Lu, S.H. Moon, T.A. Nguyen, M.A. Shepard, et al., *Medulloblastomas overexpress the p53-inactivating oncogene WIP1/PPM1D*. J Neurooncol, 2008. **86**(3): p. 245-56.
73. Doucette, T.A., Y. Yang, C. Pedone, J.Y. Kim, A. Dubuc, P.D. Northcott, et al., *WIP1 enhances tumor formation in a sonic hedgehog-dependent model of medulloblastoma*. Neurosurgery, 2012. **70**(4): p. 1003-10; discussion 1010.
74. Malek, R., J. Matta, N. Taylor, M.E. Perry, and S.M. Mendrysa, *The p53 inhibitor MDM2 facilitates Sonic Hedgehog-mediated tumorigenesis and influences cerebellar foliation*. PLoS One, 2011. **6**(3): p. e17884.
75. Abe, Y., E. Oda-Sato, K. Tobiume, K. Kawauchi, Y. Taya, K. Okamoto, et al., *Hedgehog signaling overrides p53-mediated tumor suppression by activating Mdm2*. Proc Natl Acad Sci U S A, 2008. **105**(12): p. 4838-43.
76. Feng, J., R. Tamaskovic, Z. Yang, D.P. Brazil, A. Merlo, D. Hess, et al., *Stabilization of Mdm2 via decreased ubiquitination is mediated by protein kinase B/ Akt-dependent phosphorylation*. J Biol Chem, 2004. **279**(34): p. 35510-7.
77. Kunkele, A., K. De Preter, L. Heukamp, T. Thor, K.W. Pajtler, W. Hartmann, et al., *Pharmacological activation of the p53 pathway by nutlin-3 exerts anti-tumoral effects in medulloblastomas*. Neuro Oncol, 2012. **14**(7): p. 859-69.

78. Ghassemifar, S. and S.M. Mendrysa, *MDM2 antagonism by nutlin-3 induces death in human medulloblastoma cells*. *Neurosci Lett*, 2012. **513**(1): p. 106-10.
79. Wlodarchak, N. and Y. Xing, *PP2A as a master regulator of the cell cycle*. *Crit Rev Biochem Mol Biol*, 2016. **51**(3): p. 162-84.
80. Westphal, R.S., R.L. Coffee, Jr., A. Marotta, S.L. Pelech, and B.E. Wadzinski, *Identification of kinase-phosphatase signaling modules composed of p70 S6 kinase-protein phosphatase 2A (PP2A) and p21-activated kinase-PP2A*. *J Biol Chem*, 1999. **274**(2): p. 687-92.
81. Okamoto, K., H. Li, M.R. Jensen, T. Zhang, Y. Taya, S.S. Thorgeirsson, et al., *Cyclin G recruits PP2A to dephosphorylate Mdm2*. *Mol Cell*, 2002. **9**(4): p. 761-71.
82. Mainwaring, L.A. and A.M. Kenney, *Divergent functions for eIF4E and S6 kinase by sonic hedgehog mitogenic signaling in the developing cerebellum*. *Oncogene*, 2011. **30**(15): p. 1784-97.
83. Christensen, D.J., Y. Chen, J. Oddo, K.M. Matta, J. Neil, E.D. Davis, et al., *SET oncoprotein overexpression in B-cell chronic lymphocytic leukemia and non-Hodgkin lymphoma: a predictor of aggressive disease and a new treatment target*. *Blood*, 2011. **118**(15): p. 4150-8.
84. Leopoldino, A.M., C.H. Squarize, C.B. Garcia, L.O. Almeida, C.R. Pestana, L.M. Sobral, et al., *SET protein accumulates in HNSCC and contributes to cell survival: antioxidant defense, Akt phosphorylation and AVOs acidification*. *Oral Oncol*, 2012. **48**(11): p. 1106-13.
85. Hu, X., C. Garcia, L. Fazli, M. Gleave, M.P. Vitek, M. Jansen, et al., *Inhibition of Pten deficient Castration Resistant Prostate Cancer by Targeting of the SET - PP2A Signaling axis*. *Sci Rep*, 2015. **5**: p. 15182.
86. Adachi, Y., G.N. Pavlakis, and T.D. Copeland, *Identification and characterization of SET, a nuclear phosphoprotein encoded by the translocation break point in acute undifferentiated leukemia*. *J Biol Chem*, 1994. **269**(3): p. 2258-62.

87. Hallahan, A.R., J.I. Pritchard, S. Hansen, M. Benson, J. Stoeck, B.A. Hatton, et al., *The SmoA1 mouse model reveals that notch signaling is critical for the growth and survival of sonic hedgehog-induced medulloblastomas*. *Cancer Res*, 2004. **64**(21): p. 7794-800.
88. Hatton, B.A., E.H. Villavicencio, K.D. Tsuchiya, J.I. Pritchard, S. Ditzler, B. Pullar, et al., *The Smo/Smo model: hedgehog-induced medulloblastoma with 90% incidence and leptomeningeal spread*. *Cancer Res*, 2008. **68**(6): p. 1768-76.
89. ten Klooster, J.P., I. Leeuwen, N. Scheres, E.C. Anthony, and P.L. Hordijk, *Rac1-induced cell migration requires membrane recruitment of the nuclear oncogene SET*. *EMBO J*, 2007. **26**(2): p. 336-45.
90. Lam, B.D., E.C. Anthony, and P.L. Hordijk, *Cytoplasmic targeting of the proto-oncogene SET promotes cell spreading and migration*. *FEBS Lett*, 2013. **587**(2): p. 111-9.
91. Li, M., A. Makkinje, and Z. Damuni, *The myeloid leukemia-associated protein SET is a potent inhibitor of protein phosphatase 2A*. *J Biol Chem*, 1996. **271**(19): p. 11059-62.
92. Arnaud, L., S. Chen, F. Liu, B. Li, S. Khatoon, I. Grundke-Iqbal, et al., *Mechanism of inhibition of PP2A activity and abnormal hyperphosphorylation of tau by I2(PP2A)/SET*. *FEBS Lett*, 2011. **585**(17): p. 2653-9.
93. Arif, M., J. Wei, Q. Zhang, F. Liu, G. Basurto-Islas, I. Grundke-Iqbal, et al., *Cytoplasmic retention of protein phosphatase 2A inhibitor 2 (I2PP2A) induces Alzheimer-like abnormal hyperphosphorylation of Tau*. *J Biol Chem*, 2014. **289**(40): p. 27677-91.
94. Chambon, J.P., S.A. Touati, S. Berneau, D. Cladiere, C. Hebras, R. Groeme, et al., *The PP2A inhibitor I2PP2A is essential for sister chromatid segregation in oocyte meiosis II*. *Curr Biol*, 2013. **23**(6): p. 485-90.
95. Yan, Y. and M.C. Mumby, *Distinct roles for PP1 and PP2A in phosphorylation of the retinoblastoma protein. PP2a regulates the activities of G(1) cyclin-dependent kinases*. *J Biol Chem*, 1999. **274**(45): p. 31917-24.

96. Kurimchak, A. and X. Grana, *PP2A holoenzymes negatively and positively regulate cell cycle progression by dephosphorylating pocket proteins and multiple CDK substrates*. *Gene*, 2012. **499**(1): p. 1-7.
97. Fan, Z., P.J. Beresford, D.Y. Oh, D. Zhang, and J. Lieberman, *Tumor suppressor NM23-H1 is a granzyme A-activated DNase during CTL-mediated apoptosis, and the nucleosome assembly protein SET is its inhibitor*. *Cell*, 2003. **112**(5): p. 659-72.
98. Seo, S.B., P. McNamara, S. Heo, A. Turner, W.S. Lane, and D. Chakravarti, *Regulation of histone acetylation and transcription by INHAT, a human cellular complex containing the set oncoprotein*. *Cell*, 2001. **104**(1): p. 119-30.
99. Kalousi, A., A.S. Hoffbeck, P.N. Selemenakis, J. Pinder, K.I. Savage, K.K. Khanna, et al., *The nuclear oncogene SET controls DNA repair by KAP1 and HP1 retention to chromatin*. *Cell Rep*, 2015. **11**(1): p. 149-63.
100. Yu, G., T. Yan, Y. Feng, X. Liu, Y. Xia, H. Luo, et al., *Ser9 phosphorylation causes cytoplasmic detention of I2PP2A/SET in Alzheimer disease*. *Neurobiol Aging*, 2013. **34**(7): p. 1748-58.
101. Taipale, J., J.K. Chen, M.K. Cooper, B. Wang, R.K. Mann, L. Milenkovic, et al., *Effects of oncogenic mutations in Smoothed and Patched can be reversed by cyclopamine*. *Nature*, 2000. **406**(6799): p. 1005-9.
102. Ivanov, D.P., B. Coyle, D.A. Walker, and A.M. Grabowska, *In vitro models of medulloblastoma: Choosing the right tool for the job*. *J Biotechnol*, 2016. **236**: p. 10-25.
103. Saddoughi, S.A., S. Gencer, Y.K. Peterson, K.E. Ward, A. Mukhopadhyay, J. Oaks, et al., *Sphingosine analogue drug FTY720 targets I2PP2A/SET and mediates lung tumour suppression via activation of PP2A-RIPK1-dependent necroptosis*. *EMBO Mol Med*, 2013. **5**(1): p. 105-21.
104. Siegel, R.L., K.D. Miller, and A. Jemal, *Cancer Statistics, 2017*. *CA Cancer J Clin*, 2017. **67**(1): p. 7-30.
105. Ferguson, S. and M.S. Lesniak, *Percival Bailey and the classification of brain tumors*. *Neurosurg Focus*, 2005. **18**(4): p. e7.

106. Zhao, X., Z. Liu, L. Yu, Y. Zhang, P. Baxter, H. Voicu, et al., *Global gene expression profiling confirms the molecular fidelity of primary tumor-based orthotopic xenograft mouse models of medulloblastoma*. *Neuro Oncol*, 2012. **14**(5): p. 574-83.
107. Jensen, A.M. and V.A. Wallace, *Expression of Sonic hedgehog and its putative role as a precursor cell mitogen in the developing mouse retina*. *Development*, 1997. **124**(2): p. 363-71.
108. Wang, M.Z., P. Jin, D.A. Bumcrot, V. Marigo, A.P. McMahon, E.A. Wang, et al., *Induction of dopaminergic neuron phenotype in the midbrain by Sonic hedgehog protein*. *Nat Med*, 1995. **1**(11): p. 1184-8.
109. Ye, W., K. Shimamura, J.L. Rubenstein, M.A. Hynes, and A. Rosenthal, *FGF and Shh signals control dopaminergic and serotonergic cell fate in the anterior neural plate*. *Cell*, 1998. **93**(5): p. 755-66.
110. Gajjar, A.J. and G.W. Robinson, *Medulloblastoma-translating discoveries from the bench to the bedside*. *Nat Rev Clin Oncol*, 2014. **11**(12): p. 714-22.
111. Bhatia, B., M. Hsieh, A.M. Kenney, and Z. Nahle, *Mitogenic Sonic hedgehog signaling drives E2F1-dependent lipogenesis in progenitor cells and medulloblastoma*. *Oncogene*, 2011. **30**(4): p. 410-22.
112. Kenney, A.M., H.R. Widlund, and D.H. Rowitch, *Hedgehog and PI-3 kinase signaling converge on Nmyc1 to promote cell cycle progression in cerebellar neuronal precursors*. *Development*, 2004. **131**(1): p. 217-28.
113. Morrissy, A.S., L. Garzia, D.J. Shih, S. Zuyderduyn, X. Huang, P. Skowron, et al., *Divergent clonal selection dominates medulloblastoma at recurrence*. *Nature*, 2016. **529**(7586): p. 351-7.
114. Ramaswamy, V., M. Remke, E. Bouffet, C.C. Faria, S. Perreault, Y.J. Cho, et al., *Recurrence patterns across medulloblastoma subgroups: an integrated clinical and molecular analysis*. *Lancet Oncol*, 2013. **14**(12): p. 1200-7.
115. Gilbertson, R., C. Wickramasinghe, R. Hernan, V. Balaji, D. Hunt, D. Jones-Wallace, et al., *Clinical and molecular stratification of disease risk in medulloblastoma*. *Br J Cancer*, 2001. **85**(5): p. 705-12.

116. Northcott, P.A., T. Hielscher, A. Dubuc, S. Mack, D. Shih, M. Remke, et al., *Pediatric and adult sonic hedgehog medulloblastomas are clinically and molecularly distinct*. *Acta Neuropathol*, 2011. **122**(2): p. 231-40.
117. Rutkowski, S., U. Bode, F. Deinlein, H. Ottensmeier, M. Warmuth-Metz, N. Soerensen, et al., *Treatment of early childhood medulloblastoma by postoperative chemotherapy alone*. *N Engl J Med*, 2005. **352**(10): p. 978-86.
118. Duffner, P.K., M.E. Horowitz, J.P. Krischer, H.S. Friedman, P.C. Burger, M.E. Cohen, et al., *Postoperative chemotherapy and delayed radiation in children less than three years of age with malignant brain tumors*. *N Engl J Med*, 1993. **328**(24): p. 1725-31.
119. Cavalli, F.M.G., M. Remke, L. Rampasek, J. Peacock, D.J.H. Shih, B. Luu, et al., *Intertumoral Heterogeneity within Medulloblastoma Subgroups*. *Cancer Cell*, 2017. **31**(6): p. 737-754 e6.
120. Tabori, U., L. Sung, J. Hukin, N. Laperriere, B. Crooks, A.S. Carret, et al., *Medulloblastoma in the second decade of life: a specific group with respect to toxicity and management: a Canadian Pediatric Brain Tumor Consortium Study*. *Cancer*, 2005. **103**(9): p. 1874-80.
121. Lindsey, J.C., E.C. Schwalbe, S. Potluri, S. Bailey, D. Williamson, and S.C. Clifford, *TERT promoter mutation and aberrant hypermethylation are associated with elevated expression in medulloblastoma and characterise the majority of non-infant SHH subgroup tumours*. *Acta Neuropathol*, 2014. **127**(2): p. 307-9.
122. Goodrich, L.V. and M.P. Scott, *Hedgehog and patched in neural development and disease*. *Neuron*, 1998. **21**(6): p. 1243-57.
123. Heine, V.M., M. Priller, J. Ling, D.H. Rowitch, and U. Schuller, *Dexamethasone destabilizes Nmyc to inhibit the growth of hedgehog-associated medulloblastoma*. *Cancer Res*, 2010. **70**(13): p. 5220-5.

124. Knoepfler, P.S., P.F. Cheng, and R.N. Eisenman, *N-myc is essential during neurogenesis for the rapid expansion of progenitor cell populations and the inhibition of neuronal differentiation*. *Genes Dev*, 2002. **16**(20): p. 2699-712.
125. Kimura, H., D. Stephen, A. Joyner, and T. Curran, *Gli1 is important for medulloblastoma formation in Ptc1+/- mice*. *Oncogene*, 2005. **24**(25): p. 4026-36.
126. Lee, Y., R. Kawagoe, K. Sasai, Y. Li, H.R. Russell, T. Curran, et al., *Loss of suppressor-of-fused function promotes tumorigenesis*. *Oncogene*, 2007. **26**(44): p. 6442-7.
127. Reifenberger, J., M. Wolter, R.G. Weber, M. Megahed, T. Ruzicka, P. Lichter, et al., *Missense mutations in SMOH in sporadic basal cell carcinomas of the skin and primitive neuroectodermal tumors of the central nervous system*. *Cancer Res*, 1998. **58**(9): p. 1798-803.
128. Swartling, F.J., M.R. Grimmer, C.S. Hackett, P.A. Northcott, Q.W. Fan, D.D. Goldenberg, et al., *Pleiotropic role for MYCN in medulloblastoma*. *Genes Dev*, 2010. **24**(10): p. 1059-72.
129. Hahn, H., L. Wojnowski, K. Specht, R. Kappler, J. Calzada-Wack, D. Potter, et al., *Patched target Igf2 is indispensable for the formation of medulloblastoma and rhabdomyosarcoma*. *J Biol Chem*, 2000. **275**(37): p. 28341-4.
130. Wang, J.Y., L. Del Valle, J. Gordon, M. Rubini, G. Romano, S. Croul, et al., *Activation of the IGF-IR system contributes to malignant growth of human and mouse medulloblastomas*. *Oncogene*, 2001. **20**(29): p. 3857-68.
131. Corcoran, R.B., T. Bachar Raveh, M.T. Barakat, E.Y. Lee, and M.P. Scott, *Insulin-like growth factor 2 is required for progression to advanced medulloblastoma in patched1 heterozygous mice*. *Cancer Res*, 2008. **68**(21): p. 8788-95.
132. Hartmann, W., A. Koch, H. Brune, A. Waha, U. Schuller, I. Dani, et al., *Insulin-like growth factor II is involved in the proliferation control of medulloblastoma and its cerebellar precursor cells*. *Am J Pathol*, 2005. **166**(4): p. 1153-62.

133. Hartmann, W., B. Digon-Sontgerath, A. Koch, A. Waha, E. Endl, I. Dani, et al., *Phosphatidylinositol 3'-kinase/ AKT signaling is activated in medulloblastoma cell proliferation and is associated with reduced expression of PTEN*. Clin Cancer Res, 2006. **12**(10): p. 3019-27.
134. Metcalfe, C., B. Alicke, A. Crow, M. Lamoureux, G.J. Dijkgraaf, F. Peale, et al., *PTEN loss mitigates the response of medulloblastoma to Hedgehog pathway inhibition*. Cancer Res, 2013. **73**(23): p. 7034-42.
135. Hambardzumyan, D., O.J. Becher, M.K. Rosenblum, P.P. Pandolfi, K. Manova-Todorova, and E.C. Holland, *PI3K pathway regulates survival of cancer stem cells residing in the perivascular niche following radiation in medulloblastoma in vivo*. Genes Dev, 2008. **22**(4): p. 436-48.
136. Zhang, X., L. Zhang, X. Cheng, Y. Guo, X. Sun, G. Chen, et al., *IGF-1 promotes Brn-4 expression and neuronal differentiation of neural stem cells via the PI3K/ Akt pathway*. PLoS One, 2014. **9**(12): p. e113801.
137. Johnson, S.C., P.S. Rabinovitch, and M. Kaeberlein, *mTOR is a key modulator of ageing and age-related disease*. Nature, 2013. **493**(7432): p. 338-45.
138. Parathath, S.R., L.A. Mainwaring, L.A. Fernandez, D.O. Campbell, and A.M. Kenney, *Insulin receptor substrate 1 is an effector of sonic hedgehog mitogenic signaling in cerebellar neural precursors*. Development, 2008. **135**(19): p. 3291-300.
139. Jia, J., K. Amanai, G. Wang, J. Tang, B. Wang, and J. Jiang, *Shaggy/ GSK3 antagonizes Hedgehog signalling by regulating Cubitus interruptus*. Nature, 2002. **416**(6880): p. 548-52.
140. Nolan-Stevaux, O., J. Lau, M.L. Truitt, G.C. Chu, M. Hebrok, M.E. Fernandez-Zapico, et al., *GLI1 is regulated through Smoothened-independent mechanisms in neoplastic pancreatic ducts and mediates PDAC cell survival and transformation*. Genes Dev, 2009. **23**(1): p. 24-36.

141. Stecca, B., C. Mas, V. Clement, M. Zbinden, R. Correa, V. Piguet, et al., *Melanomas require HEDGEHOG-GLI signaling regulated by interactions between GLI1 and the RAS-MEK/AKT pathways*. Proc Natl Acad Sci U S A, 2007. **104**(14): p. 5895-900.
142. Riobo, N.A., K. Lu, X. Ai, G.M. Haines, and C.P. Emerson, Jr., *Phosphoinositide 3-kinase and Akt are essential for Sonic Hedgehog signaling*. Proc Natl Acad Sci U S A, 2006. **103**(12): p. 4505-10.
143. Wang, Y., Q. Ding, C.J. Yen, W. Xia, J.G. Izzo, J.Y. Lang, et al., *The crosstalk of mTOR/S6K1 and Hedgehog pathways*. Cancer Cell, 2012. **21**(3): p. 374-87.
144. Stecca, B. and A. Ruiz i Altaba, *A GLI1-p53 inhibitory loop controls neural stem cell and tumour cell numbers*. EMBO J, 2009. **28**(6): p. 663-76.
145. Ramaswamy, V., C. Nor, and M.D. Taylor, *Erratum: p53 and Medulloblastoma*. Cold Spring Harb Perspect Med, 2016. **6**(4): p. a029579.
146. Shen, H. and P.W. Laird, *Interplay between the cancer genome and epigenome*. Cell, 2013. **153**(1): p. 38-55.
147. Audia, J.E. and R.M. Campbell, *Histone Modifications and Cancer*. Cold Spring Harb Perspect Biol, 2016. **8**(4): p. a019521.
148. Jones, P.A., J.P. Issa, and S. Baylin, *Targeting the cancer epigenome for therapy*. Nat Rev Genet, 2016. **17**(10): p. 630-41.
149. Baylin, S.B. and P.A. Jones, *Epigenetic Determinants of Cancer*. Cold Spring Harb Perspect Biol, 2016. **8**(9).
150. Hovestadt, V., M. Remke, M. Kool, T. Pietsch, P.A. Northcott, R. Fischer, et al., *Robust molecular subgrouping and copy-number profiling of medulloblastoma from small amounts of archival tumour material using high-density DNA methylation arrays*. Acta Neuropathol, 2013. **125**(6): p. 913-6.

151. Schwalbe, E.C., J.C. Lindsey, S. Nakjang, S. Crosier, A.J. Smith, D. Hicks, et al., *Novel molecular subgroups for clinical classification and outcome prediction in childhood medulloblastoma: a cohort study*. *Lancet Oncol*, 2017. **18**(7): p. 958-971.
152. Schwalbe, E.C., D. Williamson, J.C. Lindsey, D. Hamilton, S.L. Ryan, H. Megahed, et al., *DNA methylation profiling of medulloblastoma allows robust subclassification and improved outcome prediction using formalin-fixed biopsies*. *Acta Neuropathol*, 2013. **125**(3): p. 359-71.
153. Lindsey, J.C., D. Kawauchi, E.C. Schwalbe, D.J. Solecki, M.P. Selby, P.J. McKinnon, et al., *Cross-species epigenetics identifies a critical role for VAV1 in SHH subgroup medulloblastoma maintenance*. *Oncogene*, 2015. **34**(36): p. 4746-57.
154. Wang, G.G., C.D. Allis, and P. Chi, *Chromatin remodeling and cancer, Part I: Covalent histone modifications*. *Trends Mol Med*, 2007. **13**(9): p. 363-72.
155. Yi, J. and J. Wu, *Epigenetic regulation in medulloblastoma*. *Mol Cell Neurosci*, 2018. **87**: p. 65-76.
156. Northcott, P.A., Y. Nakahara, X. Wu, L. Feuk, D.W. Ellison, S. Croul, et al., *Multiple recurrent genetic events converge on control of histone lysine methylation in medulloblastoma*. *Nat Genet*, 2009. **41**(4): p. 465-72.
157. Dubuc, A.M., M. Remke, A. Korshunov, P.A. Northcott, S.H. Zhan, M. Mendez-Lago, et al., *Aberrant patterns of H3K4 and H3K27 histone lysine methylation occur across subgroups in medulloblastoma*. *Acta Neuropathol*, 2013. **125**(3): p. 373-84.
158. Roussel, M.F. and J.L. Stripay, *Epigenetic Drivers in Pediatric Medulloblastoma*. *Cerebellum*, 2018. **17**(1): p. 28-36.
159. Lee, S.J., S. Lindsey, B. Graves, S. Yoo, J.M. Olson, and S.A. Langhans, *Sonic hedgehog-induced histone deacetylase activation is required for cerebellar granule precursor hyperplasia in medulloblastoma*. *PLoS One*, 2013. **8**(8): p. e71455.

160. Miele, E., S. Valente, V. Alfano, M. Silvano, P. Mellini, D. Borovika, et al., *The histone methyltransferase EZH2 as a druggable target in SHH medulloblastoma cancer stem cells*. *Oncotarget*, 2017. **8**(40): p. 68557-68570.
161. Pajtler, K.W., C. Weingarten, T. Thor, A. Künkele, L.C. Heukamp, R. Buttner, et al., *The KDM1A histone demethylase is a promising new target for the epigenetic therapy of medulloblastoma*. *Acta Neuropathol Commun*, 2013. **1**: p. 19.
162. Malatesta, M., C. Steinhauer, F. Mohammad, D.P. Pandey, M. Squatrito, and K. Helin, *Histone acetyltransferase PCAF is required for Hedgehog-Gli-dependent transcription and cancer cell proliferation*. *Cancer Res*, 2013. **73**(20): p. 6323-33.
163. Wang, G.G., C.D. Allis, and P. Chi, *Chromatin remodeling and cancer, Part II: ATP-dependent chromatin remodeling*. *Trends Mol Med*, 2007. **13**(9): p. 373-80.
164. Jones, D.T., P.A. Northcott, M. Kool, and S.M. Pfister, *The role of chromatin remodeling in medulloblastoma*. *Brain Pathol*, 2013. **23**(2): p. 193-9.
165. Wang, X., C. Venugopal, B. Manoranjan, N. McFarlane, E. O'Farrell, S. Nolte, et al., *Sonic hedgehog regulates Bmi1 in human medulloblastoma brain tumor-initiating cells*. *Oncogene*, 2012. **31**(2): p. 187-99.
166. Tang, Y., S. Gholamin, S. Schubert, M.I. Willardson, A. Lee, P. Bandopadhyay, et al., *Epigenetic targeting of Hedgehog pathway transcriptional output through BET bromodomain inhibition*. *Nat Med*, 2014. **20**(7): p. 732-40.
167. Shi, X., Q. Wang, J. Gu, Z. Xuan, and J.I. Wu, *SMARCA4/Brg1 coordinates genetic and epigenetic networks underlying Shh-type medulloblastoma development*. *Oncogene*, 2016. **35**(44): p. 5746-5758.
168. Vaupel, P., F. Kallinowski, and P. Okunieff, *Blood flow, oxygen and nutrient supply, and metabolic microenvironment of human tumors: a review*. *Cancer Res*, 1989. **49**(23): p. 6449-65.

169. Byrd, T., R.G. Grossman, and N. Ahmed, *Medulloblastoma-biology and microenvironment: a review*. *Pediatr Hematol Oncol*, 2012. **29**(6): p. 495-506.
170. Crawford, J.R., T.J. MacDonald, and R.J. Packer, *Medulloblastoma in childhood: new biological advances*. *Lancet Neurol*, 2007. **6**(12): p. 1073-85.
171. Ellison, D., *Classifying the medulloblastoma: insights from morphology and molecular genetics*. *Neuropathol Appl Neurobiol*, 2002. **28**(4): p. 257-82.
172. Lathia, J.D., J.M. Heddleston, M. Venere, and J.N. Rich, *Deadly teamwork: neural cancer stem cells and the tumor microenvironment*. *Cell Stem Cell*, 2011. **8**(5): p. 482-5.
173. Dekkers, M.P., V. Nikolettou, and Y.A. Barde, *Cell biology in neuroscience: Death of developing neurons: new insights and implications for connectivity*. *J Cell Biol*, 2013. **203**(3): p. 385-93.
174. Huang, G.H., Q.F. Xu, Y.H. Cui, N. Li, X.W. Bian, and S.Q. Lv, *Medulloblastoma stem cells: Promising targets in medulloblastoma therapy*. *Cancer Sci*, 2016. **107**(5): p. 583-9.
175. Buffo, A. and F. Rossi, *Origin, lineage and function of cerebellar glia*. *Prog Neurobiol*, 2013. **109**: p. 42-63.
176. Martirosian, V., T.C. Chen, M. Lin, and J. Neman, *Medulloblastoma initiation and spread: Where neurodevelopment, microenvironment and cancer cross pathways*. *J Neurosci Res*, 2016. **94**(12): p. 1511-1519.
177. Quail, D.F. and J.A. Joyce, *The Microenvironmental Landscape of Brain Tumors*. *Cancer Cell*, 2017. **31**(3): p. 326-341.
178. Yang, Z.J., T. Ellis, S.L. Markant, T.A. Read, J.D. Kessler, M. Bourboulas, et al., *Medulloblastoma can be initiated by deletion of Patched in lineage-restricted progenitors or stem cells*. *Cancer Cell*, 2008. **14**(2): p. 135-45.
179. Marzban, H., M.R. Del Bigio, J. Alizadeh, S. Ghavami, R.M. Zachariah, and M. Rastegar, *Cellular commitment in the developing cerebellum*. *Front Cell Neurosci*, 2014. **8**: p. 450.

180. Bellamy, T.C., *Interactions between Purkinje neurones and Bergmann glia*. *Cerebellum*, 2006. **5**(2): p. 116-26.
181. Frick, A., D. Grammel, F. Schmidt, J. Poschl, M. Priller, P. Pagella, et al., *Proper cerebellar development requires expression of beta1-integrin in Bergmann glia, but not in granule neurons*. *Glia*, 2012. **60**(5): p. 820-32.
182. Miller, J.A., S.L. Ding, S.M. Sunkin, K.A. Smith, L. Ng, A. Szafer, et al., *Transcriptional landscape of the prenatal human brain*. *Nature*, 2014. **508**(7495): p. 199-206.
183. Wallace, V.A., *Purkinje-cell-derived Sonic hedgehog regulates granule neuron precursor cell proliferation in the developing mouse cerebellum*. *Curr Biol*, 1999. **9**(8): p. 445-8.
184. Cahoy, J.D., B. Emery, A. Kaushal, L.C. Foo, J.L. Zamanian, K.S. Christopherson, et al., *A transcriptome database for astrocytes, neurons, and oligodendrocytes: a new resource for understanding brain development and function*. *J Neurosci*, 2008. **28**(1): p. 264-78.
185. Chung, W.S., L.E. Clarke, G.X. Wang, B.K. Stafford, A. Sher, C. Chakraborty, et al., *Astrocytes mediate synapse elimination through MEGF10 and MERTK pathways*. *Nature*, 2013. **504**(7480): p. 394-400.
186. Clarke, L.E. and B.A. Barres, *Emerging roles of astrocytes in neural circuit development*. *Nat Rev Neurosci*, 2013. **14**(5): p. 311-21.
187. Sofroniew, M.V. and H.V. Vinters, *Astrocytes: biology and pathology*. *Acta Neuropathol*, 2010. **119**(1): p. 7-35.
188. Liddelow, S.A., K.A. Guttenplan, L.E. Clarke, F.C. Bennett, C.J. Bohlen, L. Schirmer, et al., *Neurotoxic reactive astrocytes are induced by activated microglia*. *Nature*, 2017. **541**(7638): p. 481-487.
189. Liddelow, S. and B. Barres, *SnapShot: Astrocytes in Health and Disease*. *Cell*, 2015. **162**(5): p. 1170-1170 e1.

190. Sevenich, L., *Brain-Resident Microglia and Blood-Borne Macrophages Orchestrate Central Nervous System Inflammation in Neurodegenerative Disorders and Brain Cancer*. *Front Immunol*, 2018. **9**: p. 697.
191. Ginhoux, F., M. Greter, M. Leboeuf, S. Nandi, P. See, S. Gokhan, et al., *Fate mapping analysis reveals that adult microglia derive from primitive macrophages*. *Science*, 2010. **330**(6005): p. 841-5.
192. Dai, X.M., G.R. Ryan, A.J. Hapel, M.G. Dominguez, R.G. Russell, S. Kapp, et al., *Targeted disruption of the mouse colony-stimulating factor 1 receptor gene results in osteopetrosis, mononuclear phagocyte deficiency, increased primitive progenitor cell frequencies, and reproductive defects*. *Blood*, 2002. **99**(1): p. 111-20.
193. Yoshida, H., S. Hayashi, T. Kunisada, M. Ogawa, S. Nishikawa, H. Okamura, et al., *The murine mutation osteopetrosis is in the coding region of the macrophage colony stimulating factor gene*. *Nature*, 1990. **345**(6274): p. 442-4.
194. Aloisi, F., *Immune function of microglia*. *Glia*, 2001. **36**(2): p. 165-79.
195. Hanisch, U.K. and H. Kettenmann, *Microglia: active sensor and versatile effector cells in the normal and pathologic brain*. *Nat Neurosci*, 2007. **10**(11): p. 1387-94.
196. Paolicelli, R.C., G. Bolasco, F. Pagani, L. Maggi, M. Scianni, P. Panzanelli, et al., *Synaptic pruning by microglia is necessary for normal brain development*. *Science*, 2011. **333**(6048): p. 1456-8.
197. Wlodarczyk, A., I.R. Holtman, M. Krueger, N. Yogev, J. Bruttger, R. Khorrooshi, et al., *A novel microglial subset plays a key role in myelinogenesis in developing brain*. *EMBO J*, 2017. **36**(22): p. 3292-3308.
198. Reed-Geaghan, E.G., J.C. Savage, A.G. Hise, and G.E. Landreth, *CD14 and toll-like receptors 2 and 4 are required for fibrillar A β -stimulated microglial activation*. *J Neurosci*, 2009. **29**(38): p. 11982-92.
199. Imai, Y. and S. Kohsaka, *Intracellular signaling in M-CSF-induced microglia activation: role of Iba1*. *Glia*, 2002. **40**(2): p. 164-74.

200. Bennett, M.L., F.C. Bennett, S.A. Liddel, B. Ajami, J.L. Zamanian, N.B. Fernhoff, et al., *New tools for studying microglia in the mouse and human CNS*. Proc Natl Acad Sci U S A, 2016. **113**(12): p. E1738-46.
201. Margol, A.S., N.J. Robison, J. Gnanachandran, L.T. Hung, R.J. Kennedy, M. Vali, et al., *Tumor-associated macrophages in SHH subgroup of medulloblastomas*. Clin Cancer Res, 2015. **21**(6): p. 1457-65.
202. Salsman, V.S., K.K. Chow, D.R. Shaffer, H. Kadikoy, X.N. Li, C. Gerken, et al., *Crosstalk between medulloblastoma cells and endothelium triggers a strong chemotactic signal recruiting T lymphocytes to the tumor microenvironment*. PLoS One, 2011. **6**(5): p. e20267.
203. Wiegering, V., M. Eyrich, S. Rutkowski, M. Wolf, P.G. Schlegel, and B. Winkler, *TH1 predominance is associated with improved survival in pediatric medulloblastoma patients*. Cancer Immunol Immunother, 2011. **60**(5): p. 693-703.
204. Zhou, P., H. Sha, and J. Zhu, *The role of T-helper 17 (Th17) cells in patients with medulloblastoma*. J Int Med Res, 2010. **38**(2): p. 611-9.
205. Pham, C.D., C. Flores, C. Yang, E.M. Pinheiro, J.H. Yearley, E.J. Sayour, et al., *Differential Immune Microenvironments and Response to Immune Checkpoint Blockade among Molecular Subtypes of Murine Medulloblastoma*. Clin Cancer Res, 2016. **22**(3): p. 582-95.
206. Singh, S.K., I.D. Clarke, M. Terasaki, V.E. Bonn, C. Hawkins, J. Squire, et al., *Identification of a cancer stem cell in human brain tumors*. Cancer Res, 2003. **63**(18): p. 5821-8.
207. Read, T.A., M.P. Fogarty, S.L. Markant, R.E. McLendon, Z. Wei, D.W. Ellison, et al., *Identification of CD15 as a marker for tumor-propagating cells in a mouse model of medulloblastoma*. Cancer Cell, 2009. **15**(2): p. 135-47.
208. Ward, R.J., L. Lee, K. Graham, T. Satkunendran, K. Yoshikawa, E. Ling, et al., *Multipotent CD15+ cancer stem cells in patched-1-deficient mouse medulloblastoma*. Cancer Res, 2009. **69**(11): p. 4682-90.

209. Vanner, R.J., M. Remke, M. Gallo, H.J. Selvadurai, F. Coutinho, L. Lee, et al., *Quiescent sox2(+) cells drive hierarchical growth and relapse in sonic hedgehog subgroup medulloblastoma*. *Cancer Cell*, 2014. **26**(1): p. 33-47.
210. Pistollato, F., E. Rampazzo, L. Persano, S. Abbadì, C. Frasson, L. Denaro, et al., *Interaction of hypoxia-inducible factor-1alpha and Notch signaling regulates medulloblastoma precursor proliferation and fate*. *Stem Cells*, 2010. **28**(11): p. 1918-29.
211. Liu, J., N. Chi, J.Y. Zhang, W. Zhu, Y.S. Bian, and H.G. Chen, *Isolation and characterization of cancer stem cells from medulloblastoma*. *Genet Mol Res*, 2015. **14**(2): p. 3355-61.
212. Folkman, J., *Angiogenesis in cancer, vascular, rheumatoid and other disease*. *Nat Med*, 1995. **1**(1): p. 27-31.
213. Slongo, M.L., B. Molena, A.M. Brunati, M. Frasson, M. Gardiman, M. Carli, et al., *Functional VEGF and VEGF receptors are expressed in human medulloblastomas*. *Neuro Oncol*, 2007. **9**(4): p. 384-92.
214. Rochkind, S., I. Blatt, M. Sadeh, and Y. Goldhammer, *Extracranial metastases of medulloblastoma in adults: literature review*. *J Neurol Neurosurg Psychiatry*, 1991. **54**(1): p. 80-6.
215. MacDonald, T.J., K.M. Brown, B. LaFleur, K. Peterson, C. Lawlor, Y. Chen, et al., *Expression profiling of medulloblastoma: PDGFRA and the RAS/MAPK pathway as therapeutic targets for metastatic disease*. *Nat Genet*, 2001. **29**(2): p. 143-52.
216. Wang, X., A.M. Dubuc, V. Ramaswamy, S. Mack, D.M. Gendoo, M. Remke, et al., *Medulloblastoma subgroups remain stable across primary and metastatic compartments*. *Acta Neuropathol*, 2015. **129**(3): p. 449-57.
217. Faria, C.C., B.J. Golbourn, A.M. Dubuc, M. Remke, R.J. Diaz, S. Agnihotri, et al., *Foretinib is effective therapy for metastatic sonic hedgehog medulloblastoma*. *Cancer Res*, 2015. **75**(1): p. 134-46.

218. Gupta, R., C. Chetty, P. Bhoopathi, S. Lakka, S. Mohanam, J.S. Rao, et al., *Downregulation of uPA/uPAR inhibits intermittent hypoxia-induced epithelial-mesenchymal transition (EMT) in DAOY and D283 medulloblastoma cells*. Int J Oncol, 2011. **38**(3): p. 733-44.
219. Hoppe-Hirsch, E., D. Renier, A. Lellouch-Tubiana, C. Sainte-Rose, A. Pierre-Kahn, and J.F. Hirsch, *Medulloblastoma in childhood: progressive intellectual deterioration*. Childs Nerv Syst, 1990. **6**(2): p. 60-5.
220. Laughton, S.J., T.E. Merchant, C.A. Sklar, L.E. Kun, M. Fouladi, A. Broniscer, et al., *Endocrine outcomes for children with embryonal brain tumors after risk-adapted craniospinal and conformal primary-site irradiation and high-dose chemotherapy with stem-cell rescue on the SJMB-96 trial*. J Clin Oncol, 2008. **26**(7): p. 1112-8.
221. Mulhern, R.K., T.E. Merchant, A. Gajjar, W.E. Reddick, and L.E. Kun, *Late neurocognitive sequelae in survivors of brain tumours in childhood*. Lancet Oncol, 2004. **5**(7): p. 399-408.
222. Wolfe, K.R., G.R. Hunter, A. Madan-Swain, A.T. Reddy, J. Banos, and R.K. Kana, *Cardiorespiratory fitness in survivors of pediatric posterior fossa tumor*. J Pediatr Hematol Oncol, 2012. **34**(6): p. e222-7.
223. Hatton, B.A., P.S. Knoepfler, A.M. Kenney, D.H. Rowitch, I.M. de Alboran, J.M. Olson, et al., *N-myc is an essential downstream effector of Shb signaling during both normal and neoplastic cerebellar growth*. Cancer Res, 2006. **66**(17): p. 8655-61.
224. Gottlieb, T.M., J.F. Leal, R. Seger, Y. Taya, and M. Oren, *Cross-talk between Akt, p53 and Mdm2: possible implications for the regulation of apoptosis*. Oncogene, 2002. **21**(8): p. 1299-303.
225. Mayo, L.D. and D.B. Donner, *A phosphatidylinositol 3-kinase/ Akt pathway promotes translocation of Mdm2 from the cytoplasm to the nucleus*. Proc Natl Acad Sci U S A, 2001. **98**(20): p. 11598-603.
226. Westermarck, J. and W.C. Hahn, *Multiple pathways regulated by the tumor suppressor PP2A in transformation*. Trends Mol Med, 2008. **14**(4): p. 152-60.

227. Janghorban, M., A.S. Farrell, B.L. Allen-Petersen, C. Pelz, C.J. Daniel, J. Oddo, et al., *Targeting c-MYC by antagonizing PP2A inhibitors in breast cancer*. Proc Natl Acad Sci U S A, 2014. **111**(25): p. 9157-62.
228. Yang, Y., Q. Huang, Y. Lu, X. Li, and S. Huang, *Reactivating PP2A by FTY720 as a novel therapy for AML with C-KIT tyrosine kinase domain mutation*. J Cell Biochem, 2012. **113**(4): p. 1314-22.
229. Malhotra, A., A. Dey, N. Prasad, and A.M. Kenney, *Sonic Hedgehog Signaling Drives Mitochondrial Fragmentation by Suppressing Mitofusins in Cerebellar Granule Neuron Precursors and Medulloblastoma*. Mol Cancer Res, 2016. **14**(1): p. 114-24.
230. Jacobsen, P.F., D.J. Jenkyn, and J.M. Papadimitriou, *Establishment of a human medulloblastoma cell line and its heterotransplantation into nude mice*. J Neuropathol Exp Neurol, 1985. **44**(5): p. 472-85.
231. Yamada, M., K. Shimizu, K. Tamura, Y. Okamoto, Y. Matsui, S. Moriuchi, et al., [*Establishment and biological characterization of human medulloblastoma cell lines*]. No To Shinkei, 1989. **41**(7): p. 695-702.
232. Keles, G.E., M.S. Berger, R. Lim, A. Zaheer, A.L. Denton, and J.R. Silber, *Expression of glial fibrillary acidic protein in human medulloblastoma cells treated with recombinant glia maturation factor-beta*. Oncol Res, 1992. **4**(10): p. 431-7.
233. Zanini, C., E. Ercole, G. Mandili, R. Salaroli, A. Poli, C. Renna, et al., *Medullospheres from DAOY, UW228 and ONS-76 cells: increased stem cell population and proteomic modifications*. PLoS One, 2013. **8**(5): p. e63748.
234. Wen, J., J. Lee, A. Malhotra, R. Nahta, A.R. Arnold, M.C. Buss, et al., *WTP1 modulates responsiveness to Sonic Hedgehog signaling in neuronal precursor cells and medulloblastoma*. Oncogene, 2016. **35**(42): p. 5552-5564.
235. Bilousova, G., A. Marusyk, C.C. Porter, R.D. Cardiff, and J. DeGregori, *Impaired DNA replication within progenitor cell pools promotes leukemogenesis*. PLoS Biol, 2005. **3**(12): p. e401.

236. Van Linden, A.A., D. Baturin, J.B. Ford, S.P. Fosmire, L. Gardner, C. Korch, et al., *Inhibition of Wee1 sensitizes cancer cells to antimetabolite chemotherapeutics in vitro and in vivo, independent of p53 functionality*. Mol Cancer Ther, 2013. **12**(12): p. 2675-84.
237. Kenney, A.M. and D.H. Rowitch, *Sonic hedgehog promotes G(1) cyclin expression and sustained cell cycle progression in mammalian neuronal precursors*. Mol Cell Biol, 2000. **20**(23): p. 9055-67.
238. Dey, A., M. Robitaille, M. Remke, C. Maier, A. Malhotra, A. Gregorieff, et al., *YB-1 is elevated in medulloblastoma and drives proliferation in Sonic hedgehog-dependent cerebellar granule neuron progenitor cells and medulloblastoma cells*. Oncogene, 2016. **35**(32): p. 4256-68.
239. Switzer, C.H., R.Y. Cheng, T.M. Vitek, D.J. Christensen, D.A. Wink, and M.P. Vitek, *Targeting SET/I(2)PP2A oncoprotein functions as a multi-pathway strategy for cancer therapy*. Oncogene, 2011. **30**(22): p. 2504-13.
240. Ivaska, J., L. Nissinen, N. Immonen, J.E. Eriksson, V.M. Kahari, and J. Heino, *Integrin alpha 2 beta 1 promotes activation of protein phosphatase 2A and dephosphorylation of Akt and glycogen synthase kinase 3 beta*. Mol Cell Biol, 2002. **22**(5): p. 1352-9.
241. Wang, D., N. Kon, G. Lasso, L. Jiang, W. Leng, W.G. Zhu, et al., *Acetylation-regulated interaction between p53 and SET reveals a widespread regulatory mode*. Nature, 2016. **538**(7623): p. 118-122.
242. Vasudevan, N.T., M.L. Mohan, M.K. Gupta, A.K. Hussain, and S.V. Naga Prasad, *Inhibition of protein phosphatase 2A activity by PI3Kgamma regulates beta-adrenergic receptor function*. Mol Cell, 2011. **41**(6): p. 636-48.
243. Gajjar, A., R. Hernan, M. Kocak, C. Fuller, Y. Lee, P.J. McKinnon, et al., *Clinical, histopathologic, and molecular markers of prognosis: toward a new disease risk stratification system for medulloblastoma*. J Clin Oncol, 2004. **22**(6): p. 984-93.

244. Ellison, D.W., M. Kocak, J. Dalton, H. Megahed, M.E. Lusher, S.L. Ryan, et al., *Definition of disease-risk stratification groups in childhood medulloblastoma using combined clinical, pathologic, and molecular variables*. J Clin Oncol, 2011. **29**(11): p. 1400-7.
245. Garner, E.F., A.P. Williams, L.L. Stafman, J.M. Aye, E. Mroczek-Musulman, B.P. Moore, et al., *FTY720 Decreases Tumorigenesis in Group 3 Medulloblastoma Patient-Derived Xenografts*. Sci Rep, 2018. **8**(1): p. 6913.